Influence of intestinal *Coriobacteriia* on host metabolism

Von der Fakultät für Mathematik und Naturwissenschaften der RWTH Aachen University
zur Erlangung des akademischen Grades
einer Doktorin der Naturwissenschaften genehmigte Dissertation

vorgelegt von

Alina Viehof-Beckmann, M. Sc.
aus
Neuss, Deutschland

Berichter: Prof. Dr. rer. nat. Thomas Clavel
Prof. Dr. med. Mathias Hornef

Tag der mündlichen Prüfung: 08.12.2025

Abstract

The intestinal microbiota and their metabolites are known to influence host metabolism, but only few bacteria involved have been described. In studies with rodents and humans, alterations in host metabolism have been associated with the presence of *Coriobacteriia*, which can deconjugate and dehydrogenate bile acids (BAs) and express lipases. Gnotobiotic mouse experiments performed by a former PhD student from the lab showed that colonisation with four *Coriobacteriia* species resulted in increased plasma cholesterol levels. In addition, white adipose tissue (WAT) mass doubled in *Coriobacteriia*-colonised mice fed a diet supplemented with primary BAs. These results indicate that *Coriobacteriia* play a causal role in host metabolism, but it remains unclear how. The aim of this PhD thesis was to investigate whether and how *Coriobacteriia*, specifically *Eggerthella lenta* and *Collinsella aerofaciens,* mediate changes in host metabolism.

In the first part of this work, the effects of colonising gnotobiotic OMM12 mice with *E. lenta* on the liver proteome and gut metabolome were investigated. *E. lenta* stably colonised the mouse intestine at high relative abundances. It had no significant effect on liver proteomes, whereas the colon metabolome differed significantly between colonisation groups. While creatine, sarcosine, N,N-dimethylarginine, and N-Acetyl-DL-methionine were decreased in *E. lenta*-colonised mice, latifolicinin C acid was elevated.

In the second part, the effects of colonising germfree (GF) mice with the four *Coriobacteriia* species *Adlercreutzia mucosicola*, *C. aerofaciens*, *E. lenta*, and *Lancefieldella parvula* (CORIO) in combination with diets differing in fat content and primary BAs on host metabolism were investigated. However, as the CORIO strains did not colonise, the GF and specific pathogen-free (SPF) mice fed the different diets were compared. Most interestingly, GF mice had a significantly elongated small intestine compared to SPF mice, regardless of diet.

In the third part, *C. aerofaciens* was studied in more detail. A total of 14 strains, isolated from human faeces, were analysed and all exhibited a consistent cell-bound lipase activity. Gnotobiotic mouse experiments were performed with the *C. aerofaciens* type strain to investigate its effects on intestinal lipid absorption using stable isotope-labelled lipids. *C. aerofaciens* successfully colonised all regions of the gut, with higher cell densities in the caecum and colon. In mice fed chow supplemented with primary BAs (sampled one hour after gavage of the labelled lipids), and in mice fed chow high in fat (sampled six hours after gavage), levels of labelled fatty acids (FAs) in plasma were higher in the *C. aerofaciens*-monocolonised mice compared to GF and SPF controls. However, statistical significance was only reached for the *C. aerofaciens*-monocolonised mice fed the high-fat diet (HFD) and sampled six hours after gavage compared to corresponding SPF mice.

In the last part, to assess the potential clinical relevance of bacterial lipase, the occurrence of dominant lipase-positive bacteria, including *C. aerofaciens*, in the stool microbiota of 338 participants from a human cohort (16S rRNA gene amplicon profiles) was analysed in relation to host body parameters. Regression analyses revealed a significant positive association between the cumulative relative abundance of lipase-positive bacteria and several host metabolic parameters, including higher body fat content and blood lipids.

The results of this this PhD thesis provide further evidence for the role of *Coriobacteriia* in metabolic health. The identification of underlying molecular mechanisms require further investigations.

Zusammenfassung

Es ist bekannt, dass Darm-Mikrobiota und ihre Metabolite den Stoffwechsel des Wirtes beeinflussen, aber nur wenige der involvierten Bakterien sind bisher beschrieben worden. In Studien mit Nagetieren und Menschen wurden Veränderungen des Wirtsstoffwechsels mit der Anwesenheit von *Coriobacteriia*, die Gallensäuren dekonjugieren und dehydrogenieren können und Lipasen exprimieren, in Verbindung gebracht. Gnotobiotische Mausexperimente, die von einer ehemaligen Doktorandin des Labors durchgeführt wurden, zeigten, dass die Kolonisierung mit vier *Coriobacteriia* Spezies zu erhöhten Plasma Cholesterin Werten führte. Darüber hinaus verdoppelte sich die Masse des weißen Fettgewebes bei den mit *Coriobacteriia* besiedelt Mäusen, die ein mit primären Gallensäuren angereichertes Futter erhielten. Diese Ergebnisse deuten darauf hin, dass *Coriobacteriia* eine kausale Rolle im Wirtsstoffwechsel spielen, aber die zugrunde liegenden Mechanismen sind noch nicht bekannt. Ziel dieser Doktorarbeit war es, zu untersuchen, ob und wie *Coriobacteriia*, insbesondere die Spezies *Eggerthella lenta* und *Collinsella aerofaciens*, Veränderungen im Wirtsstoffwechsel verursachen.

Im ersten Teil dieser Arbeit wurden die Auswirkungen der Kolonisierung von gnotobiotischen OMM12-Mäusen mit *E. lenta* auf das Leber-Proteom und das Colon-Metabolom untersucht. *E. lenta* hat den Darm der Mäuse stabil und in hoher relativer Abundanz kolonisiert. Dies hatte keine signifikante Auswirkung auf das Leber-Proteom, während sich das Metabolom im Colon zwischen den Kolonisationsgruppen signifikant unterschied. Die Werte für Kreatin, Sarkosin, N,N-Dimethylarginin und N-Acetyl-DL-Methionin waren bei Mäusen, die mit *E. lenta* kolonisiert waren, verringert, während der Latifolicin-C-Säure Wert erhöht war.

Im zweiten Teil wurden die Auswirkungen der Kolonisierung von keimfreien Mäusen mit den vier *Coriobacteriia* Spezies *Adlercreutzia mucosicola*, *C. aerofaciens*, *E. lenta* und *Lancefieldella parvula* (CORIO) in Kombination mit Diäten mit unterschiedlichem Fettgehalt bzw. Supplementierung mit primären Gallensäuren auf den Wirtsstoffwechsel untersucht. Da die Besiedlung mit den CORIO Stämmen jedoch nicht erfolgreich war, wurden keimfreie und spezifisch pathogenfreie (SPF) Mäuse, die die verschiedenen Diäten erhielten, verglichen. Interessanterweise hatten die keimfreie Mäuse im Vergleich zu den SPF-Mäusen einen deutlich verlängerten Dünndarm, unabhängig von den verschiedenen Diäten.

Im dritten Teil wurde *C. aerofaciens* detaillierter untersucht. Insgesamt wurden 14 Stämme, die aus humanen Stuhlproben isoliert wurden, analysiert, und alle wiesen eine konsistente zellgebundene Lipase Aktivität auf. Gnotobiotische Mausexperimente wurden mit dem *C. aerofaciens* Typstamm durchgeführt, um die Einflüsse auf die intestinale Lipidabsorption unter Verwendung stabiler

isotopenmarkierter Lipide zu untersuchen. *C. aerofaciens* kolonisierte erfolgreich alle Darmregionen, wobei die Zelldichten im Caecum und Colon höher waren. Bei Mäusen, die mit Futter angereichert mit primären Gallensäuren gefüttert wurden (Probenahme eine Stunde nach der Gavage mit markierten Lipiden), und bei Mäusen, die mit fettreichem Futter gefüttert wurden (Probenahme sechs Stunden nach der Gavage), war der Plasmaspiegel an markierten Fettsäuren bei den *C. aerofaciens*-monokolonisierten Mäusen höher als bei den keimfreien und SPF Kontrollmäusen. Eine statistische Signifikanz wurde jedoch nur bei den *C. aerofaciens*-monokolonisierten Mäusen im Vergleich zu den SPF Mäusen, die mit einer fettreichen Diät gefüttert wurden und bei denen die Probenahme sechs Stunden nach der Gavage erfolgte, erreicht.

Um die potentielle klinische Relevanz der bakteriellen Lipasen zu untersuchen, wurde im letzten Teil das Vorkommen dominanter Lipase-positiver Bakterien, einschließlich *C. aerofaciens*, in Stuhlmikrobiota von 338 Teilnehmern einer humanen Kohorte (16S rRNA Gen Amplikon Profile) im Zusammenhang mit verfügbaren Körperparametern analysiert. Regressionsanalysen ergaben einen signifikanten positiven Zusammenhang zwischen der kumulativen relativen Abundanz der Lipase-positiven Bakterien und mehreren Stoffwechselparametern des Wirts, einschließlich eines höheren Körperfettgehalts und erhöhten Blutfettwerte.

Die Ergebnisse dieser Doktorarbeit liefern weitere Beweise für die Rolle von *Coriobacteriia* in der metabolischen Gesundheit. Die Identifizierung der zugrunde liegenden molekularen Mechanismen erfordert jedoch weitere Untersuchungen.

Acknowledgments

First of all, I would like to express my sincere gratitude to my supervisor, Professor Thomas Clavel, for his exceptional support and guidance throughout my PhD journey. His expertise and encouragement have not only been essential to the completion of this thesis, but have also played a crucial role in shaping my development as a scientist.

I would also like to thank my colleagues in AG Clavel, both past and present: Afrizal, Andrea Martinez Aguirre, Amy Coates, Atscharah Panyot, Candice Raynaud, Catherine Gonzalez, Charlie Pauvert, Daniel Friske, David Wylensek, Esther Wortmann, Johanna Bosch, Johannes (Jojo) Masson, Katharina Grünwald, Maja Magel, Marko Baloh, Maurice Heitzer, Neeraj Kumar, Nicole Treichel, Ntana Kousetzi, Sareh Tavakol, Selina Nüchtern, Soheila Razavi, Susan Jennings, Theresa Streidl, Thomas Hitch, and all the students and Hiwis. I really appreciate their support and scientific input, as well as the coffee breaks filled with conversations about topics beyond work. The positive working atmosphere has helped me to stay on track, even during challenging times.

In addition, I am grateful for the opportunity to supervise Emily Richter during her Master's thesis and I greatly appreciate the valuable work and results she contributed to this project.

Next, I would like to thank all the collaborators whose valuable contributions have greatly enriched this project: Beatrice Engelmann, Caroline Schneider, Diana Möckel, Josef Ecker, Johannes Plagge, Kristin Schubert, Ramona Brück, Roman Bülow, Sarah Schraven, Sven Hermeling, Sven-Bastiaan Haange, and Thriveni Basavanapura.

Last but not least, I would like to express my heartfelt gratitude to my husband, family and friends, who are always there for me and put up with all my moods.

Contributions

The contributions of collaborators to this thesis are summarised in **Table 1** and are described in detail at the end of each corresponding material and methods section.

Table 1: Contributions of the collaborators to each part of this thesis. The percentages are own estimates and relate to the sum of all tasks for the given results chapter.

Name of collaborators	Type of contribution	Contribution to whole chapter
4.1 Influence of *Eggerthella lenta* on liver proteome and gut metabolome		
Theresa Streidl	Mouse experiment and sampling	20%
Beatrice Engelmann Sven-Bastiaan Haange	Metabolomics of colon content	10%
Kristin Schubert	Proteomics of liver tissue	10%
4.2 Comparison of gut physiology and metabolism in germfree and SPF mice on different diets		
Theresa Streidl	Help with mouse experiment and sampling	10%
Diana Möckel Ramona Brück Sarah Schraven	µCT scans of mice	10%
Nicole Treichel Ntana Kousetzi	DNA isolation and 16S rRNA gene amplicon sequencing of gut content	5%
Roman Bülow	Histological analysis	5%
4.3 Influence of *Collinsella aerofaciens* on lipid absorption		
Emily Richter	Isolation and analysis of bacterial strains	10%
Atscharah Panyot Esther Wortmann Susan Jennings	Help with mouse experiment and sampling	5%
Johannes Plagge Josef Ecker Sven Hermeling	Fatty acid measurements	15%
Nicole Treichel Ntana Kousetzi	DNA isolation and 16S rRNA gene amplicon sequencing of gut content	5%
4.4 Occurrence of lipase-positive bacteria in human stool from a population study		
Nicole Treichel Ntana Kousetzi	DNA isolation and 16S rRNA gene amplicon sequencing of gut content	10%
Johannes Masson	Lipase activity screening	5%
Caroline Schneider Thriveni Basavanapura	Help with statistical analysis	15%

Glossary

ACN	acetonitrile
AUC	area under the curve
BA	bile acid
BCAA	branched-chain amino acid
BHI	brain heart infusion
BMI	body mass index
BSH	bile salt hydrolase
C.A	*Collinsella aerofaciens*
CA	cholic acid
CD	control diet
CDCA	chenodeoxycholic acid
CFU	colony forming unit
Cgr2	cardiac glycoside reductase 2
CORIO	*Coriobacteriia* consortium (consisting of *Adlercreutzia mucosicola*, *Collinsella aerofaciens*, *Eggerthella lenta*, and *Lancefieldella parvula*)
DCA	deoxycholic acid
DNA	deoxyribonucleic acid
DTT	1,4-Dithiothreitol
FA	fatty acid
GF	germfree
HDL	high-density lipoprotein
HFD	high-fat diet
HSDH	hydroxysteroid dehydrogenases
IBD	inflammatory bowel disease
IVC	individually ventilated cage
LCA	lithocholic acid
LDL	low-density lipoprotein
MAG	metagenome-assembled genome
MCA	muricholic acid
MUFA	monounsaturated fatty acid
OGTT	oral glucose tolerance test
OMM	Oligo-Mouse-Microbiota
OTU	Operational Taxonomic Unit

PBS	Dulbecco's Phosphate Buffered Saline
PCA	principal component analysis
PUFA	polyunsaturated fatty acid
rRNA	ribosomal ribonucleic acid
SAFA	saturated fatty acid
SIHUMI	simplified human microbiota
SPF	specific pathogen-free
T2D	type 2 diabetes
UDCA	ursodeoxycholic acid
WAT	white adipose tissue
αMCA	*alpha*- muricholic acid
βMCA	*beta*-muricholic acid
µCT	micro computed tomography

Table of contents

1. Introduction

This PhD thesis investigated the interactions between specific bacteria from the human gut, the *Coriobacteriia*, and host metabolism in mice. Accordingly, this introduction provides background information about the gut microbiome, its influence on host health and especially metabolism, the processes underlying intestinal lipid metabolism, bacteria involved in lipid metabolism and those that play a role in regulating host metabolism in general, including species of the class *Coriobacteriia*.

1.1 The gut microbiome

A microbiome is a complex ecosystem comprising microbes, their genomes, and environmental factors (Marchesi *et al.* 2015). The microbes within a microbiome include bacteria, archaea, eukaryotic microorganisms, and viruses. The adult human body carries a similar number of prokaryotic cells as human eukaryotic cells, with approximately 4 x 10^{13} prokaryotic cells on average, which make up a mass of approximately 200 g (Sender *et al.* 2016). The majority of the prokaryotic cells are located in the intestine (Sender *et al.* 2016), and the majority of intestinal bacteria are anaerobic or facultative anaerobic species due to the low partial pressure of oxygen in the gut lumen (Donaldson *et al.* 2016). The most dominant bacterial phyla in the human gut are *Bacillota* (formerly *Firmicutes*) and *Bacteroidota* (formerly *Bacteroidetes*), but other phyla, including *Actinomycetota* (formerly *Actinobacteria*), *Pseudomonadota* (formerly *Proteobacteria*), *Fusobacteriota*, and *Verrucomicrobiota* also represent dominant populations (Arumugam *et al.* 2011; Eckburg *et al.* 2005). The composition and density of the microbial community varies along the length of the intestine. The small intestine harbours up to 10^7 cells/g, has a shorter transit time, is more acidic, is characterised by a higher partial pressure of oxygen and higher concentrations of antimicrobial molecules compared to the colon, which harbours approximately 10^{11} to 10^{12} cells/g (Marchesi 2011; O'Hara *et al.* 2006; Shalon *et al.* 2023). The phylum *Pseudomonadota* has a higher relative abundance in the small intestine, whereas *Actinomycetota*, *Bacteroidota*, and *Bacillota* have an increased relative abundance in stool (Shalon *et al.* 2023).

The following section summarises the methods that can be used to study the gut microbiome and its interaction with the host.

1.1.2 Analysis of the gut microbiome

Microbiome research began with cultivation-based methods, with substantial progress in the 1960s due to the advent of modern anaerobic techniques (Arank *et al.* 1969; Killgore *et al.* 1973). It was

already possible in the 1970s to identify over 100 distinct bacterial species and subspecies in faecal samples using anaerobic cultivation techniques (Moore *et al.* 1974). Cultivation is still a valuable tool in microbiome research, although a substantial fraction of the gut microbiota is still uncultured (Almeida *et al.* 2021; Thomas *et al.* 2019). In 1977, Woese *et al.* (1977) published a molecular method for the phylogenetic analysis of bacteria based on their 16S ribosomal ribonucleic acid (rRNA) sequence. The 16S rRNA gene is ubiquitous (i.e., present in all prokaryotes) and has both highly conserved, and hypervariable regions, that enable to distinguish different bacterial taxa. Several culture-independent techniques based on the 16S rRNA gene became available and have been used for decades (e.g., denaturing gradient gel electrophoresis, fluorescence *in situ* hybridisation, or Sanger sequencing of cloned 16S rRNA genes) (Dave *et al.* 2012). With the advent of next-generation sequencing technologies combined with advanced bioinformatics in the mid-2000s, it became possible to use high-throughput 16S rRNA gene amplicon sequencing for rapid profiling of prokaryotic taxa in complex samples at lower cost and higher resolution. Whilst 16S rRNA gene amplicon sequencing approaches target only one bacterial gene, shotgun sequencing (i.e., metagenomics) enables the analysis of entire genomes from the microorganisms in a sample. Shotgun sequencing facilitates the analysis of community composition at the strain level (Truong *et al.* 2017), and the analysis of the functional potential within microbial communities (Almeida *et al.* 2021; Quince *et al.* 2017). These high-throughput sequencing techniques have facilitated the investigation of the composition and function of hundreds to thousands of microbiomes. Large-scale sequencing projects (e.g., MetaHit, HMP) have provided important insights into the associations between microbiota composition and health and disease (Human Microbiome Project 2012; Qin *et al.* 2010). Although studies using next-generation sequencing techniques have been essential in providing important insights into microbiomes, the results are mainly descriptive, and the methods are prone to technical issues (Abellan-Schneyder *et al.* 2021; Reitmeier *et al.* 2021; Roume *et al.* 2023). For instance, sequencing-based studies erroneously proposed the existence of a microbiota in the placenta, which has been known to be a sterile organ (Blaser *et al.* 2021; Kennedy *et al.* 2023; Leiby *et al.* 2018; Panzer *et al.* 2023; Perez-Munoz *et al.* 2017).

Gnotobiotic mouse models can be used to test the causal role of microbiomes or simplified communities and to study the molecular mechanisms underlying microbe-host interactions under controlled conditions (Basic *et al.* 2019). The term gnotobiology is derived from the Greek words “gnotos”, meaning known, and “bios”, meaning life. Gnotobiotic animals include germfree (GF) animals and animals that are colonised with defined microorganisms. The first GF animals were created in the 1890s by George H. F. Nuttall and Hans Thierfelder, who delivered GF guinea pigs by Cesarina section and fed them sterile milk and feed (Nuttall *et al.* 1896). GF mice have been available since 1954 (Basic *et al.* 2019; Pleasants 1959). Gnotobiotic mice can be maintained and bred in positive pressure

isolators, which provide a closed and sterile environment (Trexler *et al.* 1957). Alternatively, for short-term experiments, mice can be housed in airtight, individually ventilated cages with air filters, which can be opened under biosafety cabinets for mouse handling (e.g., the IsoCage P system from Techniplast) (Basic *et al.* 2019). GF mice show multiple physiological changes compared to normally colonised mice. Among other effects, their caecum is enlarged (Schaedler *et al.* 1965) and the development of the immune system is affected by the lack of microbial stimulation (Round *et al.* 2009). To study microbe-host interactions, GF mice can be monocolonised with a specific bacterium of interest. Such a simplified model allows to study how the bacterium affects the host. Mice can also be colonised with simplified microbial consortia (Basic *et al.* 2019; Jennings *et al.* 2024). These mice can be more like complex colonised mice, but still have a reduced complexity and all members of the microbiome are known. An example of a simplified microbial consortium is the Oligo-Mouse-Microbiota (OMM) consortium, consisting of 12 strains representing members of the major bacterial phyla in the mouse gut. The OMM12 consortium has been shown to provide partial colonisation resistance against the pathogen *Salmonella enterica* serovar Typhimurium in mice (Brugiroux *et al.* 2016). Moreover, GF mice can be colonised with complex microbiota such as faecal samples from humans or rodents. Several studies have used this method to show that disease phenotypes can be transmitted via the transfer of the microbial communities (Ridaura *et al.* 2013; Routy *et al.* 2018; Schaubeck *et al.* 2016). The influence of gut microbes on the health of their host is discussed in more detail in the following section.

1.1.2 Influence of the gut microbiome on host health

The gut microbiome interacts with the immune system and with metabolic and other physiological processes. It thereby plays a critical role not only in maintaining health, but also in contributing to disease development when imbalanced (de Vos *et al.* 2022; Lynch *et al.* 2016). In a healthy state, gut microbes fulfil important functions such as the fermentation of food compounds, the production of vitamins, protection against pathogens, and stimulation of the immune system (Hillman *et al.* 2017). The gut microbiome has been found to play a role in various diseases such as irritable bowel syndrome, inflammatory bowel disease (IBD), colorectal cancer, obesity, type 2 diabetes (T2D), non-alcoholic fatty liver disease, cardiovascular diseases, and neurological disorders (de Vos *et al.* 2022; Hills *et al.* 2019; Nesci *et al.* 2023). The influence of the microbiome can be mediated by microbial components such as lipopolysaccharides and metabolites such as short-chain fatty acids, BAs or neurotransmitters that can interact with host receptors (Cani 2018; de Vos *et al.* 2022). Although numerous descriptive studies have supported the relationship between gut microbiome composition and disease, there is no definitive disease-specific consensus on microbial shifts. This is partly due to the enormous complexity and inter-individual variability of the gut microbiome. Evidence from intervention studies in

gnotobiotic animal models and humans strongly suggests that the microbiome plays a causal role in several diseases. It is now important for current research to focus on identification of specific microbial molecules and description of the underlying mechanisms. Elucidating these details will be crucial to translating associative findings into targeted strategies for disease prevention or treatment.

Considerable research has been dedicated to the role of the microbiome in the development of metabolic diseases such as obesity and diabetes. For example, it has been observed that individuals with a low gut bacterial gene count are characterised by greater overall adiposity, insulin resistance, and dyslipidaemia (Le Chatelier *et al.* 2013). The following section provides a more detailed review of the interactions between the gut microbiome and host metabolism.

1.1.3 Gut microbiome and host metabolism

The relationship between the gut microbiome and host metabolic health has been extensively studied. Several human studies have linked changes in the gut microbiota to T2D and obesity. For example, Qin *et al.* (2012) analysed faecal metagenomes from 345 Chinese individuals to identify markers associated with T2D, including a decrease in butyrate-producing bacteria, an increase in both, opportunistic species within the family *Enterobacteriaceae* and microbial functions related to sulphate reduction and oxidative stress resistance. Karlsson *et al.* (2013) studied faecal metagenomes in 145 European women with T2D, impaired or normal glucose tolerance. They observed compositional and functional changes in women with T2D, but also emphasised that predictive tools should be population-specific due to confounding effects of age and geographical location. However, the data of these two studies was confounded by metformin intake (Forslund *et al.* 2015). Pedersen *et al.* (2016) investigated the faecal microbiome and serum metabolome in 277 non-diabetic Danish individuals. They observed increased levels of branched-chain amino acids (BCAAs) in serum and an enriched biosynthetic potential for BCAAs in the microbiome. *Segatella copri* (formerly *Prevotella copri*) and *Phocaeicola vulgatus* (formerly *Bacteroides vulgatus*) were identified as the main species responsible for the association between BCAA biosynthesis and insulin resistance. Wu *et al.* (2020) studied the microbiota profiles of nearly 1,500 Swedish individuals naive for antidiabetic treatment. They found that changes in the overall gut microbiota profiles were associated with insulin resistance, but not with fasting glucose. In particular, the occurrence of several butyrate-producing bacteria was reduced in both the prediabetes and T2D groups.

A lot of research has also found associations between human gut microbiome and obesity. For instance, Ley *et al.* (2006) observed that the relative abundance of the phylum *Bacteroidota* (formerly *Bacteroidetes*) was decreased, whereas the relative abundance of *Bacillota* (formerly *Firmicutes*) was increased in obese compared to lean subjects. When the obese subjects were placed on a calorie-

restricted diet for one year and lost weight, the relative abundance of *Bacteroidota* increased. Since then, the "Firmicutes/Bacteroidetes ratio" has often been referred to as a marker of obesity. However, the aforementioned results are based on an analysis of only 12 subjects. Moreover, several studies have demonstrated that this finding is inconsistent across human studies (Sze *et al.* 2016; Tims *et al.* 2013; Walker *et al.* 2023; Walters *et al.* 2014; Yun *et al.* 2017). Turnbaugh *et al.* (2009) analysed the faecal microbiome of 154 individuals, including adult female monozygotic and dizygotic twin pairs concordant for leanness or obesity, as well as their mothers. They identified associations between obesity and a lower diversity, a decreased relative abundance of *Actinomycetota* (formerly *Actinobacteria*), and an increased relative abundance of *Bacteroidota*. Fu *et al.* (2015) examined the microbiota profiles of participants of the Dutch population cohort LifeLines-DEEP (n = 893) and identified several bacterial taxa associated with changes in body mass index (BMI) and the blood lipids high-density lipoprotein (HDL) and triglycerides. For example, members of the genus *Eggerthella* were associated with increased triglyceride and decreased HDL levels in blood. Nevertheless, these studies only describe associations and did not analyse causality (studies that tested causality are summarised at the end of this section).

Several studies have also compared GF and colonised animals to investigate the relationship between gut microbiota on host metabolism. Velagapudi *et al.* (2010) conducted a comparative analysis of the metabolome in serum and lipidome in serum, adipose tissue, and liver from GF and conventionalised mice. They found increased levels of metabolites involved in energy metabolism (e.g., pyruvic acid) and decreased levels of cholesterol and FAs in the serum metabolome of conventionalised mice. Lipidome analysis revealed decreased triglyceride levels in the serum but an increase in adipose tissue and liver of conventionalised mice compared to GF mice. Martinez-Guryn *et al.* (2018) observed an impaired lipid digestion and absorption in GF compared to SPF mice. Studies using gnotobiotic zebrafish have also shown that microbiota play a key role in lipid absorption and metabolism. Semova *et al.* (2012) observed enhanced FA uptake and lipid storage in enterocytes and hepatocytes in conventionalised compared to GF zebrafish. Similarly, Sheng *et al.* (2018) found increased lipid accumulation and altered expression pattern of genes associated with lipid metabolism in the intestinal epithelium of conventionalised zebrafish when compared with GF and antibiotic-treaded zebrafish.

Not only does the presence of the microbiota affect host lipid metabolism, but several studies have also shown that diet plays an important role in this relationship. Several studies have found that GF mice can be protected from diet-induced obesity (Bäckhed *et al.* 2007; Just *et al.* 2018; Martinez-Guryn *et al.* 2018; Rabot *et al.* 2010), but this phenotype depends on the type of diet used (Fleissner *et al.* 2010; Kübeck *et al.* 2016). Rabot *et al.* (2010) observed that GF mice fed a lard-based high fat diet had

lower body weight, excreted more lipids in their faeces and showed improved glucose tolerance and insulin sensitivity, as well as decreased plasma total cholesterol levels compared to conventionalised mice. In the study by Bäckhed *et al.* (2007), GF mice fed a Western diet high in fat (beef tallow) and sucrose GF gained significantly less body weight compared to conventionalised mice. Fleissner *et al.* (2010) were able to reproduce these results using the same Western diet with beef tallow, but when using a coconut oil-based HFD, the GF mice gained as much or even more body weight and fat than the conventionalised mice. Kübeck *et al.* (2016) found that mice fed a cholesterol-rich, lard-based HFD were protected from diet-induced obesity, whereas mice fed a cholesterol-free, palm oil-based HFD were susceptible.

To further investigate the relationship between intestinal microbiota, obesity and metabolism, various studies have transplanted obesity-associated microbiota into GF mice. In contrast to the studies mentioned above, this approach enables the investigation of causality, albeit with some limitations: for example, the microbiota composition is altered due to the transfer from human to rodents, which is often not analysed; the number of used human donors is usually very low; changes in the phenotype of recipient mice may be statistically significant but their amplitude marginal (Walter *et al.* 2020). In a study by Turnbaugh *et al.* (2006), caecal microbiota from obese mice homozygous for a mutation in the leptin gene and wild type lean control mice were used to colonise GF mice. Transplantation of the obesity-associated microbiota resulted in a significantly greater increase in body fat (+47% vs. +27%) over a two-week period. Martinez-Guryn *et al.* (2018) colonised GF mice with jejunal microbiota from conventional mice fed either a high-fat or low-fat diet. The mice transplanted with the HFD microbiota showed increased absorption of radiolabelled lipids compared to the mice transplanted with the low-fat microbiota, regardless of whether they were maintained on a low- or high-fat diet. Ridaura *et al.* (2013) transplanted human faecal microbiota from twins discordant for obesity into GF mice fed a low-fat diet. The transplantation of faecal material, as well as a culture collection obtained from faeces of the obese twin led to an increased body and fat mass in the mice. Cohousing of mice transplanted with the faecal microbiota from the obese and lean twins prevented the increased body and fat mass gain.

In summary, the gut microbiome is known to play a causal role in modulating host metabolism and the response to HFDs, but the underlying mechanisms remain unclear. Currently, only a limited number of bacteria with causal effects on host metabolism are known (see section **1.3**), and further research is necessary to gain a deeper understanding. The following section focuses on lipid digestion and absorption in the intestine, which is one specific aspect of lipid metabolism that can be affected by microbiota.

1.2 Intestinal lipid digestion and absorption

The main dietary fats consumed by humans are triglycerides, cholesterol esters, and phospholipids (Hussain 2014). In addition, endogenous lipids from the bile or shed enterocytes are present in the gut (Ko *et al.* 2020; Shiau *et al.* 1985). Lipid digestion begins in the mouth and stomach but mainly occurs in the small intestine. Small intestinal lipid digestion, absorption and transport via chylomicrons is summarised in **Figure 1.** The first step is the emulsification of large fat droplets by BAs, which increases the water-lipid surface area, making the lipids more accessible to enzymes produced in the pancreas and secreted into the duodenum (Ko *et al.* 2020; Senior 1964). Triglycerides are then hydrolysed by pancreatic lipases, releasing free FAs, monoacylglycerol, and glycerol (Winkler *et al.* 1990). Phospholipids are hydrolysed by the pancreatic enzyme phospholipase A2 to lysophospholipids and free FAs, whilst cholesteryl esters are hydrolysed by carboxyl ester hydrolase yielding cholesterol and free FAs (Ko *et al.* 2020). Together with BAs the hydrolysed lipids form smaller mixed micelles, which can diffuse to the brush border of the enterocytes. FAs and monoacylglycerols can be taken up into the enterocytes either by passive diffusion across the apical membrane or by protein-mediated transport (Chow *et al.* 1979; Iqbal *et al.* 2009; Mansbach *et al.* 2007). Cluster of differentiation 36 (CD36) is a key protein involved in the import of FAs into enterocytes (Ko *et al.* 2020). Along the intestine, it is mainly expressed in the proximal part of the small intestine (Lobo *et al.* 2001; Nassir *et al.* 2007). The uptake of cholesterol from the intestinal lumen into enterocytes is mediated by Niemann-Pick C1-like 1 (NPC1L1) protein (Altmann *et al.* 2004). Inside the endoplasmic reticulum of enterocytes, FAs, monoacylglycerol, lysophospholipids, and cholesterol are then re-esterified to triglycerides, cholesterol esters, and phospholipids by a variety of enzymes (Hussain 2014; Ko *et al.* 2020). The lipid molecules are then either packaged into chylomicrons for excretion, used in FA oxidation, or stored in cytosolic lipid droplets. Cytosolic lipid droplets consist of a core of neutral lipids (mainly triglycerides and cholesterol esters) surrounded by a phospholipid monolayer and are mobilised in fasting state (Demignot *et al.* 2014; Martin *et al.* 2006). Chylomicrons are large lipoproteins which transport dietary lipids to various tissues. Their core mainly consists of triglycerides and cholesterol esters and is surrounded by a phospholipid monolayer and specific proteins, including apolipoprotein B-48, which is essential for chylomicrons (van Greevenbroek *et al.* 1998; Zilversmit 1968). Pre-chylomicrons formation begins in the endoplasmic reticulum and the final modification and maturation occurs in the Golgi apparatus before the chylomicrons are packaged into versicles and secreted by exocytosis at the basolateral membrane of the enterocytes (Ko *et al.* 2020; van Greevenbroek *et al.* 1998). The chylomicrons then enter the lacteal and lymphatic system and are transported to various organs and tissues. Whereas triglycerides are exclusively secreted via the chylomicron pathway, cholesterol can also be secreted via the HDL pathway (Hussain 2014).

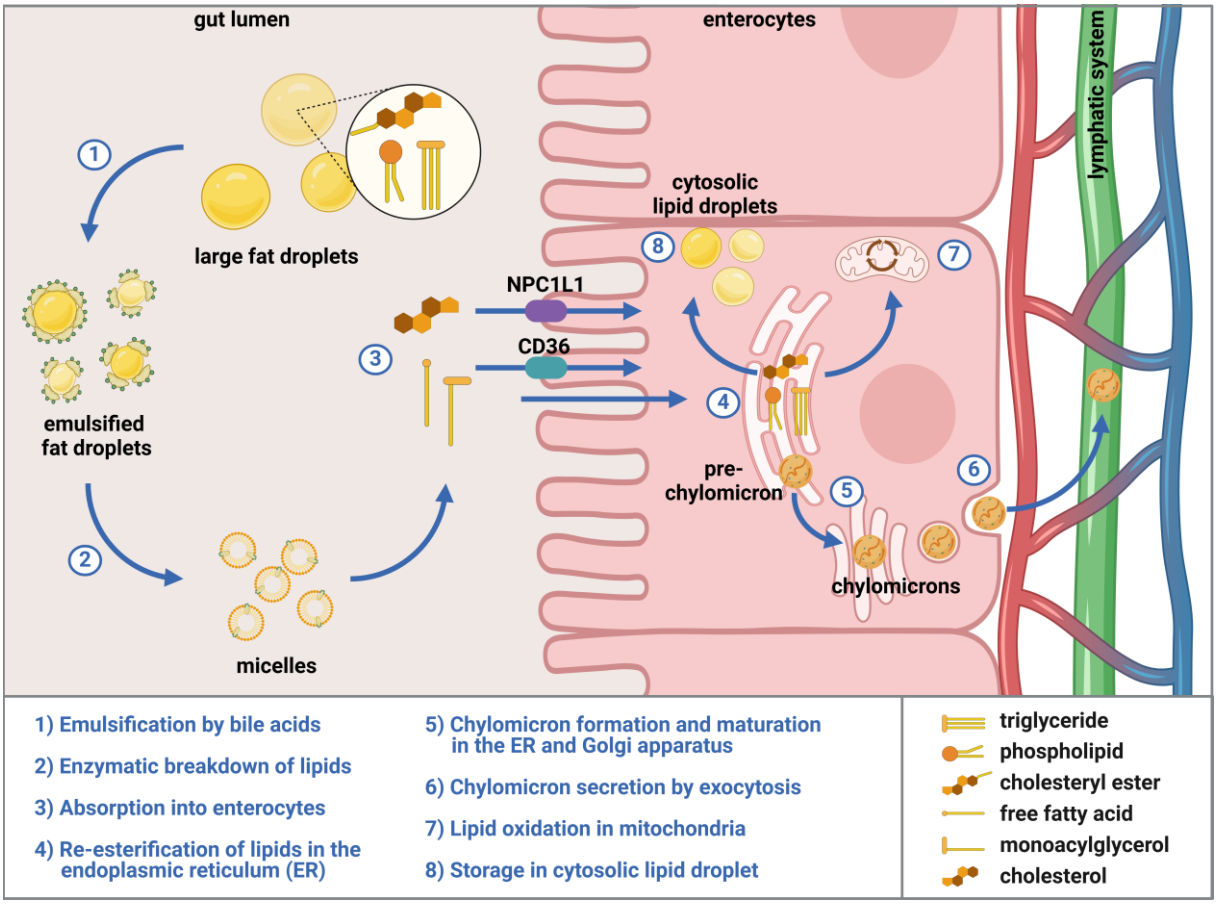

Figure 1: Summary of lipid digestion, absorption, and transport by chylomicrons in the small intestine. Created in https://BioRender.com

As previously stated above in section **1.1.3**, several studies have demonstrated that the gut microbiota plays a role in regulating host metabolism and the response to HFDs. However, the underlying mechanisms remain unclear, and further research is required to identify specific bacteria that causally affect lipid absorption. A common argument against the influence of bacteria on lipid absorption is that lipids are efficiently absorbed in the proximal small intestine, where bacterial density and diversity are low. However, it has been shown that faecal fat excretion increases as dietary lipid amounts increase (Booth *et al.* 1961; Cummings *et al.* 1978; Kasper 1970; Walker *et al.* 1973). Some studies even suggested that lipid absorption can take place in more distal parts of the intestine. Snipes (1977) observed lipid droplets inside the enterocytes of the caecum and colon of mice after force feeding with large amounts of fat (0.5-1.0 ml three times daily), although, the subsequent processing of fat was observed to be way less efficient than in the proximal small intestine. Booth *et al.* (1961) showed that, when rats were gavage with an increasing amount of radioactively labelled triolein (up to 500 mg), the percentage of absorption from the ileum and/or colon increased to up to 16% of the administered dose. Ammon *et al.* (1973) perfused the colon of 9 healthy human volunteers with electrolyte solutions with C18 FAs and observed that 350-400 mg FAs per hour were absorbed on average in the colon.

Although more research is required, some bacteria that can affect lipid absorption have already been identified. Wu *et al.* (2024) observed that *Megamonas rupellensis* colonisation in mice promoted HFD-induced obesity through enhanced lipid transport and absorption, particularly in the jejunum. They confirmed that *M. rupellensis* degrades myo-inositol *in vitro* and *in vivo*, which leads to an increase in lipid transport and absorption. Araujo *et al.* (2020) used *in vitro* and *in vivo* murine models and bacterial mutants to discover that acetate produced by *Escherichia coli* promotes FA oxidation in the enterocytes, and L-lactate produced by *Lactobacillus paracasei* inhibits lipid oxidation and therefore increases cytosolic lipid droplet size and amount in enterocytes.

In summary, while the proximal small intestine is the primary site for lipid digestion and absorption, some evidence suggests that microbial metabolic activities, including those in distal regions of the gut, may modulate this process in ways that are not yet fully understood. One way in which bacteria can affect lipid absorption is through the conversion of BAs, a process described in more detail in the following section.

1.2.1 Bile Acids

BAs play a crucial role in the emulsification and absorption of lipids and fat-soluble vitamins. Furthermore, they serve as important signalling molecules that regulate lipid and glucose metabolism and immune signalling (Collins *et al.* 2023). For instance, BAs engage with nuclear receptors such as nuclear farnesoid X receptor (FXR) and transmembrane receptors such as G protein-coupled membrane receptor 5 (TGR5), which play a key role in the regulation of metabolic pathways (Wahlstrom *et al.* 2016).

Primary BAs are synthesised from cholesterol in hepatocytes (Russell 2003): cholic acid (CA) and chenodeoxycholic acid (CDCA) in the human liver; a greater diversity, including alpha-muricholic acid (αMCA), beta-muricholic acid (βMCA) and ursodeoxycholic acid (UDCA) in the mouse liver (Honda *et al.* 2020; Sayin *et al.* 2013). BAs are conjugated to the amino acids taurine and glycine to enhance their hydrophilicity. The ratio of glycine- to taurine-conjugated BAs in humans is approximately three to one, whereas in mice, BAs are predominantly conjugated to taurine (Collins *et al.* 2023). Conjugated BAs are then stored in the gallbladder and are released into the duodenum upon stimulation by a meal (Collins *et al.* 2023). Approximately 95% of the BAs in the in the small intestine are reabsorbed before reaching the terminal ileum (Perino *et al.* 2021; Ridlon *et al.* 2006). The reabsorbed BAs are transported back to the liver via the hepatic portal vein, a process known as enterohepatic circulation. The remaining 5% enter the colon and are excreted within stool.

The BAs in the small intestine and those escaping the enterohepatic circulation in more distal regions can be metabolised by bacterial enzymes. In a first step, the BAs are deconjugated through the activity of bile salt hydrolases (BSHs). BSH is widespread across all major bacterial phyla within the human gut microbiota, however, the substrate specificity, genetic regulation, and occurrence of isoforms varies drastically between strains (Collins *et al.* 2023; Ridlon *et al.* 2006). The benefit of BA deconjugation for the bacteria is not clear and multiple hypothesis exist. Glycine and taurine can potentially be used as nutrient source, or the change in microbiota profiles due to the higher toxicity of the deconjugated BAs could be beneficial to BSH-expressing species (Guzior *et al.* 2021; Ridlon *et al.* 2006). The deconjugation to free primary BAs enables further metabolism to secondary BAs. Several intestinal bacterial species express hydroxysteroid dehydrogenases (HSDHs), which are position-specific and stereo-specific enzymes responsible for the oxidation and epimerisation of the C3-, C7- and C12-hydroxyl groups of BAs (Guzior *et al.* 2021; Ridlon *et al.* 2006). Both α- and β-HSDH are required for the epimerisation of BAs. For example, the oxidation of CA to the stable intermediate 7-oxoDCA via 7α-HSDH can be followed by the reduction to 7-epiCA via 7β-HSDH. HSDHs are widespread throughout the gut microbiome. Lucas *et al.* (2021) found that more than half of 70 common human intestinal bacterial species tested possessed HSDH activity. The advantage of BA dehydrogenation for the bacteria may be the reduced hydrophobicity and toxicity, or it may be useful for energy production (Ridlon *et al.* 2006). Furthermore, primary BAs can be metabolised by bacteria via dehydroxylation at the C7 position. Several enzymes encoded in the *bai* operon are responsible for this modification. CA can be metabolised to deoxycholic acid (DCA), CDCA to lithocholic acid (LCA), and muricholic acid (MCA) to murideoxcholic acid (MDCA) (Collins *et al.* 2023). Compared to HSDHs, the *bai* operon is less widespread among bacterial species of the human microbiome. Vital *et al.* (2019) conducted a metagenomic analysis of two datasets and found that MAGs exhibiting the *bai* gene accounted for 0.51–0.73% of the total MAGs present in stool samples. In 2020, it was discovered that BAs also can be re-conjugated to amino acids by microbial enzymes (Quinn *et al.* 2020). Lucas *et al.* (2021) demonstrated that these microbial bile salt conjugates can be formed from both primary and secondary BAs and 15 different amino acids. They found that 28 of the 70 common human intestinal bacterial species tested were able to produce microbial bile salt conjugates, especially members of the families *Bifidobacteriaceae*, *Lachnospiraceae*, and *Bacteroidaceae*. The reason for the re-conjugation of BAs by bacteria remains unclear; potential explanations include the export of toxic intracellular BAs, specific roles in bacterial metabolism, or the production of BA metabolites that harm other bacteria and provide a growth advantage (Ay *et al.* 2022). The chemical transformation of BAs by bacteria alters their solubility, toxicity, and signalling functions, impacting their role in lipid and glucose metabolism, as well as immune regulation. For example, Paik *et al.* (2022) discovered that the secondary BAs 3-oxoLCA and isoLCA inhibit the differentiation of pro-inflammatory T helper 17 cells, which play a key

role in IBD. Lynch *et al.* (2023) found that the heterologous expression of *Turicibacter* BSH genes in *Bacteroides thetaiotaomicron* was sufficient to alter host lipid metabolism in monocolonised mice, including decreased serum triglycerides and WAT mass. Similarly, Joyce *et al.* (2014) found that colonisation of GF mice with *Escherichia coli* heterologously expressing *Lactobacillus salivarius* BSH genes altered gene expression of key regulators of lipid metabolism in the ileum and liver.

Besides the influence of gut microbes on the BA pool, BAs can influence the composition, diversity, and metabolic activity of the gut microbiota (Collins *et al.* 2023). Due to their amphiphilic structure, BAs can be toxic to bacteria. Antimicrobial toxicity increases with increasing hydrophobicity and free BAs are generally more toxic than their conjugated counterparts (Sannasiddappa *et al.* 2017; Sung *et al.* 1993; Tian *et al.* 2020). Gram-negative bacteria and bacteria expressing BA-modifying enzymes and BA exporters show greater tolerance towards BAs (Collins *et al.* 2023). For example, Pedersen *et al.* (2022) found that co-cultivation with *E. lenta* alleviated the CA and CDCA-induced growth inhibition of strains such as *Thomasclavelia ramosa* (formerly *Clostridium ramosum*), probably due to the formation of oxidised and epimerised BAs by *E. lenta*.

In summary, BAs play a crucial role in lipid absorption, metabolic signalling, and immune regulation and their composition and function are significantly influenced by microbial transformations, which include deconjugation, oxidation and epimerisation, 7α-dehydroxylation, and re-conjugation. These modifications impact BA toxicity, solubility, and signalling functions, and consequently shape host metabolism and gut microbiota composition. Beyond the critical role of BAs in lipid absorption, microbial lipases may also contribute to the digestion and absorption of lipids in the gut. The next section reviews the influence of microbial lipases on lipid digestion and absorption.

1.2.2 Influence of microbial lipases

Lipases are serine hydrolases that catalyse the hydrolysis of triglycerides into glycerol and FAs by acting at the oil-water interface. Microbial lipases are expressed by bacteria, fungi and yeasts and are used in various industries (e.g., detergents, biofuels, food) and for environmental applications (Javed *et al.* 2018; Kanmani *et al.* 2015). Lipase-expressing bacteria are widespread in the human gut microbiome. Hoyles (2009) screened approximately 4,000 isolates from the stool of 15 human donors and identified 378 strains with lipase activity, representing 0.1% to 18.5% of the total isolates per donor. An analysis of metagenome-assembled genomes (MAGs) from different human body sites showed that the majority (75%) of lipase-positive species originated from stool samples and belonged to the dominant phyla of the human gut microbiome (Hitch *et al.* 2020).

The role of bacterial lipases in the digestion and absorption of fat in the gut is not well understood, although some studies have suggested that they play a role. Feeding lipase isolated from *Burkholderia*

plantarii to dogs with pancreatic duct ligation resulted in increased absorption of dietary lipids (Suzuki *et al.* 1999; Suzuki *et al.* 1997). In addition, Drouault *et al.* (2002) found that the consumption of *Lactococcus lactis* heterologously expressing lipase from *Staphylococcus hyicus* increased lipid absorption in pigs with pancreatic duct ligation. Ran *et al.* (2015) found that supplementation with *Acinetobacter* lipase resulted in increased weight gain of carp fed a diet rich in palm oil. In addition to bacterial lipases, lipases expressed by other gut microbes, such as yeast, have been found to influence lipid metabolism: Feng *et al.* (2022) identified the high lipase-expressing yeast strain *Trichosporon asahii* Y2 which, when fed to SPF mice, increased intestinal lipase activity and exacerbated HFD-induced obesity and hyperlipidaemia.

Microbial expression of lipase may confer benefits such as enhanced nutrient acquisition and modulation of microbial composition and can play a role in pathogenesis. Some bacteria, such as species of the genera *Bilophila* and *Alistipes,* can utilise the released FAs for growth (Agans *et al.* 2018). Many bacteria may also be able to use the released glycerol as carbon and energy source (da Silva *et al.* 2009). Hitch *et al.* (2020) reported a higher fraction of lipase-positive species that contained the genes for the glycerol degradation pathway II compared with the *beta*-oxidation pathway. Some bacteria can also metabolise glycerol to acrolein, an antimicrobial compound and toxin that can alter microbial composition (Cleusix *et al.* 2007; Ramirez Garcia *et al.* 2021; Zhang, Sturla*, et al.* 2018). Furthermore, bacterial lipases can act as virulence factors and play a role in pathogenesis (Chen *et al.* 2019; Ghadimi *et al.* 2024).

In summary, the specific contributions of microbial lipases to lipid digestion and absorption in the gut remain poorly understood. While evidence from a few animal models indicates that microbial lipases may influence lipid absorption and metabolism, particularly in combination with a HFD, further research is needed to gain a deeper understanding.

1.3 Bacteria with a causal impact on host metabolism

While many studies investigating the influence of bacteria on host metabolism have found associations between the occurrence of certain bacteria and changes in host metabolism, only a few specific bacterial species with causal effects are known. Some bacterial species with known causal effects on host metabolism are described below and summarised in **Table 2.**

Akkermansia muciniphila has been shown to have beneficial effects on metabolic health by modulating various physiological processes (Ioannou *et al.* 2024). For instance, Plovier *et al.* (2017) showed that the administration of pasteurised *A. muciniphila* reduced fat mass, insulin resistance and dyslipidaemia, and improved intestinal barrier function in mice fed a HFD. This was due to the outer

membrane protein Amuc_1100, which interacts with Toll-Like Receptor 2. In addition, *A. muciniphila* was found to secrete another protein, P9, which induces GLP-1 secretion and increases thermogenesis in brown adipose tissue (Yoon *et al.* 2021). Another specific bacterium is the probiotic strain *Lactobacillus rhamnosus* GG, which was shown to compete with the host for FA absorption in the gut, resulting in reduced body weight, fat mass and lipid accumulation in the liver in mice (Jang *et al.* 2019). In contrast, one example of a potentially detrimental species in terms of host metabolism is *T. ramosa*, which enhanced diet-induced obesity in gnotobiotic mice (Woting *et al.* 2014). This was linked to elevated levels of glucose transporter 2 (Glut2) and FA translocase (CD36), leading to increased nutrient absorption. Using monocolonised mice, cell lines and organoids, Mandic *et al.* (2019) further showed that *T. ramosa* can stimulate serotonin secretion from intestinal enterochromaffin cells, leading to increased intestinal lipid absorption. Monocolonisation of mice with *Enterobacter cloacae* has also been shown to enhance HFD-induced obesity in mice, including elevated serum endotoxin levels and increased systemic inflammation (Fei *et al.* 2013). In addition, Yan *et al.* (2016) found that *E. cloacae* monocolonisation of mice on a HFD altered gene expression in colon tissue related to inflammation and metabolism. Finally, Chen *et al.* (2021) discovered that colonisation of GF mice with *S. copri* induced chronic inflammation via TLR4 and mTOR pathways and promoted fat accumulation by upregulating lipogenesis genes and downregulating genes associated with lipolysis, lipid transport and muscle growth.

Table 2: Overview of bacteria with a causal impact on host metabolism. This table summarises the observed impacts on the host, and key findings and mechanisms for each described bacterial species.

Bacterium	Impact on host	Key findings and mechanisms	Literature
A. muciniphila	- reduction in body fat - improved insulin resistance - reduced dyslipidaemia - improved intestinal barrier function	- surface protein Amuc_1100 interacts with TLR2 - secretion of protein P9 enhances GLP-1 secretion and promotes thermogenesis in brown adipose tissue	Ioannou *et al.* (2024) Plovier *et al.* (2017) Yoon *et al.* (2021)
***L. rhamnosus* GG**	- reduced body weight and fat mass -reduced hepatic lipid accumulation	- competition with the host for FA absorption in the gut	Jang *et al.* (2019)
T. ramosa	- enhanced HFD-induced obesity - increased absorption of nutrients and lipids	- increased expression of Glut2 and CD36 - stimulation of serotonin secretion from intestinal enterochromaffin cells	Mandic *et al.* (2019) Woting *et al.* (2014)
E. cloacae	- enhanced HFD-induced obesity - increased inflammatory processes	- elevated serum endotoxin levels - increased systemic inflammation markers - altered gene expression in colon tissue (inflammation and metabolism related)	Fei *et al.* (2013) Yan *et al.* (2016)
S. copri	- induced chronic inflammation - increased fat accumulation	- activation of TLR4 and mTOR signalling pathways - upregulation of lipogenesis genes - downregulation of genes involved in lipolysis, lipid transport and muscle growth	Chen *et al.* (2021)

However, *S. copri* is a good example of the importance of studying intra-species diversity, which can be observed in several bacterial species (Chen-Liaw *et al.* 2025). De Filippis *et al.* (2019) have shown how dietary habits can drive the selection of specific strains of *S. copri* with different functional potentials. Strains associated with an omnivorous diet had a higher prevalence of genes related to branched-chain amino acid biosynthesis, whilst those associated with a fibre-rich diet had an increased potential for carbohydrate catabolism. Sorbara *et al.* (2020) analysed the genomes of 273 isolates of the family *Lachnospiraceae* and also observed intra-species diversity in pathways that could potentially play a role in host health. Strain-level diversity, although relatively understudied, has the potential to explain discrepancies in associations between bacterial species and their impact on host metabolism.

In summary, despite some reports on specific bacteria with causal effects on host metabolism, there is no data on many commensal gut species. The following section focuses on the class of *Coriobacteriia*, whose presence has been associated with alterations in host metabolism.

1.4 *Coriobacteriia*

Coriobacteriia is a class of bacteria belonging to the phylum *Actinomycetota* (formerly *Actinobacteria*). Formerly, all members of the *Coriobacteriia* belonged to a single order (*Coriobacteriales*) and a single family (*Coriobacteriaceae*) (Gupta *et al.* 2013). After reclassification, the family *Coriobacteriaceae* was split into several families within the class *Coriobacteriia*, including *Atopobiaceae* and *Coriobacteriaceae*, both belonging to the order *Coriobacteriales*, and *Eggerthellaceae*, belonging to the class *Eggerthellales* (Gupta *et al.* 2013; Nouioui *et al.* 2018). *Coriobacteriia* are usually Gram-positive, non-motile, non-spore-forming, non-haemolytic, mesophilic bacteria that are typically shaped like rods or coccobacilli and grow as single cells, pairs, or chains (Clavel *et al.* 2014). Most *Coriobacteriia* are obligate anaerobes, but some species are also known to be aerotolerant, microaerophilic or facultative anaerobe (Clavel *et al.* 2009; Clavel *et al.* 2014; Kraatz *et al.* 2011; Rodriguez Jovita *et al.* 1999). *Actinomycetota*, including *Coriobacteriia*, are often underrepresented in 16S rRNA gene amplicon sequencing because of factors such as extraction methods and primer selection, which may be due to their hydrophobic cell walls and high G+C content of deoxyribonucleic acid (DNA) (Maukonen *et al.* 2012; Sim *et al.* 2012; Thorasin *et al.* 2015). Nonetheless, their presence and abundance has been linked to alterations in host metabolism in several studies with rodents and humans (described in the following paragraphs).

Several studies found increased relative abundance of *Coriobacteriia* associated with HFD feeding and obesity in rats and mice (Campbell *et al.* 2019; Chen *et al.* 2018; Feng *et al.* 2024; Lin *et al.* 2024; Park *et al.* 2020; Tang *et al.* 2024; Zhao *et al.* 2017). Furthermore, Claus *et al.* (2011) observed a strong correlation between *Coriobacteriaceae* (and *Coriobacteriales*), increased hepatic triglycerides and decreased hepatic glucose and glycogen levels in mice. Martinez *et al.* (2013) observed significant correlations between *Coriobacteriaceae* and host lipid metabolism in hamsters. The relative abundance of *Coriobacteriaceae* was associated with increased cholesterol absorption, plasma cholesterol, plasma triglycerides and liver cholesterol, and decreased cholesterol synthesis and liver triglycerides.

Studies in humans have also highlighted associations between the occurrence of *Coriobacteriia* and metabolic disorders such as obesity (Cancello *et al.* 2019; Nirmalkar *et al.* 2018; Zhang *et al.* 2009) or diabetes (Afolayan *et al.* 2020; Crusell *et al.* 2018; Doumatey *et al.* 2020; Lv *et al.* 2023). Romo-Vaquero *et al.* (2019) reported a positive correlation between *Coriobacteriaceae* and BMI, as well as total

cholesterol, low-density lipoprotein (LDL) and apolipoprotein A-1 blood levels (n = 249, healthy adult individuals). Similarly, Gallardo-Becerra *et al.* (2020) observed a positive correlation between the relative abundance of *Coriobacteriia* and BMI and blood triglycerides, while noting a negative correlation with blood HDL in a cohort of 27 children. Morales *et al.* (2022) found that *Actinomycetota* and *Coriobacteriaceae* had a significantly higher relative abundance in hypercholesterolemic individuals compared to controls (n = 57, adult individuals). Additionally, Castro-Mejia *et al.* (2022) reported that increased levels of total cholesterol and LDL was linked to higher relative abundances of *Coriobacteriaceae* (n = 262, adult individuals). However, it is important to note that some studies have reported conflicting results. For example, Kim *et al.* (2020) studied a cohort of overweight and obese adult individuals (n = 747), categorised into metabolically healthy and unhealthy groups, and found that *Coriobacteriaceae* were more prevalent in the metabolically healthy subgroup. Furthermore, Hu *et al.* (2021) observed a decreased relative abundance of *Coriobacteriaceae* in pregnant women with gestational diabetes mellitus (n = 402).

Collinsella aerofaciens and *Eggerthella lenta* are the two *Coriobacteriia* species that are the focus of this thesis and are described in more detail below. They are among the best-studied members of the bacterial class of *Coriobacteriia* and dominant and prevalent members of the human intestinal microbiome (Almeida *et al.* 2019; Qin *et al.* 2010).

Collinsella aerofaciens, formerly *Bacteroides aerofaciens* or *Eubacterium aerofaciens*, was first isolated from human faeces by Eggerth in 1935. The species is Gram-positive, non-flagellated, non-spore-forming, obligate anaerobic and the cells are typically rod to cocci shaped, variable in size (approximately 0.3-0.7 × 1.2-4.3 µm) and form chains (Eggerth 1935; Kageyama *et al.* 1999). *C. aerofaciens* has been shown to display *in vitro* lipase activity in the rhodamine B agar plate assay (Just 2017; Streidl 2021; Thorasin *et al.* 2015). In addition, the species is known to express BA-modifying enzymes, including BSH and 3α-, 7β- and 12α-HSDH (Liu *et al.* 2011; Lucas *et al.* 2021; Wegner *et al.* 2017). The experiments of Lucas *et al.* (2021) suggested that *C. aerofaciens* may also have 7α-HSDH activity and may be able to re-conjugate BAs with the amino acids glycine, alanine, phenylalanine, and leucine. The occurrence of *C. aerofaciens* has been associated with various diseases, including metabolic disorders. For example, Companys *et al.* (2021) reported that *C. aerofaciens* was more abundant in obese compared to lean individuals (n = 128). Gallardo-Becerra *et al.* (2020) observed that *C. aerofaciens* had a higher relative abundance in obese children with metabolic syndrome compared to normal weight and obese children without metabolic syndrome (n = 27). Notably, they also identified a significant positive correlation between the relative abundance of *C. aerofaciens* and blood triglyceride levels, in addition to a negative correlation with HDL. Liu *et al.* (2021) observed increased relative abundance of *C. aerofaciens* in children with type 1 diabetes (n = 98). Moreover, Purohit *et al.*

(2024) reported an increased relative abundance of *C. aerofaciens* in individuals with non-alcoholic fatty liver disease compared to healthy controls (n = 47).

Eggerthella lenta, formerly *Bacteroides lentus* or *Eubacterium lentum*, was also first isolated from human faeces by Eggerth in 1935. The bacterium is Gram-positive, non-flagellated, non-spore-forming, obligate anaerobic and the cells are rod-shaped, measuring approximately 0.2-0.4 × 0.2-2.0 µm in size and often form chains (Eggerth 1935; Wade *et al.* 1999). *E. lenta* strains are functionally very versatile. *E. lenta* is able to metabolise BAs via the enzymes BSH, and 3α-, 3β-, 7α- and 12α-HSDH (Harris *et al.* 2018; Ridlon *et al.* 2006; Wegner *et al.* 2017). Moreover, *E. lenta* strains are able to metabolise neurotransmitters (Maini Rekdal *et al.* 2020), hormones (Bokkenheuser *et al.* 1977; McCurry *et al.* 2024), drugs (Haiser *et al.* 2013; Maini Rekdal *et al.* 2019; Saha *et al.* 1983) and dietary phytochemicals (Bess *et al.* 2020; Clavel *et al.* 2006; Takagaki *et al.* 2015; Woting *et al.* 2010). Paik *et al.* (2022) showed that *E. lenta* is capable of metabolising the secondary BA LCA to 3-oxoLCA and isoLCA, which suppress T_H17 cell differentiation, a mechanism potentially relevant to the pathophysiology of IBD. However, Alexander *et al.* (2022) found that *E. lenta* activates T_H17 cells in gnotobiotic mice via the bacterial enzyme cardiac glycoside reductase 2 (Cgr2) and that dietary arginine supplementation prevents this inflammation induction due to Cgr2 sensitivity to this substrate. The relative abundance of *E. lenta* has also been associated with metabolic disorders. For example, Qin *et al.* (2012) analysed the gut metagenomes of 345 individuals and reported an enrichment of *E. lenta* in individuals with T2D, however, their results were confounded by metformin intake (Forslund *et al.* 2015). Also Koh *et al.* (2018) observed an increased relative abundance of *E. lenta* in individuals with T2D (n = 33) compared to controls (n = 43) and linked this to the ability of the species to produce imidazole.

In summary, the presence of *Coriobacteriia* has been associated with changes in lipid metabolism, obesity, and diabetes. Several studies suggest that alterations in the relative abundance of *Coriobacteriia* may be linked to metabolic dysregulation, although there are also conflicting results, and no underlying mechanisms have been reported yet.

A former PhD student from the lab studied the effect of a minimal consortium consisting of the four *Coriobacteriia* species *A. mucosicola*, *C. aerofaciens*, *E. lenta*, and *L. parvula* (CORIO) on host metabolism in gnotobiotic mice (Just 2017). The mice colonised with CORIO were compared to GF and SPF controls. They were fed with one of the following three experimental diets for a duration of 16 weeks: synthetic control diet (CD), palm oil-based HFD, or CD supplemented with primary BAs (0.1% CA and 0.1% CDCA). The colonisation of the CORIO mice in the different gut regions was examined by qPCR at the endpoint. All four CORIO strains were detected, though at rather low densities and inter-individual differences were observed. *C. aerofaciens* and *E. lenta* colonised at higher densities than the other two strains, and all strains tended to be more abundant in the proximal part of the intestine and in the HFD-fed mice. Independent of diet, CORIO mice showed elevated cholesterol levels in plasma.

Notably, the WAT mass increased twofold in CORIO mice fed the BA-supplemented diet, independent of the body weight. Additionally, the plasma levels of insulin and leptin, the leptin expression in WAT, and the hepatic triglyceride and total FA levels were increased in CORIO mice fed the BA diet. In addition to the literature aforementioned, these results from this gnotobiotic experiment indicate that *Coriobacteriia* play a causal role in host metabolism, which was the basis of this PhD thesis.

2. Hypothesis and aims of the thesis

In my PhD thesis I focus on the role of *Coriobacteriia*, because their occurrence has been linked to alterations in host metabolism in studies with rodents and humans. Furthermore, a previous gnotobiotic mouse experiment from the lab showed that colonisation with a consortium of four *Coriobacteriia* strains (CORIO) in combination with a diet supplemented with primary BAs resulted in increased WAT mass.

Here, we hypothesise that *Coriobacteriia*, in particular *E. lenta* and *C. aerofaciens,* which can deconjugate and dehydrogenate BAs and express lipases, have causal effects on host metabolism.

In the first part, I studied how colonisation of gnotobiotic OMM12 mice with *E. lenta* influences the liver proteome and gut metabolome.

In the second part, I aimed to investigate how colonisation with the CORIO consortium (*A. mucosicola, C. aerofaciens, E. lenta, L. parvula*) in combination with diets varying in fat content and primary BAs influences host metabolism. However, as colonisation of the intestine with the CORIO strains failed, GF and SPF mice fed the different diets were compared.

In the third part, I investigated whether specific colonisation of GF mice with *C. aerofaciens* in combination with diets high in fat or supplemented with primary BAs affects intestinal lipid absorption using stable isotope-labelled lipids.

In the fourth and final part, I assessed the potential clinical relevance of dominant lipase-positive bacteria, including *C. aerofaciens*, by analysing their occurrence in the stool microbiome of 338 participants from a human cohort in relation to host body parameters.

3. Material and Methods

In this part the technical and methodological background of the work performed during my PhD thesis and the contributions made by collaborators are described in detail. The first section describes the general handling procedure for anaerobic bacteria and the following sections (**3.2; 3.3; 3.4; 3.5**) present the different experiments that correspond to the main results sections.

3.1 Handling of anaerobic bacteria

In multiple parts of the project, anaerobic bacteria were used. Here I describe the general preparation of anaerobic culture media and the procedures used to grow bacteria under anaerobic conditions and to store them.

3.1.1 Media preparation

The Hungate technique was used for anaerobic liquid cultures (Hungate *et al.* 1966). For the preparation of media in Hungate tubes, all ingredients, except L-cysteine and 1,4-Dithiothreitol (DTT) (see concentrations below), were dissolved in deionised water and heated to 100°C to remove soluble oxygen. Afterwards, L-cysteine and DTT were added. Each Hungate tube was filled with the heated medium (9 ml), gassed with 89.3% N_2, 6% CO_2, and 4.7% H_2 for 3 min, and sealed with a rubber stopper and a screw cap. The Hungate tubes were then autoclaved (121°C, 20 min) and stored at room temperature.

For the preparation of solid media, 1.5% (w/v) agar was added. All ingredients, except L-cysteine, DTT and other heat-sensitive ingredients, such as rhodamine B, were dissolved in deionised water and autoclaved at 121°C for 20 min. After cooling down to approximately 55°C, heat-sensitive ingredients were added from filter-sterilised stock solutions. The medium was then poured into Petri dishes under a laminar flow cabinet to ensure sterility. The medium was left to stand for approx. 30 min to solidify and the plates were stored at 4°C. Before use for anaerobic cultivation, the plates were imported into the anaerobic chamber (MBraun; 89.3% N_2, 6% CO_2, 4.7% H_2) at least 24 h before starting the work.

Unless otherwise stated, all media for anaerobic cultivation were supplemented with 0.05% (w/v) L-cysteine and 0.02% (w/v) DDT as reducing agents, and 0.0001% (1 mg/L) resazurin as redox potential indicator.

3.1.2 Cultivation and storage

For anaerobic cultivation, the strains were either incubated on agar plates at 37°C in an anaerobic chamber (MBraun, Garching, Germany; 89.3% N_2, 6% CO_2, 4.7% H_2) or in broth in Hungate tubes. For subculturing outside the anaerobic chamber, the rubber stopper of the Hungate tubes was flamed twice using ethanol, and a sterile, gassed syringe was used to transfer bacterial suspensions from one tube to the other under a laminar flow cabinet. Depending on the experiment, Hungate tubes were inoculated in different ways: using freshly thawed cryo-stocks, existing liquid cultures, or cell material obtained from a single colony grown on agar plate. In the latter case, inoculation occurred within the anaerobic chamber by manually removing the stopper and screw cap.

For long time storage of bacterial strains, fresh liquid cultures were mixed 1:1 with sterile, anoxic medium containing 40% glycerol in a gassed syringe under a laminar flow cabinet. The mixture was aliquoted (ca. 500 µl) into screw cap tubes, then placed on dry ice and stored at -75°C.

3.1.3 Contributions

The general handling of anaerobic bacteria was done by myself. Student assistants (AG Clavel) helped with the preparation of media that were routinely used.

3.2 Influence of *Eggerthella lenta* on liver proteome and gut metabolome

In this chapter, samples from a previous gnotobiotic mouse experiment were analysed to study the effect of the *Coriobacteriia* species *E. lenta* on liver proteome and gut metabolome. The content of this chapter is already published under Viehof *et al.* (2024).

3.2.1 Gnotobiotic mouse experiment

The gnotobiotic mouse experiment was conducted by Theresa Streidl in the context of her own PhD thesis (Streidl 2021). The experiment was ethically approved by the local authority (Regierung von Oberbayern, approval no. 55.2-1-54-2532-156-2013) and was performed in the mouse facility of ZIEL - Institute for Food & Health at Technical University of Munich.

In brief, GF male C57BL/6N mice (n = 6-8 per group) were colonised with microbial suspensions containing the strains of the synthetic community OMM12 (Brugiroux *et al.* 2016) with or without the CORIO strains (*A. mucosicola* DSM 19490^T, *C. aerofaciens* DSM 3979^T, *E. lenta* DSM 2243^T, and *L. parvula* DSM 20469^T) via oral gavage three times within one week at the age of five weeks. From week eight onwards, the diet was changed from autoclaved standard chow to a semi-synthetic control diet (CD) for two weeks. Thereafter, the mice were fed either CD, CD supplemented with the primary BAs CA (0.1%) and (0.1%) CDCA (CD-BA), lard-based HFD with 48% energy from fat (HFD), or HFD supplemented with BAs CA (0.1%) and (0.1%) CDCA (HFD-BA) for eight weeks. Before euthanising the mice with CO_2, they were fasted for a minimum of 6 h and blood glucose was measured. During necropsy, systemic EDTA-plasma was obtained from vena cava and content of the caecum and colon, and liver lobes were snap frozen.

3.2.2 Metabolomics of colon content

Colon content was mixed with 5x acetonitrile (ACN):H2O solvent and 4 steel beads for subsequent extraction in the bead mill (10 min, 30 Hz). After centrifugation (14,000 rpm, 2 min), 100 µl of the supernatant were added to 500 µl MeOH:ACN:H2O (2:3:1) and vortexed thoroughly for 5 min. After sonication for 5 min, samples were centrifuged (14.000 rpm, 5 min), 550 µl were transferred to a new tube, evaporated to dryness (SpeedVac, Eppendorf) and kept at -80°C until further use. Prior to analysis, samples were resuspended in 100 µl 0.1% FA and 1% ACN in water. Samples measured in positive and negative ionisation mode were further diluted 1:10.

For measurement, 10 or 5 µl (positive and negative ionisation, respectively) of each extract was injected into a HPLC system coupled online with a 6546 UHD Accurate-Mass Q-TOF (Agilent

Technologies). Metabolites were separated with an Agilent Zorbax Eclipse Plus C18 column (2.1 x 100 mm, 1.8 µm) equipped with a matching pre-column (2.1 x 50 mm, 1.8 µm). The autosampler was kept at 5°C and column oven was set to 45°C. Separation was achieved using a binary solvent system of A (0.1% FA in water) and B (0.1% FA in ACN). The gradient was as follows: 0-5.5 min: 1% B; 5-20 min: 1-100% B; 20-22 min: 100% B; 22-22.5: 100-1% B; 22.5-25 min: 1% B. Metabolites were eluted at a constant flow rate of 0.3 ml/min with the autosampler at 5°C and column oven at 45°C. Eluted compounds were measured with the QTOF operated in centroid mode. Full scan data was generated with a scan range of 50-1000 m/z in both ionisation modes. Out of the survey scan, the 2 most abundant precursor ions with charge state = 1 were subjected to fragmentation. The dynamic exclusion time after two acquired spectra was set to 0.1 min.

The spectral data (.d files) were imported into the Progenesis QI software (Non-Linear Dynamics). The two ionisation modes were analysed separately. The adduct ions were [M+H] and [M+H-H2O] for positive mode and [M-H], [M-H2O-H] and [M+FA-H] for negative mode. Chromatograms were aligned using an automatically chosen reference chromatogram from the dataset. The following software-guided peak-picking tool resulted in a data matrix including retention time, mass-to-charge ratio, and corresponding normalised peak area. For the *in silico* database search, the Fecal Metabolome Database was used as resource. After exporting the results (compound measurement and putative identifications) for all measured compounds, the data was further processed by only keeping peaks which were putatively identified with an MS2 fragment spectrum and a minimum Progenesis score of 40. Only those annotations with the highest Progenesis score were kept if peaks were annotated to multiple compounds.

Principal component analysis (PCA) of metabolome peaks was done in R with significance of group differences calculated by PERMONOVA using the adonis2 function in the R package vegan (Oksanen *et al.* 2022). Differences in annotated metabolites were calculated by a Kruskal-Wallis test with correction for multiple testing by Benjamini-Hochberg method followed by posthoc Dunn-test for pairwise comparisons using R.

3.2.3 Proteomics of liver tissue

Proteins from liver samples were extracted by adding 800 µl ice-cold lysis buffer (150 mM NaCl, 10 mM Tris (pH 7.2), 0.1% SDS, 1% Triton X-100, 1% deoxycholate, 5 mM EDTA, pH 7.4, cOmplete™ protease inhibitor) to frozen samples, followed by bead milling (10 min, frequency 30) and 1 h incubation on ice. Lysates were centrifuged (12,000 rpm, 15 min, 4°C), supernatants were recovered, and protein concentration was determined by DC protein assay (BIO-RAD) according to the manufacturer's instructions.

For each sample, 20 µg protein lysate was used for sample preparation, as described previously (Wang *et al.* 2021). Briefly, proteins were reduced with tris(2-carboxyethyl)phosphine hydrochloride and alkylated with iodoacetamide. A protein clean-up was conducted using paramagnetic beads in 70% ethanol and ACN without acidification of the samples, as described previously (Wang *et al.* 2021). Proteins were then proteolytic cleaved using Trypsin (Promega) in a 1:50 ratio (trypsin:protein) for 16 h at 37°C. Next, samples were labelled using 5x tandem mass tags (TMT, TMT-10plex, Thermo Scientific) for 1 h at room temperature, followed by adding 1 µl 5% (v/v) hydroxylamine in 100 mM TEAB to quench the labelling. Samples were combined into 7 mixes, each containing 1 replicate of the different treatments. After peptide clean-up with 100% ACN, peptides were eluted in 2 fractions using 87% ACN in 10 mM ammonium formate (pH 10, Sigma Aldrich) for fraction 1 and 2% dimethylsulfoxide (Sigma Aldrich) for fraction 2.

LC–MS/MS analysis was then performed using an UltiMate 3000 RSLCnano system (Dionex), coupled online to a Q Exactive HF mass spectrometer (Thermo Fisher Scientific) by a chip-based electrospray ionisation source (TriVersa NanoMate, Advion), as previously described (Streidl *et al.* 2021; Wang *et al.* 2021). First, peptides were loaded on a trapping column with 5 µL/min by using 98% water / 2% ACN / 0.05% trifluoroacetic acid (Acclaim PepMap 100 C18, 3 µm, nanoViper, 75 µm x 5 cm, Thermo Fisher Scientific) and peptides were then separated on an analytical column (Acclaim PepMap 100 C18, 3 µm, nanoViper, 75 µm x 25 cm, Thermo Fisher). A 150 min non-linear gradient was applied starting from 0.1% formic acid in water to 80% ACN/ 0.08% formic acid in water. From each MS, the top 15 precursor ions were selected with an isolation window of 0.7 m/z.

MS raw data were processed against the *Mus musculus* UniProtKB reference proteome from 16th November 2021 using ProteomeDiscoverer 2.2 with carbamidomethylation. TMT set as fixed, and methionine oxidation and acetylation of protein N-terminus set as variable modifications. Reporter ion intensities were corrected according to the manufacturer's instructions. A total of 1,914 proteins were identified. Samples were normalised against a pool control containing a mixture of all samples included in each TMT mix. Samples were filtered for proteins quantified in at least four replicates per condition resulting in 1,710 proteins.

For proteomics, after log2-transformation, fold changes were calculated to the respective controls with adjusted p-values calculated with the Benjamini-Hochberg method. Proteins were considered significantly altered with an adjusted p-value ≤ 0.05. The analysis was conducted in R-3.5.0 using the following packages: mixOmics (Rohart *et al.* 2017), ggplot2 (Wickham 2016b), qpcR (Spiess 2018), corrplot (Wei *et al.* 2017), PerformanceAnalytics (Peterson *et al.* 2014), calibrate (Graffelman *et al.* 2005), dendsort (Sakai *et al.* 2014), dendextend (Galili 2015), ComplexHeatmap (Gu *et al.* 2016), limma (Ritchie *et al.* 2015), plyr (Wickham 2016a), reshape2 (Wickham 2007), xlsx (Dragulescu *et al.* 2018),

DEP (Zhang, Smits*, et al.* 2018), ggsci (Xiao 2018), ggpubr (Kassambara 2023), pheatmap (Kolde 2012), circlize (Gu *et al.* 2014).

3.2.4 Contributions

The gnotobiotic mouse experiment was conducted by Theresa Streidl in the context of her own PhD thesis (Streidl 2021). Proteomics and metabolomics measurements were performed at the Department of Molecular Systems Biology at Helmholtz Centre for Environmental Research (UFZ) in Leipzig, Germany. Sample preparation and metabolomics measurements were conducted by Beatrice Engelmann. Raw data processing and statistical analysis of this data was conducted by Sven-Bastiaan Haange. Proteomics measurement and raw data processing was done by Kristin Schubert. I performed all downstream data analysis and statistics, interpreted the data, and wrote the manuscript.

3.3 Comparison of gut physiology and metabolism in germfree and SPF mice on different diets

Due to our previous experiments indicating that a consortium of four CORIO strains in combination with primary BAs in diet modulated host metabolism (Just 2017), we conducted a new gnotobiotic mouse experiment to further study the effects of CORIO.

3.3.1 Preparation of gavage suspensions

Mice were colonised with fresh cultures of *A. mucosicola DSM 19490^T, C. aerofaciens DSM 3979^T, E. lenta DSM 2243^T, and L. parvula DSM 20469^T* (CORIO consortium). The four strains were each grown in Hungate tubes containing anoxic BHI medium without resazurin. For each batch of mice, fresh cryo-aliquots were used for reactivating the strains and then subcultured at least twice. On the day of gavage, cultures grown for approx. 48 h were mixed in sterile and gassed Hungate tubes in a ratio of 2:1:1:1 (*A. mucosicola*: *C. aerofaciens*: *E. lenta*: *L. parvula*). This fresh bacterial mixture was then used to gavage the mice inside an isolator (NKP isotec).

3.3.2 Gnotobiotic mouse experiment

This mouse experiment was performed under LANUV ethical approval 81-02.04.2018.A292. Mice colonised with the CORIO consortium aforementioned were compared to GF and SPF mice.

The detailed experimental design is depicted in **Figure 2A**. GF C57BL/6N mice originated from our own breeding colony (University Hospital of RWTH Aachen, Germany, LANUV approval no. 81-02.04.2018.A396) and were housed in a flexible film isolator type 2D (NKP isotec). To obtain SPF mice with the same genetic background, GF mice were colonised passively by cohousing with SPF mice and were bred in individually ventilated cages (IVC, GM500, Tecniplast). Mice of the first generations were used as SPF control mice in this experiment. The mice were fed a standard chow *ad libitum* (GF and gnotobiotes: γ-irradiated ssniff Spezialdiäten ref. V1124-927; SPF: autoclaved ssniff Spezialdiäten ref. V1124-300) and were given autoclaved tap water. Mice were weaned in the fifth week of life and only male mice were used for this experiment due to their sensitivity to HFD-induced metabolic changes.

The CORIO mice were colonised with 200 µl of fresh bacterial culture (see **3.3.1**) via oral gavage three times at intervals of approx. 48 h during the seventh week of life. From the age of 8 weeks on, all mice were fed with one of four different experimental diets for 12 weeks: control diet (CD; ssniff Spezialdiäten ref. S5745-E902), CD supplemented with the primary BAs CA (0.1%) and CDCA (0.1%) (CD-BA; ssniff Spezialdiäten ref. S5745-E905), lard-based HFD with 48 kJ% fat (HFD; ssniff Spezialdiäten

ref. S5745-E930), or HFD supplemented with the primary BAs CA (0.1%) and CDCA (0.1%) (HFD-BA; ssniff Spezialdiäten ref. S5745-E935).

During allocation of the mice into groups, attention was paid to obtain a distribution of littermates across multiple cages and experimental groups (diet, colonisation) while minimising the number of imports into the isolators to minimise the risk of contaminations. The litters used for this experiment were generated in eleven batches throughout a period of eight months. GF and SPF mice were bred separately, as SPF mice were colonised with complex microbiota from birth on. The distribution of mice within the experimental groups according to cages and litters is displayed in **Figure 2B**.

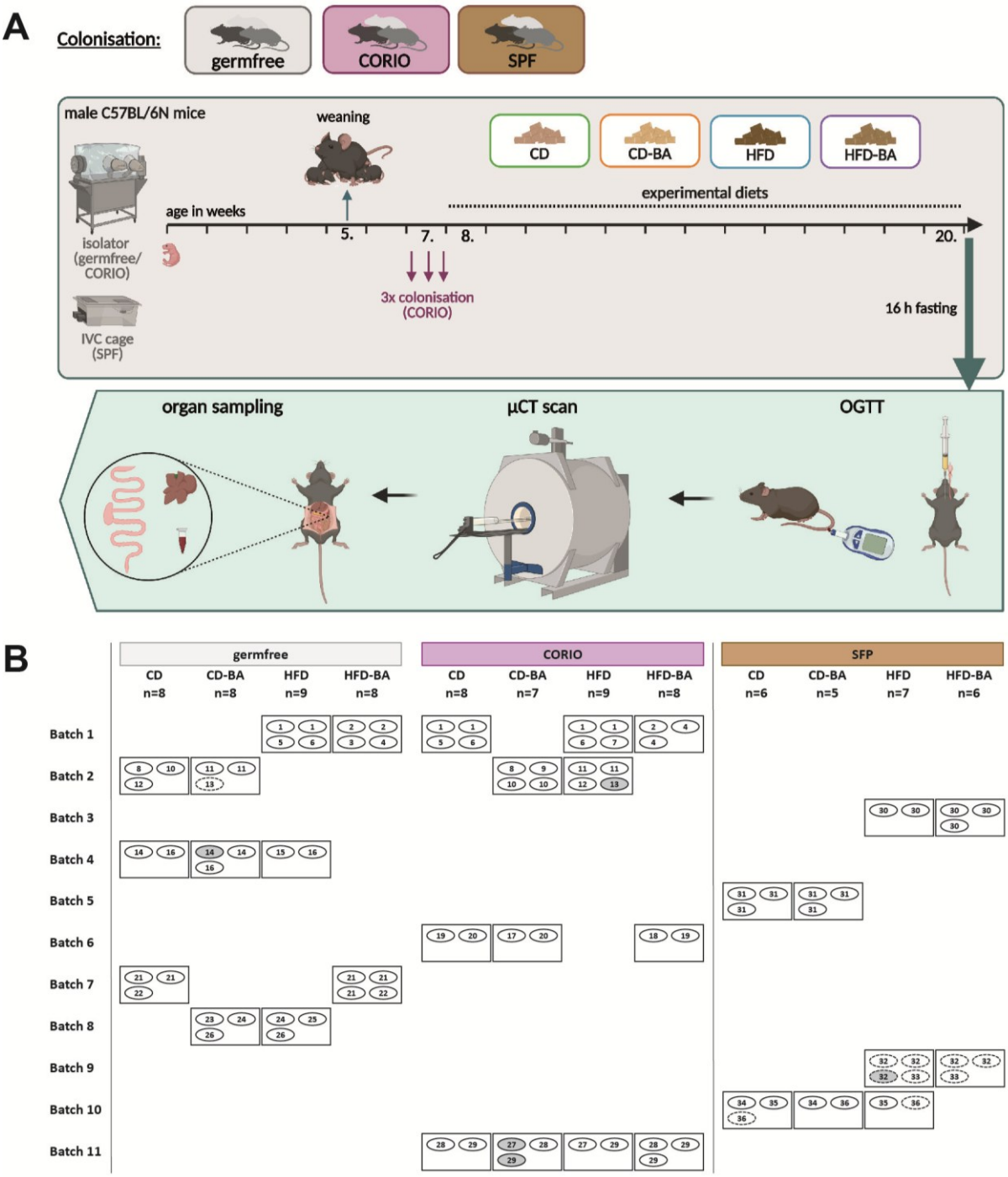

Figure 2: Experimental design and distribution of the mice into the experimental groups. A Experimental design of the gnotobiotic experiment. GF and SPF C57BL/6N mice were bred separately in an isolator or IVC cages, respectively. Mice were weaned during the fifth week of life. In the seventh week of life, CORIO mice were colonised three times via oral gavage with 200 µl of a mixture of fresh bacterial cultures (*A. mucosicola, C. aerofaciens, E. lenta*, and *L. parvula*). From the eighth week of life onwards, they were fed with one of four experimental diets for a period of twelve weeks: control diet (CD), CD supplemented with the primary BAs CA and CDCA (CD-BA), lard-based high-fat diet with 48 kJ% fat (HFD), or HFD supplemented with the primary BAs CA and CDCA (HFD-BA). At the end of the experiment, mice were fasted for 16 h followed by an OGTT and µCT scan. They were then culled for organ sampling. This part of the figure is created with BioRender. **B** Distribution of the mice into the experimental groups (colonisation, diet) according to cages and litters. GF and SPF mice were bred separately, as SPF mice used were colonised with complex microbiota from birth on. Litters were generated in 11 batches. The rectangles represent individual cages, and the ovals represent individual mice. Identical numbers within the ovals indicate mice that originated from the same litter. Only male mice were used in this experiment due to their sensitivity to HFD-induced metabolic changes. Ovals with a dotted frame represent mice that had to be separated in individual cages due to severe fighting behaviour. Ovals with a grey filling represent mice that died suddenly or had to be removed from the experiment due to reaching a too high burden score before the end of experiment.

At the end of the experiment, mice were exported from the isolator into isocages (ISO30P, Tecniplast) and fasted for 16 h. An oral glucose tolerance test (OGTT) was then performed. Therefore, the mice were gavaged with a sterile 40% glucose solution (2 mg glucose/ g body weight) and blood glucose was measured after 0, 15, 30, 60, and 120 min. A small drop of blood from the tail was used for measurement with a glucose meter (Freestyle Freedom Lite, Abbott).

Next, micro computed tomography (µCT) scans were done to quantify the visceral and subcutaneous fat volume. *In vivo* µCT imaging was performed using a µCT optical imaging system (MILabs B.V.) with the ultra-focus fast scan mode. The X-ray tubes of the µCT were operated at a voltage of 65 kV with a current of 0.13 mA. To cover the entire mouse, a continuous rotation scan was performed with one full rotation, exposure time of 75 ms and total scan duration of 27s. Animals were anaesthetised using 2% isoflurane in air for the entire imaging protocol (flow rate 1 L/min). After acquisition, volumetric data sets were reconstructed using MILabs Auto Rec 1.6. Organs and fat were segmented using Imalytics Preclinical 2.1.9.11 (Gremse-IT) (Gremse *et al.* 2016). The volumetric fat percentage was computed as the ratio of (subcutaneous and visceral) fat volume to the entire body volume.

Once the µCT scan was finished, the mice were culled by isoflurane overdose and subsequent final blood withdrawal from the vena cava. The blood was put on ice for at least 5 min and then centrifuged (4,500 rpm, 10-15 min, 4°C). The serum was then aliquoted, frozen on dry ice, and stored at -75°C.

The whole gut was collected and divided into small intestine, caecum, and colon. The caecum was weighed, and the length of small intestine and colon were measured with a ruler after being carefully placed in a straight position with only slight stretching. For the small intestine, the length was rounded to values with 0.5 cm intervals. An example for the methodology of small intestine length measurement is depicted in **Figure 3**. Then content from the different gut regions was collected and frozen on dry ice. Small tissue pieces of the distal small intestine and proximal colon were either directly frozen on dry ice or fixed in formalin for downstream analyses. The liver was also weighed, and parts were frozen on dry ice or fixed in formalin for downstream analyses. Inguinal and epididymal WAT were weighed. Samples of mesenteric, inguinal and epididymal WAT were frozen on dry ice. All frozen samples were stored at -75°C.

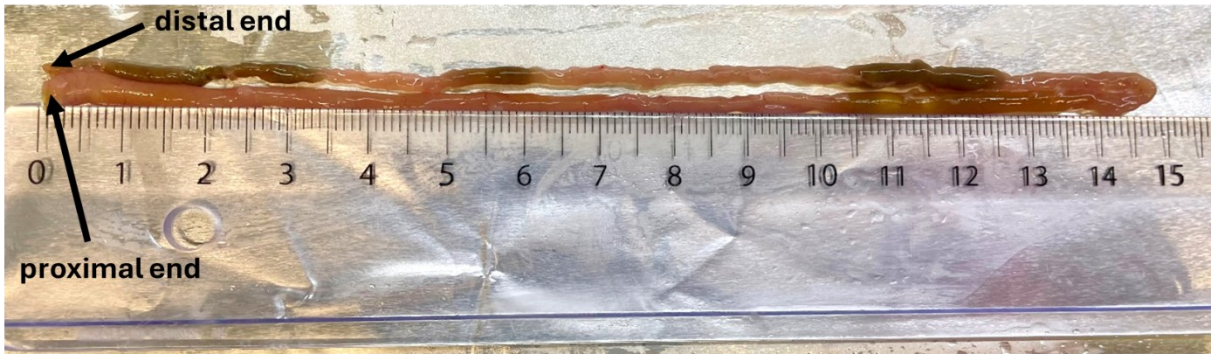

Figure 3: Example picture illustrating the methodology for measuring the length of the small intestine. The small intestine was excised immediately after the stomach and at the junction with the caecum. It was then measured with a ruler after being folded into two parts with the same length and carefully placed in a straight position with only slight stretching. The proximal end (junction to the stomach) and the distal end (junction to caecum) of the small intestine are marked with arrows.

3.3.3 DNA isolation

Metagenomic DNA was isolated from frozen caecum content of the SPF mice. Therefore, a modified version of the protocol by Godon *et al.* (1997) was performed as followed: The caecum content was re-suspended in 600 µl Stool DNA Stabilizer (STRATEC). The suspension was then transferred into screw cap tubes with 500 mg zirconium beads (0.1 mm diameter; Carl Roth). Next, 250 µl 4M guanidinium thiocyanate and 500 µl 5% N laurolylsarcosine were added and mixed by vortexing followed by incubation at 70°C for 60 min. Afterwards, samples were subjected to mechanical disruption using a bead-beater FastPrep-24 5G (MP Biomedicals) for three times with each cycle of 40 seconds at a speed of 6.6 m/s. Between cycles, dry ice was added into the cooling adaptor to prevent overheating of the samples. After cell lysis, 15 mg polyvinylpolypyrrolidone was added to the samples that were then mixed by vortexing. After centrifugation (15,000 g, 4°C, 3 min), supernatants were transferred into new tubes; this step was done twice in a row and the two supernatants of any given sample pooled. 5 µl RNase (10 mg/ml) was added to 500 µl of the clear supernatant followed by incubation at 37°C for 20-30 min with shaking (700 rpm). Finally, the isolated DNA was purified using the NucleoSpin® gDNA Clean-up kit (Machery-Nagel, Germany) according to manufacturer's instruction.

3.3.4 High-throughput 16S rRNA gene amplicon sequencing

The V3 and V4 regions of 16S rRNA genes were amplified using primers 341f and 785r (Klindworth *et al.* 2013) and a 2-step (15 + 10 cycles) procedure to limit amplification bias (Berry *et al.* 2011). Libraries were purified using the AMPure XP system (Beckmann Coulter), pooled in equimolar amounts, and sequenced in paired-end modus using a MiSeq system (Illumina) according to manufacturer's instructions. Raw amplicon sequences were processed using the IMNGS pipeline (Lagkouvardos *et al.* 2016), which is based on the UPARSE approach (Edgar 2013). Analysis parameters were: number of

allowed mismatches in the barcode: 1; minimum quality score for trimming of unpaired reads: 20; sequence length: 350-500; maximal rate of expected errors in paired sequences: 0.005; maximum mismatches during merging of reads: 50; length of trimming: 20; minimum abundance cut off: 0.0025. Operational Taxonomic Units (OTUs) were clustered at 97% sequence similarity. Sequence alignment and taxonomic classification was done by SINA 1.6.1, using the taxonomy of SILVA release 138.1 (Pruesse *et al.* 2012), as part of the IMNGS pipeline. Although some of the taxonomic classifications are not up to date, the names provided by the IMNGS pipeline have been used and the correct taxonomic names are given in the text. Further analysis was done in R using Rhea (Lagkouvardos *et al.* 2017).

3.3.5 Histological analysis of the small intestine

A 1.5 cm piece of the distal small intestine (0.5 cm before caecum) was fixed in formalin for 24 h and then moved into 70% ethanol for storage. After paraffin embedding, samples were cut into 4 µm thick sections and mounted on microscope slides. Sections were stained with haematoxylin and eosin and covered with a glass cover slip.

3.3.6 Contributions

The mouse experiment and sampling were conducted by myself and Theresa Streidl (AG Clavel, University Hospital of RWTH Aachen, Germany). The µCT scans were done and analysed by Diana Möckel, Ramona Brück, and Sarah Schraven at the Institute for Experimental Molecular Imaging (ExMI) at RWTH in Aachen, Germany. DNA isolation and 16S rRNA gene amplicon sequencing was done by Ntana Kousetzi and Nicole Treichel (AG Clavel). Preparation of the histological samples was conducted at the Immunohistochemistry Facility of the Interdisciplinary Center for Clinical Research (IZKF) within the Faculty of Medicine at RWTH Aachen University, Germany. Analysis of the histology samples was done by Roman Bülow (Institute of Pathology, University Hospital of RWTH Aachen, Germany). I analysed all host-derived data, performed 16S rRNA gene amplicon data analysis, and created the figures.

3.4 Influence of *Collinsella aerofaciens* on lipid absorption

In this chapter, two gnotobiotic mouse experiments were performed to test whether *C. aerofaciens* alters lipid absorption. Beforehand, strains of this species were isolated from human stool and tested phenotypically to assess intra-species differences.

3.4.1 Strain level diversity of *Collinsella aerofaciens*

As part of Emily Richter's Master's thesis titled "Characterizing the lipase activity of *Collinsella aerofaciens* strains, isolated from human feces", 14 in-house *C. aerofaciens* isolates from human faecal samples, which have available draft genome sequences, along with the *C. aerofaciens* type strain (DSM 3979^T) used in all mouse experiments, were tested for their lipolytic activity and their capacity to metabolise CA.

Rhodamine B plate assay: Isolates were qualitatively screened for lipolytic activity, as described by Kouker *et al.* (1987). The BHI agar plates contained 37 g/L BHI base, 15g/L agar, 10 mg/L rhodamine B (Sigma-Aldrich), 25 ml/L olive oil, 250 µL/L Tween®80 (Carl-Roth), 0.5 g/L L-cysteine, and 0.2 g/L DTT. Before pouring the agar into Petri dishes, the medium was mixed well on a magnetic stirrer and shaken to homogenise the medium. The isolates and a lipolytic-negative strain of *Escherichia coli* (negative control) were plated on the agar and incubated anaerobically at 37°C for one to three days. After colonies were grown on the plaes, 20 µL of porcine pancreatic lipase (20 g/L stock solution; Sigma-Aldrich) was pipetted onto a free spot on the agar and served as a positive control. Plates were then incubated aerobically at 37 °C for 2 h. Fluorescence, caused by lipolytic activity and interactions of the released FAs with rhodamine B, was examined under UV light (302 nm) using the GelStudio SA (Analytic Jena).

To determine whether lipolytic activity was present in culture supernatants or the pellet fraction, isolates were grown in Hungate tubes with BHI medium supplemented with 1% olive oil and 200 µL/L Tween®80 for 7 to 8 d at 37 °C. Cultures were shaken by hand once a day, to facilitate emulsification. Under sterile aerobic conditions, cultures were centrifuged at 12,000 g for 10 min. 50 µL of the supernatant was pipetted onto rhodamine B olive oil agar plates, and 2 full inoculation loops of pelleted cell material was spread onto rhodamine B olive oil agar plates. Additionally, the remaining pellet material was washed once in Dulbecco's Phosphate Buffered Saline (PBS) and 2 full inoculation loops of the washed pellet were spread onto rhodamine B olive oil agar. As in the regular rhodamine B plate assay, *E. coli* was grown on the plates as a negative control (1 day anaerobic incubation at 37°C) and porcine pancreatic lipase was used as a positive control (20 µL of 20 g/L stock solution, incubated

aerobically for 2 h at 37°C). Fluorescence screening was performed as for the regular rhodamine B plate assay.

Search for *in silico* predicted lipase genes in *C. aerofaciens* isolates: In the context of the PhD thesis of Theresa Streidl (Streidl 2021) five potential lipase genes were predicted *in silico* for *C. aerofaciens* DSM 3979^T. This was done by annotating the identified open reading frames against the databases eggNOG (Huerta-Cepas *et al.* 2019), UniProt (Consortium 2019), and the Lipase Engineering Database (Fischer *et al.* 2003) with the following filtering: subject-cover ≥40%; query-cover ≥40%; percentage ID ≥40%. Subsequently, the sequences were analysed for lipase motifs using InterPro (Mitchell *et al.* 2019) and MotifFinder (Ogiwara *et al.* 1996). The results showed that four of the five potential lipase genes were identified as members of the α/β hydrolase fold superfamily, which is a superfamily of hydrolytic enzymes including lipases.

On the basis of these findings and based on the observation that all 14 analysed *C. aerofaciens* isolates showed lipolytic activity, it was investigated in how far the *in silico* predicted lipase genes were present in the in-house sequenced genomes of all *C. aerofaciens* isolates. A protein BLAST was performed to compare the potential lipase protein sequences to protein sequences encoded within the genome of the 14 *C. aerofaciens* isolates. Genome nucleotide sequences were translated into amino acid sequences using *Prodigal* (Hyatt *et al.* 2010), whereas the lipase gene sequences were translated using MEGA 7, both with default settings. A sequence identity score greater than 30% was considered as a positive match. The potential lipase genes were furthermore checked for transmembrane regions, by submitting the protein sequences to the online tool TMHMM (Transmembrane Hidden Markov Model, version 2.0) (Sonnhammer *et al.* 1998).

Cholic acid metabolism: To determine whether *C. aerofaciens* is capable of metabolising CA, the *C. aerofaciens* isolates were grown anaerobically in liquid BHI medium supplemented with 50 µM CA for 48 h. Therefore, 100 µL of a sterile filtered stock solution with 1.08 g/L CA sodium (Sigma-Aldrich) was added to autoclaved Hungate tubes containing 4.4 mL of liquid anaerobic BHI medium with 0.2 g/L DTT and 0.5 g/L L-cysteine, resulting in a final concentration of 50 µM CA per culture. Each Hungate tube was inoculated with 0.5 ml of a freshly grown overnight culture. Sterile PBS was used as a negative control. Two positive controls were used: (i) 500 µL of the secondary BA producing species *Clostridium scindens*; (ii) 500 µL of human faecal slurry (diluted approximately 1:20 in BHI). Before (T_0) and after 48 h of incubation at 37 °C under anaerobic conditions (T_{48}), 500 µL culture was sampled from each Hungate tube using a syringe, and centrifuged at 11,000 g for 5 min. Two 200 µL aliquots of the supernatants were stored at -75 °C. The samples were sent to Tarek Moustafa (Medical Department of Gastroenterology and Hepatology, Medical University Graz) and the concentrations of CA and DCA were measured by HPLC/MS. The decrease in CA concentration after the 48 h of incubation was

calculated for all *C. aerofaciens* isolates. Since not all T_0 samples of the *C. aerofaciens* cultures were measured, the mean of the measured T_0 concentrations (n = 4) was used. A unique T_0 value was used only in the case of strain CLA-ER-H11, as the CA concentration at T_0 was very different from the T_0 concentrations in all other cultures.

Phylogenetic tree: A maximum likelihood (ML) phylogenetic tree was constructed using all in-house sequenced genomes of the 14 isolates and the *C. aerofaciens* type strain (n = 15), multiple species of the genus *Collinsella* (n = 13) and *Coriobacterium glomerans* (the type species of the type genus within family *Coriobacteriaceae*), using *Phylophlan* (Asnicar *et al.* 2020). The results were visualised with the online tool *iTOL* (interactive Tree Of Life) (Letunic *et al.* 2021).

3.4.2 Preparation of the bacterial gavage suspensions

In the two gnotobiotic mouse experiments described in section **3.4.4**, GF mice were colonised with either *C. aerofaciens* DSM 3979^T or SPF microbiota.

For *C. aerofaciens* colonisation, fresh bacterial cultures were used. Therefore, *C. aerofaciens* DSM 3979^T was cultured at 37°C in anoxic BHI medium in Hungate tubes. For each batch of mice, a new cryo-aliquot was used to prepare the working culture. After activation of the cryopreserved bacteria, the culture was transferred into a new Hungate tube min. two and max. five times before it was used for colonisation. Mice were gavaged with a fresh and densely grown bacterial culture (6-16 h incubation at 37°C).

For colonisation with complex SPF microbiota, frozen aliquots of gut content from SPF mice were used. For preparation of the frozen aliquots, six SPF mice were culled (for scientific procedures in accordance with the German Animal Protection Law (TierSchG)), and their entire gut content (including small intestine, caecum and colon) were emptied into a 50 ml screw cap tube under a laminar flow cabinet. Anaerobic FMT medium (18.75% maltodextrin, 6.25% trehalose, 0.5% ascorbic acid, and 0,05% L-cystein in 0.9% NaCl solution; filter sterilised) (Burz *et al.* 2019) was added in a 1:4 ratio (w/v; gut content: FMT medium). After vortexing, the mixture was aliquoted into screw cap tubes and immediately frozen on dry ice. The aliquots were stored at -75°C until further use. New SPF gut content aliquots were prepared for each of the two animal experiments. The SPF donor mice were held under the same hygiene conditions, but a difference in microbiota profiles is expected.

3.4.3 Preparation of the deuterium-labelled lipid gavage solutions

To quantify lipid absorption in gnotobiotic mice, stable isotope-labelled lipids (i.e., deuterium-labelled FAs and triglycerides) were used. Deuterium is a natural non-radioactive isotope of hydrogen that enables clear and detailed tracking of metabolic pathways. In this experiment we used palmitic acid labelled with five deuterium atoms (hexadecanoic-15,15,16,16,16-d5 acid; CND Isotopes, item no. D-5397) and tripalmitin labelled with 93 deuterium atoms (glyceryl tri(hexadecanoate-d31; CND Isotopes, item no. D-5213), later referred to as D5-palmitic acid and D93-tripalmitin, respectively.

The gavage solution was prepared as follows: A isooctane:isopropanol 3:1 (v/v) mixture was added to the weighed D5-palmitic acid (13 mg/ml) and D93-tripalmitin (15 mg/ml). The solution was sonicated at 37°C in an ultrasonic water bath (Sonorex super RK 102H, Bandelin) until the lipids were fully dissolved and 200 µl portions were aliquoted into 1.5 ml tubes. The solvent was then fully evaporated from the tubes using a vacuum concentrator (Concentrator plus, Eppendorf). Lipid aliquots were then stored in the dark at 4°C and 100 µl olive oil ("Italienisches Natives Olivenöl Extra", Rewe Beste Wahl) was added 1-3 days before they were used for gavage. The final gavage solution contained 99 mM D5-palmitic acid and 33 mM D93-tripalmitin.

On the day of the experiment, the aliquots were sonicated at 37°C for 30 min in an ultrasonic water bath and it was made sure that all residues are dissolved. Afterwards, the aliquots were kept at 37°C in a water bath and were briefly sonicated in an ultrasonic water bath for 1 min prior to gavage.

3.4.4 Gnotobiotic mouse experiments

These mouse experiments were performed under LANUV ethical approval 81-02.04.2018.A292. In both experiments, GF C57BL/6N mice were either colonised with fresh culture of *C. aerofaciens* DSM 3979^T or SPF gut microbiota, or they stayed GF. Both experiments were very similar, with the following differences: male mice only were used in Experiment 2; mice in Experiment 2 originated from the Charles River Laboratories breeding and not from our own GF breeding colony (due to a contamination and the need to reset our facility); the feeding started in the fifth or sixth week of life in Experiment 1 or 2, respectively. The next two paragraphs describe each of the experiments separately.

Experiment 1:

The experimental design is depicted in **Figure 4A**. The mice originated from our own GF breeding colony (University Hospital of RWTH Aachen, Germany, LANUV approval no. 81-02.04.2018.A396). Both male and female mice were used. After weaning during the fifth week of life, the mice were immediately exported from the breeding isolator (flexible film isolator type 2D, NKPisotec) into isocages of the ISOcage P System (ISO30P, Tecniplast; GF or *C. aerofaciens* colonisation) or IVC-cages

(GM500, Tecniplast; SPF colonisation). Mice were given autoclaved tap water and fed for two weeks with either: (i) normal breeding chow (chow; ssniff Spezialdiäten ref. 1124-90); (ii) breeding chow supplemented with 0.1% CA and 0.1% CDCA (chow-BA; ssniff Spezialdiäten ref. S0382-P910), or (iii) breeding chow-based HFD with 48 kJ% from palm oil (chow-HFD; ssniff Spezialdiäten ref. S0382-S910). All diets were sterilised by irradiation (2 x 25 kGy). For colonisation with *C. aerofaciens* or SPF microbiota, mice were given the bacteria (see preparation of gavage suspension in section **3.4.2**) orally (100 µl) and rectally (50 µl) three times (every second day) during the first week of feeding and one more time in the middle of the second week. Mice with a body weight below 15 g were gavaged with a decreased total volume of 10 µl/g body weight. For each cage, a fresh culture of *C. aerofaciens* in Hungate tube or a freshly thawed cryo-aliquot containing SPF gut content suspension was used.

At the end of the experiment mice, were gavaged orally with 100 µl olive oil containing 2.6 mg D5-palmitic acid (hexadecanoic-15,15,16,16,16-d5 acid) and 3.0 mg D93-tripalmitin (glyceryl tri(hexadecanoate-d31)). One or six h after the gavage with the deuterium-labelled lipids, mice were culled for organ sampling.

During allocation of the mice into groups (**Figure 4B**), attention was paid to obtain a distribution of littermates across multiple cages while minimising the risk of cross-contaminations. Additionally, an equal distribution of male and female mice within each group was intended.

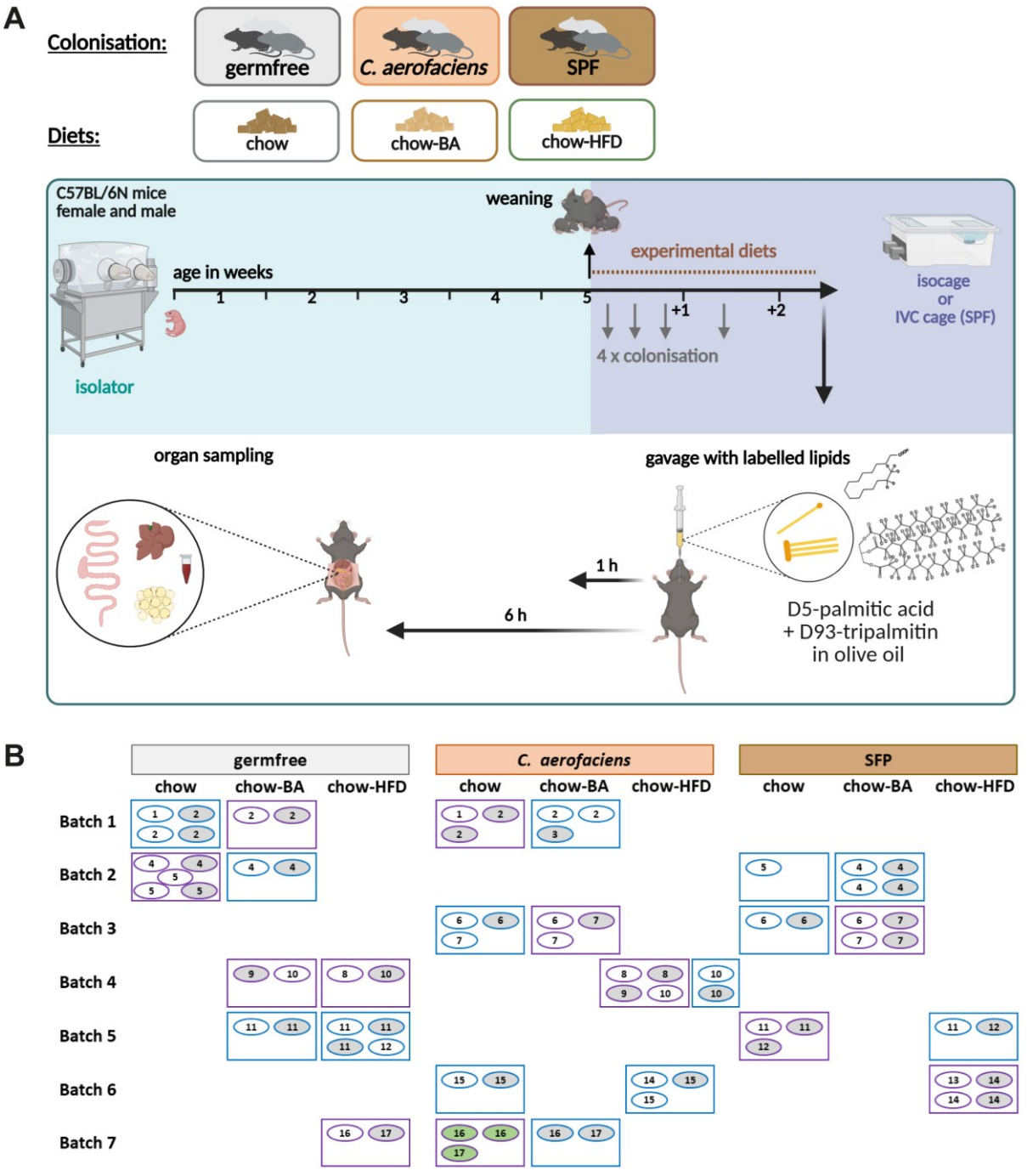

Figure 4: Experimental design and distribution of mice within the experimental groups of lipid absorption experiment 1. **A** Experimental design of the gnotobiotic experiment. During the fifth week of life, GF C57BL/6N mice bred in our own facility were weaned and exported from the breeding isolator into isocages (GF, *C. aerofaciens*) or IVC cages (SPF). After the export, mice were fed with one of three different diets for two weeks: chow, chow supplemented with 0.1% CA and 0.1% CDCA (chow-BA), or chow with 48kJ% from palm oil (chow-HFD). During these two weeks, the mice were given either *C. aerofaciens* or SPF microbiota in total four times or stayed GF. At the end of the experiment, mice were gavaged orally with 100 µl olive oil containing 2.6 mg D5-palmitic acid (hexadecanoic-15,15,16,16,16-d5 acid) and 3.0 mg D93-tripalmitin (glyceryl tri(hexadecanoate-d31)). They were culled for organ sampling either 1 or 6 h after lipid gavage. This part of the figure is created with BioRender. **B** Distribution of the mice within the experimental groups (colonisation, diet, sampling timepoint), taking into account cages and litters. Litters were generated in multiples batches (numbers on the left) throughout a period of nine months. The rectangles represent individual cages, and the ovals within the cages represent individual mice. Identical numbers within the ovals indicate mice that originated from the same litter. Mice were housed in sex-specific cages (violet, female; blue, male). The filling colour of the ovals represents the sampling timepoint after lipid gavage (white, 1 h; grey, 6 h; green, sampled for colonisation control).

Experiment 2:

The experimental design is depicted in **Figure 5A**. The GF C57BL/6N mice originated from the Charles River Laboratories (item no. 24105930). In this experiment only male mice were used due to sex differences observed for some FA data in experiment 1. Mice arrived in Aachen at an age of 4-5 weeks and were imported into a GF isolator (flexible film isolator type 2D, NKPisotec). After one week of acclimatisation time, mice were exported into isocages of the ISOcage P System (ISO30P, Tecniplast; GF or *C. aerofaciens* colonisation) or IVC-cages (GM500, Tecniplast; SPF colonisation). They were given autoclaved tap water and fed for two weeks with either: (i) breeding chow supplemented with 0.1% CA and 0.1% CDCA (chow-BA; ssniff Spezialdiäten ref. S0382-P910), or (ii) a breeding chow-based HFD with 48 kJ% from palm oil (chow-HFD; ssniff Spezialdiäten ref. S0382-S910). All experimental diets were sterilised by irradiation (2 x 25 kGy). Mice were colonise as described for experiment 1.

At the end of the two-week long experiment, mice were gavaged orally with 100 µl olive oil containing 2.6 mg D5-palmitic acid (hexadecanoic-15,15,16,16,16-d5 acid) and 3.0 mg D93-tripalmitin (glyceryl tri(hexadecanoate-d31)). Mice fed with chow-BA were culled 1 h after lipid gavage and mice fed with chow-HFD were culled 6 h after gavage.

Information about the litter affiliation was not available for the mice in experiment 2. The mice arrived in two batches and during allocation of mice into groups a distribution across multiple cages was considered while minimising the risk of cross-contamination. The distribution of mice to cages and groups is displayed in **Figure 5B**

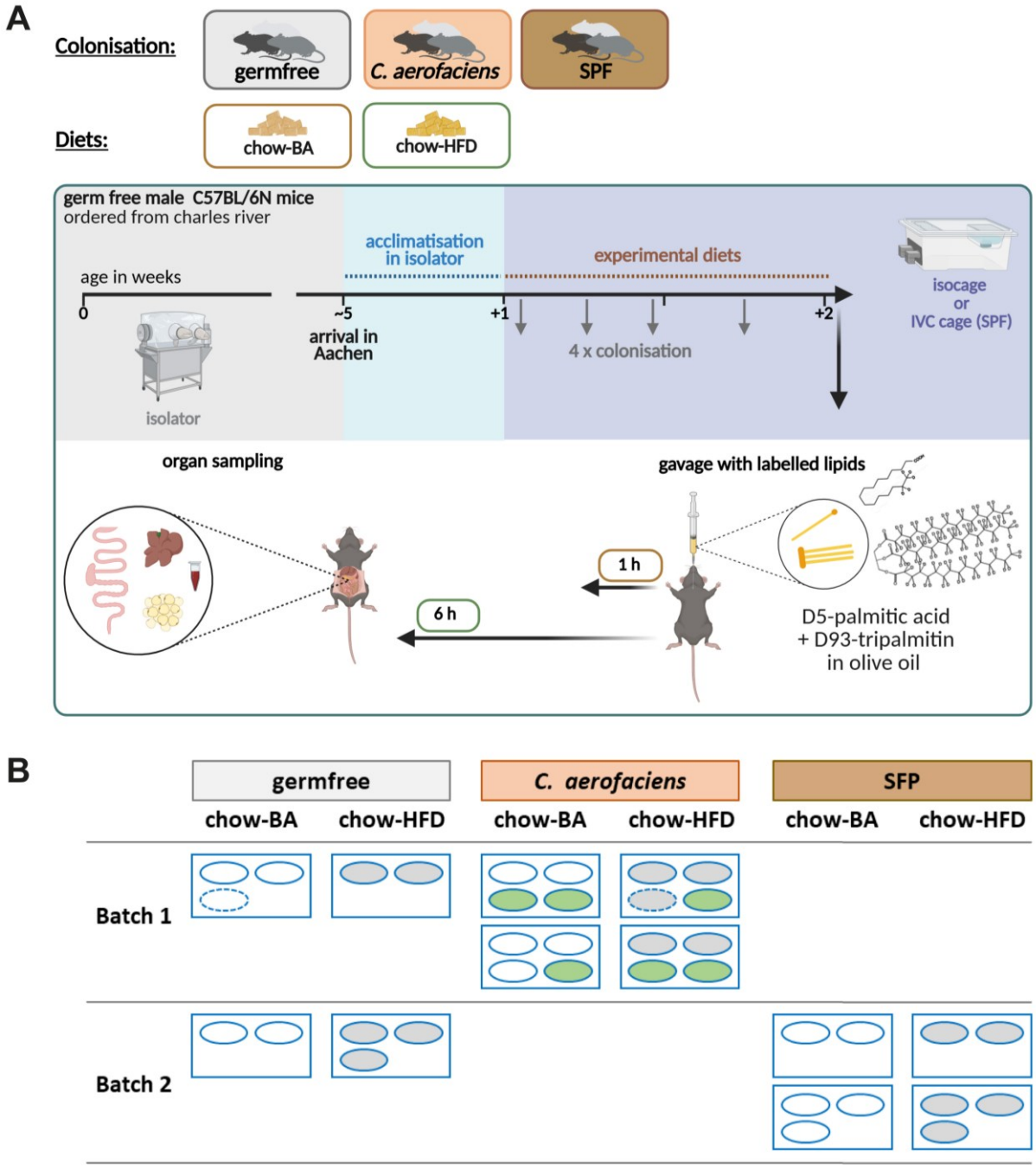

Figure 5: Experimental design and distribution of mice within the experimental groups of lipid absorption experiment 2. **A** Male GF C57BL/6N mice ordered from Charles River arrived in Aachen at an age of approx. five weeks. After one week of acclimatisation time in an isolator, mice were exported into isocages (GF, *C. aerofaciens*) or IVC cages (SPF). After the export, they were fed for two weeks with either chow supplemented with 0.1% CA and 0.1% CDCA (chow-BA), or chow with 48kJ% from palm oil (chow-HFD). During these two weeks, the mice were given either *C. aerofaciens* or SPF microbiota in total four times or stayed GF. At the end of the experiment, mice were gavaged orally with 100 µl olive oil containing 2.6 mg D5-palmitic acid (hexadecanoic-15,15,16,16,16-d5 acid) and 3.0 mg D93-tripalmitin (glyceryl tri(hexadecanoate-d31)). Mice fed with chow-BA were culled 1 h after lipid gavage and mice fed with chow-HFD were culled 6 h after gavage. This part of the figure is created with BioRender. **B** Distribution of the mice within the experimental groups (colonisation, diet, sampling timepoint) according to cages. Mice arrived in Aachen in two batches. The rectangles represent individual cages, and the ovals within the cages represent individual mice. The filling colour of the ovals represent the sampling timepoint after lipid gavage (white, 1 h; grey, 6 h; green, sampled for colonisation control). Only male mice were used in this experiment. Ovals with a dotted border represent mice that had to be separated into individual cages due to severe fighting behaviour.

In both lipid absorption experiments, faecal samples of GF mice were taken whenever possible and checked for sterility by Gram-staining and aerobic and anaerobic cultivation on complex media agar plates. To confirm that the colonisation with *C. aerofaciens* was successful, faecal samples of the corresponding mice were treated the same. Successful colonisation was assumed if colonies grew on the anaerobic but not on the aerobic agar plates and cells with the expected shape were visible under the microscope after Gram-staining.

3.4.5 Sampling procedure

Mice were culled with an isoflurane overdose and subsequent blood withdrawal by heart puncture using a syringe fitted with a 24 G cannula flushed with EDTA. To obtain plasma, EDTA blood was centrifuged for 10 min at 4,000 g and 4°C. If the gall bladder was filled, the bile was removed with a fine dosage syringe and snap frozen. Before further organ sampling, the liver was perfused with 0.9% NaCl solution. Therefore, the portal vein was cut close to the liver and 0.9% NaCl solution was injected in the vena cava until the liver lost its red colouring. Parts of the perfused left liver lobes were snap frozen. Samples of mesenteric, inguinal, and epididymal WAT were also snap frozen. The gut was taken out and handled on a sampling board cooled with ice. The length of the intestine was measured, and it was divided into three sections (proximal, middle, distal) as depicted in **Figure 6**. The length of the colon and the weight of the caecum were measured. The content of each of the three small intestine sections, caecum, and colon was emptied into separate reaction tubes. Afterwards the gut tissues were flushed with 0.9% NaCl solution and the middle 2 cm of each small intestine part and the colon were snap frozen. All samples were stored at -75°C until further use.

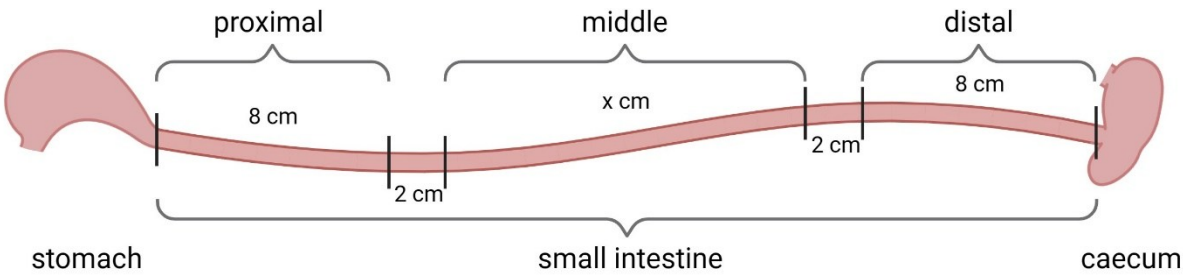

Figure 6: Sampling scheme for the small intestine. The small intestine was divided into three sections: a proximal 8 cm segment after the stomach; a distal 8 cm segment before the caecum; and a middle section. After removal of the proximal and distal part, 2 cm from each end were excluded and the rest was collected as the representative middle segment of the small intestine. This figure is created with BioRender.

3.4.6 CFU counts for colonisation check

To test for colonisation with *C. aerofaciens,* extra mice were sampled and the number of CFUs per g gut content was determined in the different gut regions. In the lipid absorption Experiment 1, the quantitative colonisation check was conducted with three mice fed with the chow diet. In Experiment 2, three mice fed with chow-BA or chow-HFD were used. After culling, the body was disinfected with 70% ethanol and moved under a laminar flow cabinet. Only sterile or disinfected instruments and materials were used for sampling. The gut was removed and divided into three sections of the small intestine (proximal, middle and distal, see **Figure 6**), caecum, and colon. The content of the gut sections was emptied into 2 ml reaction tubes, mixed well, and a smaller portion was moved into a new reaction tube. These gut content samples were weighed and transferred into the anaerobic chamber (MBraun). Samples were then diluted with anaerobic PBS in 1:10 steps. Subsequently, 10 µl of the 10^{-1} to 10^{-8} dilutions were pipetted onto BHI agar plates in duplicates and then tilted to spread the drops over the plate. Plates were incubated at 37°C in the anaerobic chamber and colony forming units (CFUs) were counted after 2 to 4 days. Only dilutions that resulted in a CFU number ≥ 5 and ≤ 50 were considered for calculation of the mean number of CFUs per g gut content for each gut section and mouse.

3.4.7 Fatty acid analysis

The FA analysis was done as described previously in Ecker *et al.* (2012).

3.4.8 DNA isolation

For experiment 2 metagenomic DNA was isolated from frozen caecum content of the *C. aerofaciens* and SPF mice. The DNA isolation protocol is described in section **3.3.3.**

3.4.9 High-throughput 16S rRNA gene amplicon sequencing

Amplification and sequencing of the 16S rRNA gene was performed as described in section **3.3.4**.

The parameters used for the IMNGS pipeline (Lagkouvardos *et al.* 2016) were: Number of allowed mismatches in the barcode: 1; minimum quality score for trimming of unpaired reads: 20; sequence length: 350-500; maximal number of expected errors in paired sequences: 0.005; maximum mismatches during merging of reads allowed: 50; length of trimming: 20; minimum abundance cut-off: 0.0025. OTUs were clustered at 97% sequence similarity. The negative control did not show any contamination (< 100 reads). Analysis for the *C. aerofaciens*-monocolonised and SPF mice was done separately. Further analysis was done in R using Rhea (Lagkouvardos *et al.* 2017).

3.4.10 Contributions

The work on strain-level diversity was performed by Emily Richter, who did her Master's thesis titled "Characterizing the lipase activity of *Collinsella aerofaciens* strains, isolated from human feces" under my supervision. During the animal experiments and sampling, I received help from Atscharah Panyot, Esther Wortmann, and Susan Jennings (AG Clavel, University Hospital of RWTH Aachen, Germany). FA measurement and analysis was done by Johannes Plagge, Sven Hermeling, and Josef Ecker at the Research Group Lipid Metabolism at the ZIEL Institute for Food & Health, Technical University in Munich, Germany. DNA isolation and 16S rRNA gene amplicon sequencing was done by Ntana Kousetzi and Nicole Treichel (AG Clavel). I planned and performed the mouse experiments and analysed all the data.

3.5 Occurrence of lipase-positive bacteria in human stool from a population study

In this last chapter, I investigated whether there is an association between the relative abundance of lipase-positive bacteria, including *C. aerofaciens*, and metabolic parameters and host body composition of individuals within a nested cohort (n = 348) of the KORA population study (Cooperative Health Research in the Region of Augsburg). An initial statistical analysis of the KORA cohort was performed in the PhD thesis of Theresa Streidl (Streidl 2021). While the focus of her analysis was on correlations between the relative abundance of *Coriobacteriia* and metadata variables, the focus of this analysis was on regression analysis of the relative abundance of the lipase-positive fraction in faecal microbiota. I analysed the data of 338 participants with available body composition data from MRI scans, faecal microbiota profiles with > 5,000 reads per sample, and not taking antibiotics.

3.5.1 DNA isolation

The extraction of DNA from stool samples of KORA subjects, which was partly performed by myself, is also described in the PhD thesis of Theresa Streidl (Streidl 2021). The isolation protocol was similar to that described in **3.3.3** with additional enzymatic steps to increase the DNA yield from *Coriobacteriia*. 15 mg lysozyme dissolved in 40 µl Tris-EDTA buffer were added to 500 µl of the stool samples stored in Stool DNA Stabilizer (STRATEC) and incubated at 37°C for 30 min. Then 50 µl 10% sodium dodecyl sulfate (Carl Roth) and 600 µg proteinase K (Carl Roth) were added followed by a 1 h incubation at 50°C. Next, 250 µl 4M guanidinium thiocyanate and 500 µl 5% N laurolylsarcosine were added, mixed by vortexing, and the suspension was then transferred into screw cap tubes containing 500 mg zirconium beads (0.1 mm diameter; Carl Roth). After incubation at 70°C for 60 min, samples were subjected to mechanical disruption using a bead-beater FastPrep-24 5G (MP Biomedicals) for three times with each cycle of 40 seconds at a speed of 6.6 m/s. Between cycles, dry ice was added into the cooling adaptor to prevent overheating of the samples. After cell lysis, 15 mg polyvinylpolypyrrolidone was added to the samples that were then mixed by vortexing. After centrifugation (15,000 g, 4°C, 3 min), supernatants were transferred into new tubes; this step was done twice in a row and the two supernatants of any given sample pooled. 5 µl RNase (10 mg/ml) was added to 500 µl of the clear supernatant followed by incubation at 37°C for 20-30 min with shaking (700 rpm). Finally, the isolated DNA was purified using the NucleoSpin® gDNA Clean-up kit (Machery-Nagel, Germany) according to manufacturer's instruction.

3.5.2 High-throughput 16S rRNA gene amplicon sequencing

The amplification and sequencing of the 16S rRNA gene is described in the PhD thesis of Theresa Streidl (Streidl 2021). Raw amplicon sequences were processed using the IMNGS pipeline (Lagkouvardos et al. 2016), which is based on the UPARSE approach (Edgar 2013).

The parameters I used for the final IMNGS-based analysis (Lagkouvardos *et al.* 2016) were: Number of allowed mismatches in the barcode: 1; minimum quality score for trimming of unpaired reads: 20; sequence length: 350-500; maximal number of expected errors in paired sequences: 0.005; maximum mismatches during merging of reads allowed: 50; length of trimming: 20; minimum abundance cutoff: 0.0025. OTUs were clustered at 97% sequence similarity. Samples less than 5000 reads were removed, and the analysis was repeated. Further analysis of the 16S rRNA gen amplicon data, including *de novo* clustering, was done in R using Rhea (Lagkouvardos *et al.* 2017).

3.5.3 Calculation of the lipase-positive fraction

To calculate the cumulative relative abundance of lipase-positive bacteria, the results of a screening of bacteria isolated from human faecal samples for lipolytic activity in the rhodamine B plate assay done by Johannes Masson (AG Clavel, University Hospital of RWTH Aachen) were used. This screening resulted in 15 lipase-positive isolates (14 species), including the *Coriobacteriia* species *C. aerofaciens*. The 16S rRNA gene sequences of these lipase-positive isolates were used in a BLAST search against the OTU sequences of the amplicon data from the 338 analysed KORA participants and the following filtering was applied: min. identity, 97%; min. query coverage, 80%. A total of 10 OTUs had >97% identity with one of the lipase-positive isolates. The cumulative relative abundance of these OTUs was calculated and is referred to as the lipase-positive fraction.

3.5.4 Statistical Analysis

The statistical analysis of the cohort data was done in IBM SPSS Statistics (version 29.0.0.0 (241)). Redundant variables were removed before doing the statistical analysis and all variables included in the analysis are listen in **Table S2** and **Table S3**. To test whether there were differences in variables between the three *de novo* clusters computed for the microbiota profiles in R using Rhea (Lagkouvardos *et al.* 2017), a one-way ANOVA followed by Benjamini-Hochberg was performed for numerical variables and a Chi2 test (performed separately for cluster 1 vs. 2, 1 vs. 3, and 2 vs.3) followed by Benjamini-Hochberg was performed for categorical variables. Next, a multiple linear regression analysis corrected for age and sex was performed (model including a constant term), with

the relative abundance of the lipase-positive fraction and the confounding factors age and sex as independent variables.

3.5.4 Contributions

The KORA study was initiated and financed by the Helmholtz Zentrum München – German Research Center for Environmental Health, which is funded by the German Federal Ministry of Education and Research (BMBF) and by the State of Bavaria. The KORA Study Group consists of Annette Peters, Birgit Linkohr, Harald Grallert, Margit Heier, and their co-workers, who are responsible for the design and conduct of the KORA studies. Initial planning of the analysis and the first statistical analysis of the data was done by Theresa Streidl (AG Clavel, University Hospital of RWTH Aachen, Germany). DNA isolation was done by Ntana Kousetzi (AG Clavel) and myself. 16S rRNA gene amplicon sequencing was done by Ntana Kousetzi and Nicole Treichel (AG Clavel). I conducted the downstream analysis of 16S rRNA gene amplicon data. The screening of bacterial strains isolated from human faecal samples for lipolytic activity was conducted by Johannes Masson. Statistical analysis was done by myself with advice from Caroline Schneider and Thriveni Basavanapura Raju (AG Schneider, Medical Clinic III, University Hospital of RWTH Aachen, Germany).

4. Results

The results are divided into four main chapters, all focussed on studying the class *Coriobacteriia*, which includes dominant gut bacteria. Chapter **4.1** reports the influence of *E. lenta* colonisation of OMM12 mice on the liver proteome and gut metabolome. In Chapter **4.2**, GF and SPF mice fed with different diets were compared, as the four CORIO strains did not colonise the gnotobiotic mice. In Chapter **4.3**, the influence of *C. aerofaciens* on intestinal lipid absorption was studied in mice. In Chapter **4.4**, the occurrence of dominant lipase-positive bacteria, including *C. aerofaciens*, in the stool of human KORA participants was analysed in relation to host body parameters.

4.1 Influence of *Eggerthella lenta* on liver proteome and gut metabolome

This chapter presents the analysis of samples derived from a gnotobiotic mouse experiment conducted as part of the PhD thesis by Theresa Streidl (Streidl 2021). The data presented here has been published under Viehof *et al.* (2024). In the gnotobiotic mouse experiment, GF mice were colonised with cryopreserved caecal suspensions of OMM12 mice, either with or without the CORIO consortium, and were fed with four different experimental diets for eight weeks. The diets varied in fat content and primary BA supplementation: experimental control diet (CD), CD supplemented with 0.1% CA and 0.1% CDCA (CD-BA), lard-based high-fat diet (HDF), or lard-based high-fat diet supplemented with 0.1% CA and 0.1% CDCA (HFD-BA). The experiment was terminated upon completion of the feeding intervention, at which point the mice had reached 18 weeks of age.

The presence of the OMM12 and CORIO species in the caecum was evaluated by 16S rRNA gene amplicon sequencing. *Beta*-diversity analysis demonstrated that the microbial communities primarily differed between the two colonisation groups ($p = 0.001$, PERMANOVA; **Figure 7A**). The influence of the dietary intervention resulted in statistically significant differences in overall microbiota profiles for only two comparisons (E.L HFD vs. E.L HFD-BA, adj. $p = 0.0482$; MM CD vs. MM CD-BA, adj. $p = 0.028$). Although all four CORIO strains were present in the gavage solution as tested by 16S rRNA gene amplicon sequencing (data not shown), only *E. lenta* successfully colonised the intestine of the mice with a median relative abundance of 27.5% (**Figure 7B**). The relative abundance of *E. lenta* was increased in the diet groups with primary BA supplementation, reaching statistical significance compared to the HFD group. Out of the twelve OMM12 strains ten were detected in the gavage solution and caecum of the mice. *Bifidobacterium animalis* DSM 26074 and *Acutalibacter muris* DSM 26090^T were not detected, which agrees with previous mouse studies (Brugiroux *et al.* 2016; Eberl *et al.* 2019).

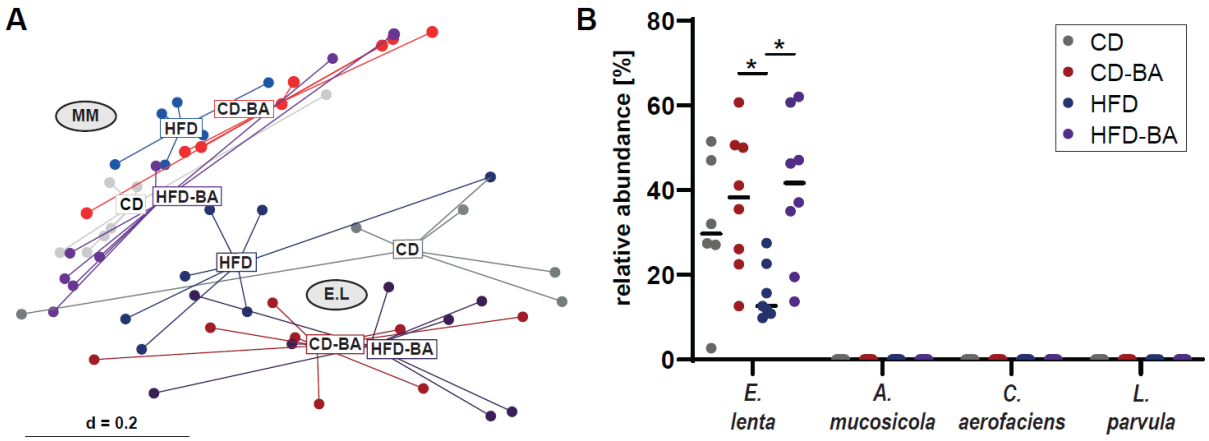

Figure 7: Caecal colonisation profiles by 16S rRNA gene amplicon sequencing. A *Beta*-diversity analysis of colonisation/diet groups shown as a multidimensional scaling plot of generalised UniFrac distances (p = 0.001; PERMANOVA). **B** Relative abundance of the CORIO strains in the E.L mice. Each dot is corresponding to an individual mouse, black bars indicate the median values. Statistics: only results for the detected CORIO strain *E. lenta* were compared statistically using Mann-Whitney tests with Benjamini-Hochberg adjustment. Stars indicate significant differences between colonisation groups (*adj. p < 0.05). Abbreviations: MM, mice colonised with the mouse synthetic community OMM12; E.L, mice colonised with OMM12 and *E. lenta*; CD, control diet; CD-BA, control diet supplemented with 0.1% CA and 0.1% CDCA; HFD, lard-based high-fat diet; HFD-BA, HFD supplemented with 0.1% CA and 0.1% CDCA. A previous version of this figure was published in the PhD thesis by Theresa Streidl (Streidl 2021) and in Viehof *et al.* (2024).

To investigate the effects of colonisation and diet on the host, a proteomics analysis of the liver was conducted. Principal component analysis (PCA) demonstrated that diet, but not colonisation, had a significant effect on the liver proteomes (**Figure 8**). The fat content of the diets was identified as the main contributing factor.

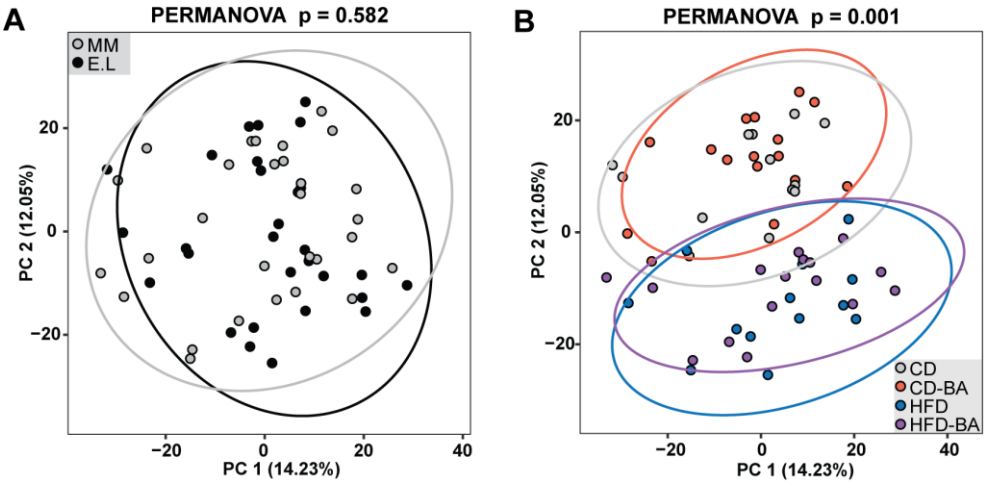

Figure 8: Effects of *E. lenta*-colonisation and diet on liver proteomes. A Principal component analysis (PCA) of liver proteomes according to colonisation group (p = 0.582; PERMANOVA). **B** PCA of liver proteomes according to diet groups (p = 0.001; PERMANOVA). Abbreviations: MM, mice colonised with the mouse synthetic community OMM12; E.L, mice colonised with OMM12 and *E. lenta*; CD, control diet; CD-BA, control diet supplemented with 0.1% CA and 0.1% CDCA; HFD, lard-based high-fat diet; HFD-BA, HFD supplemented with 0.1% CA and 0.1% CDCA. A previous version of this figure was published in Viehof *et al.* (2024).

A comparison of fold-changes in single proteins between the two colonisation groups for each of the four diets revealed no significant differences in protein expression due to the colonisation with *E. lenta*. In contrast, the diet had significant effects on individual proteins. A comparison of the mice fed the diets with a low-fat content compared with the HFDs revealed multiple significant changes (**Figure 9**). An examination of the top ten upregulated or downregulated proteins for the comparisons between CD vs. HFD and CD-BA vs. HFD-BA in both colonisation groups revealed that five proteins were consistently altered across all comparisons (**Figure 9C** and **D**). Fatty acid-binding protein 5 (UniProtKB ID: Q05816), which facilitates the intracellular transport of long-chain FAs and related active lipids, was consistently upregulated in the low-fat diet fed mice and had the highest Log2(FC) in all comparisons, ranging from 4.23 to 4.84. Furthermore, the following proteins were consistently upregulated in the low-fat diet groups: cytoplasmic aspartate aminotransferase (UniProtKB ID: P05201), which plays a key role in amino acid metabolism; ATP-citrate synthase (UniProtKB ID: Q3V117), which catalyses a critical step in cholesterol and FA synthesis; and thyroid hormone-inducible hepatic protein (UniProtKB ID: Q62264), which plays a role in in the regulation of lipogenesis and is important for the biosynthesis of triglycerides with medium-length FA chains. Whereas cholesteryl ester hydrolase (UniProtKB ID: Q9Z0M5), which is crucial for the intracellular hydrolysis of cholesteryl esters and triglycerides, was consistently upregulated in the HFD groups.

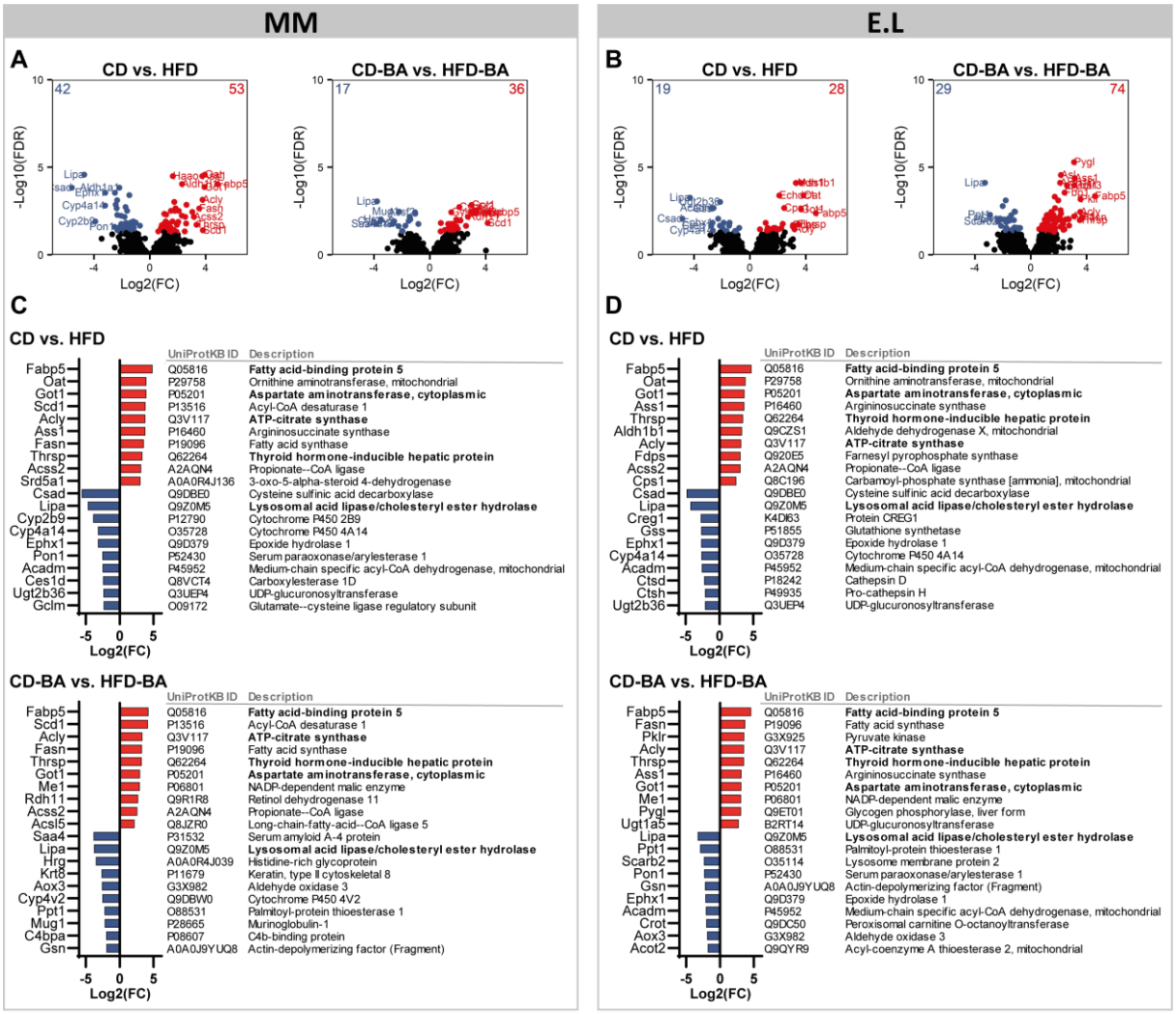

Figure 9: Effect of fat supplementation on liver proteomes for each colonisation group. A Volcano plots of proteins altered in MM mice fed diets without vs. with additional fat (48kJ%). Significant up- and downregulated proteins are displayed as coloured dots and their numbers are shown in the top corners of the graphs. **B** Same as in panel A, for E.L mice. **C** Top ten significantly up- and downregulated proteins with the highest Log2(FC) values for MM mice. **D** Same as in panel C, for E.L mice. Abbreviations: MM, mice colonised with the mouse synthetic community OMM12; E.L, mice colonised with OMM12 and *E. lenta*; CD, control diet; CD-BA, control diet supplemented with 0.1% CA and 0.1% CDCA; HFD, lard-based high-fat diet; HFD-BA, HFD supplemented with 0.1% CA and 0.1% CDCA. A previous version of panel A and B of this figure was published in Viehof *et al.* (2024).

The supplementation of primary BAs also had a significant effect on individual proteins in the liver (**Figure 10**), although this effect was less pronounced than that observed with fat supplementation. It was not possible to identify any proteins that were consistently altered across all comparisons. When comparing CD vs. CD-BA in OMM12 mice, only two significantly changed proteins were observed. Retinal dehydrogenase 1 (UniProtKB ID: P24549), which catalyses the oxidation of retinal to retinoic acid, was upregulated in liver of mice fed CD, and haloacid dehalogenase-like hydrolase domain-containing protein 3 (UniProtKB ID: Q9CYW4) was downregulated. The protein cysteine sulfinic acid decarboxylase (UniProtKB ID: Q9DBE0), which catalyses the decarboxylation of specific amino acids, exhibited the most substantial upregulation, and serum amyloid A-4 protein (UniProtKB ID: P31532),

which functions as an acute-phase protein involved in the immune response, exhibited the most substantial downregulation in HFD vs. HFD-BA fed mice of the OMM12 colonisation group. In the *E. lenta*-colonised mice, peroxisomal acyl-coenzyme A oxidase 1 (UniProtKB ID: Q9R0H0), which catalyses the initial rate-limiting step of peroxisomal ß-oxidation, was found to be the most substantially upregulated protein in CD vs. CD-BA fed mice. The protein corticosteroid 11-betadehydrogenase isozyme 1 (UniProtKB ID: P50172), which is involved in the conversion of biologically active glucocorticoids into corticosterone, was most substantially downregulated in *E. lenta*-colonised mice fed the CD diet. A comparison of HFD vs. HFD-BA in the OMM12 and *E. lenta* colonised mice revealed only a single significantly altered protein: mitochondrial carbamoyl-phosphate synthase [ammonia] (UniProtKB ID: Q8C196), which is involved in the urea cycle and plays an important role in removing excess ammonia from the cell, was found to be downregulated in HFD vs. HFD-BA fed mice.

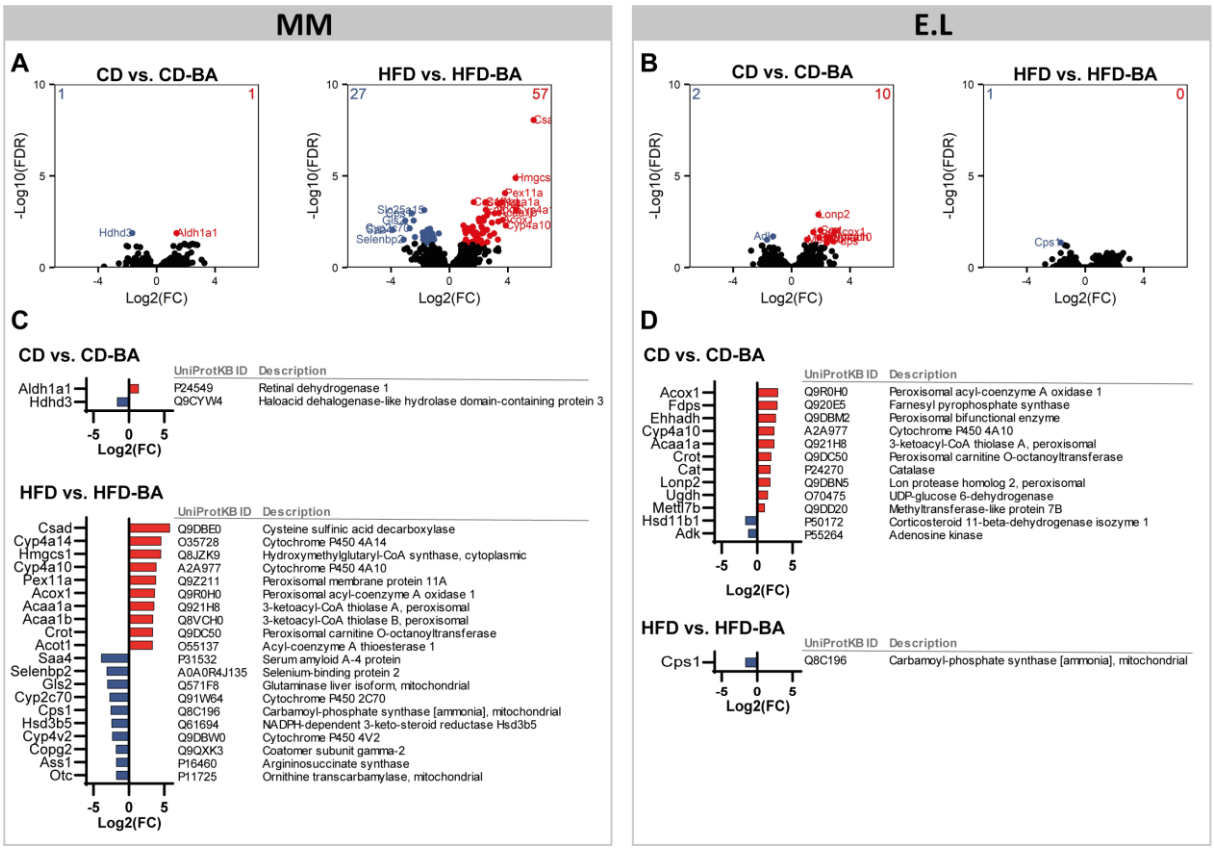

Figure 10: Effect of primary bile acid supplementation on liver proteomes in each colonisation group. A Volcano plots of proteins altered in MM mice fed diets with or without primary BAs (0.1% CD and 0.1% CDBA). Significant up- and downregulated proteins are displayed as coloured dots, and their numbers are shown in the top corners of the graphs. **B** Same as in panel A, for E.L mice. **C** Top ten significantly up- and downregulated proteins with the highest Log2(FC) values for MM mice. **D** Same as in panel C, for E.L mice. Abbreviations: MM, mice colonised with the mouse synthetic community OMM12; E.L, mice colonised with OMM12 and *E. lenta*; CD, control diet; CD-BA, control diet supplemented with 0.1% CA and 0.1% CDCA; HFD, lard-based high-fat diet; HFD-BA, HFD supplemented with 0.1% CA and 0.1% CDCA. A previous version of panel A and B of this figure was published in Viehof *et al.* (2024).

As *E. lenta* is a functionally versatile bacterial species, we investigated whether *E. lenta* colonisation had an effect on metabolomes in the colon. The use of non-targeted metabolomics allowed the identification of 381 and 576 metabolite peaks in positive and negative ionisation mode, respectively. Of those peaks, 71 and 87 could be annotated, respectively. PCA of all detected metabolite peaks revealed significant differences between the colonisation groups in the positive ionisation mode ($p = 0.001$, PERMANOVA; **Figure 11A**), but not in the negative ionisation mode ($p = 0.548$, PERMANOVA; **Figure 11C**). A significant effect of diet on the overall metabolome was observed for both ionisation modes ($p = 0.001$, PERMANOVA; **Figure 11B** and **D**).

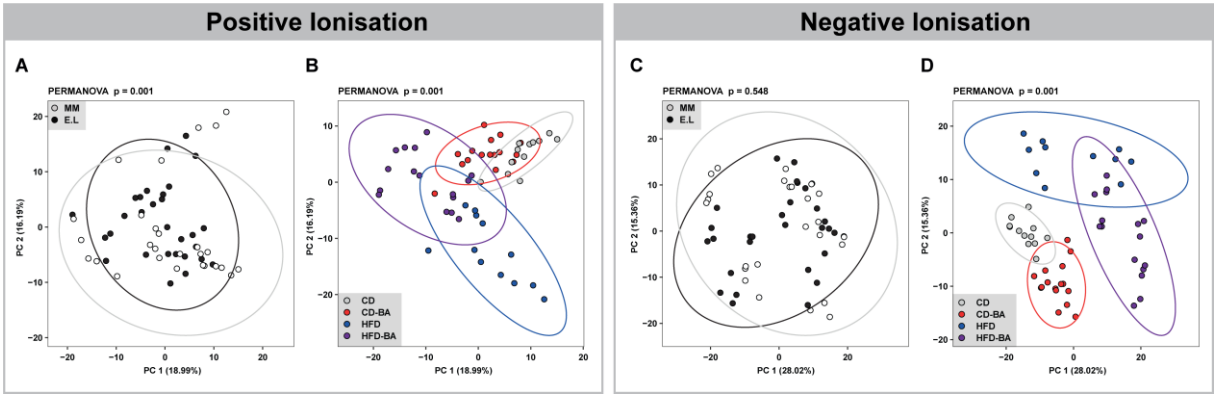

Figure 11: Effects of *E. lenta*-colonisation and diet on metabolomes in the colon of gnotobiotic mice. PCA of all identified metabolite peaks detected in positive ionisation mode according to **A** colonisation, **B** diet. **C** Same as in panel A, for negative ionisation mode. **D** Same as in panel B, for negative ionisation mode. Abbreviations: MM, mice colonised with the mouse synthetic community OMM12; E.L, mice colonised with OMM12 and *E. lenta*; CD, control diet; CD-BA, control diet supplemented with 0.1% CA and 0.1% CDCA; HFD, lard-based high-fat diet; HFD-BA, HFD supplemented with 0.1% CA and 0.1% CDCA. A previous version of this figure was published in Viehof *et al.* (2024).

Differences in the detection of individual annotated metabolites between the colonisation groups were analysed for each diet group. A Kruskal-Wallis test was conducted, followed by a post hoc Dunn's test to examine pairwise comparisons. A total of 33 metabolites in positive ionisation mode and 32 metabolites in negative ionisation mode exhibited significant alterations due to *E. lenta*-colonisation in at least one diet group (**Figure 12A** and **B**). Five metabolites were consistently altered as a result of colonisation in at least three of the four diet groups. These metabolites are marked in grey in panels **A** and **B** of **Figure 12**, while the peak intensity for each individual mouse is plotted in panels **C** and **D** of **Figure 12**. The metabolites creatine (detected in both ionisation modes), sarcosine, N,N-dimethylarginine, and N-Acetyl-DL-methionine were significantly decreased in *E. lenta*-colonised mice, while latifolicinin C acid was significantly increased in *E. lenta*-colonised mice.

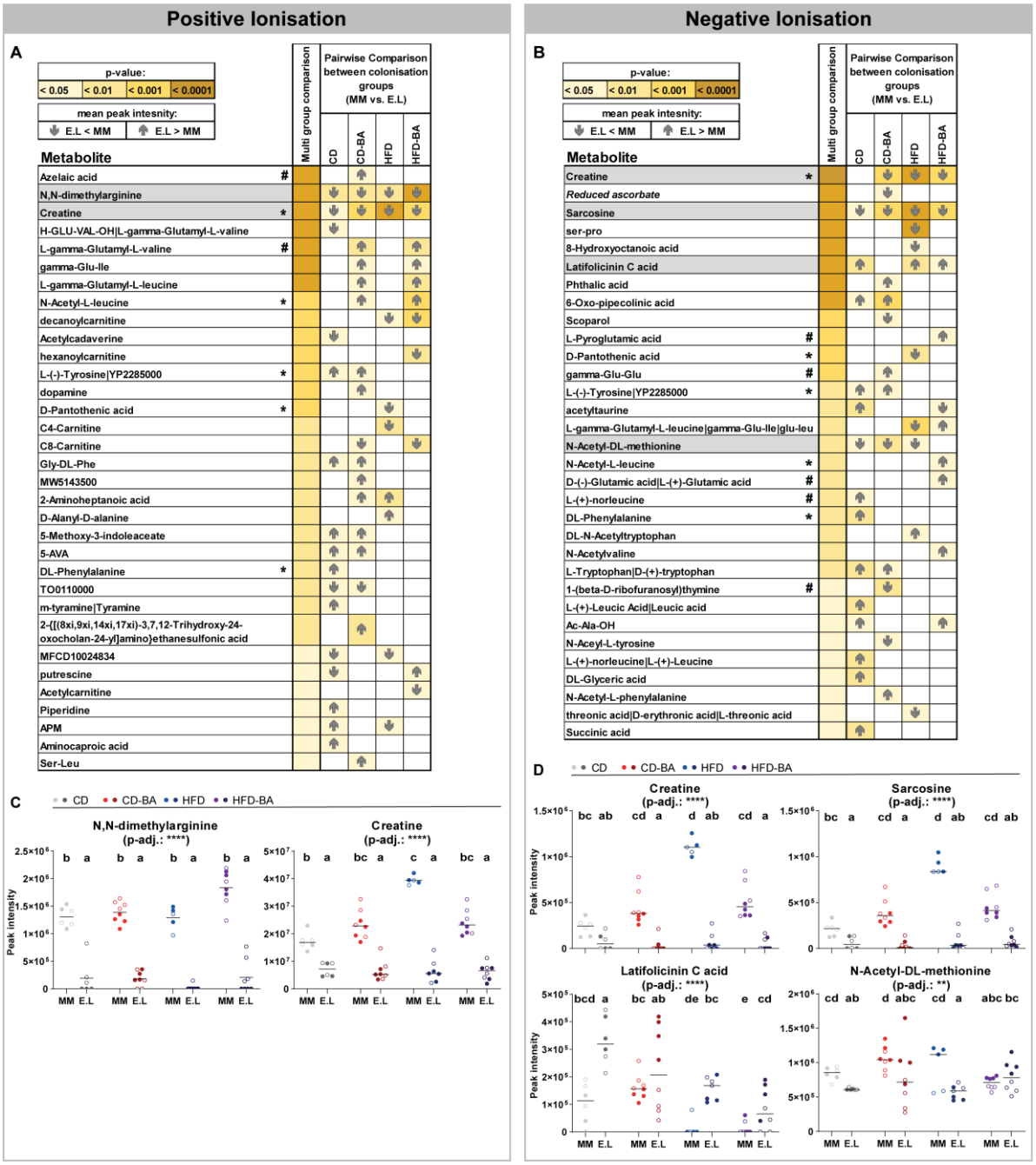

Figure 12: Effects of *E. lenta*-colonisation on annotated metabolites in the colon. A Annotated metabolites with significant differences between E.L and MM mice within at least one dietary group as measured in positive ionisation mode. The symbols after metabolite names indicate those detected in the two ionisation modes and statistically significant in both (*) or only in the specific ionisation mode (#). The first coloured column indicates significance according to multi-group comparisons (Kruskal-Wallis with Benjamini-Hochberg adjustment). The remaining columns indicate the results of post hoc Dunn's test for comparisons between E.L and MM mice per diet. The colour gradient (pale yellow to brown) shows the strength of significance, and the grey arrows indicate the direction of changes as specified in the figure legend. **B** Same as in panel A, for negative ionisation mode. **C** Peak intensity of the individual metabolites exhibiting significant pairwise comparisons between the two colonisation groups in at least three of the four diets, measured in positive ionisation mode. These metabolites are marked with grey boxes in panel A. Dots represent the values for individual mice; black bars indicate median values; within each group, mice housed in different cages are indicated with empty or filled circles. Statistics: **p-adj. < 0.01, **** p-adj. < 0.0001, Kruskal-Wallis; for each metabolite, different letters indicate significance between the corresponding groups, Dunn's test. **D** Same as in panel A, for negative ionisation mode. Abbreviations: MM, mice colonised with the mouse synthetic community OMM12; E.L, mice colonised with OMM12 and *E. lenta*; CD, control diet; CD-BA, control diet supplemented with 0.1% CA and 0.1% CDCA; HFD, lard-based high-fat diet; HFD-BA, HFD supplemented with 0.1% CA and 0.1% CDCA. A previous version of this figure was published in Viehof *et al.* (2024).

In summary, *E. lenta* stably colonised the mouse caecum at high relative abundances. The presence of *E. lenta* had no significant effect on the liver proteome when compared to the effects of diets, whilst the colon metabolome differed significantly between the colonisation groups.

4.2 Comparison of gut physiology and metabolism in germfree and SPF mice on different diets

This chapter reports a gnotobiotic mouse experiment originally conducted to investigate the impact of colonisation with the CORIO consortium on host metabolism. GF mice were gavaged with a mixture of fresh cultures of the four CORIO strains: *A. mucosicola*, *C. aerofaciens*, *E. lenta*, and *L. parvula*. These CORIO mice were compared to GF and SPF mice. The mice were fed with four different semi-synthetic experimental diets for 12 weeks, which differed due to their fat content and the addition of primary BAs: experimental control diet (CD), CD supplemented with 0.1% CA and 0.1% CDCA (CD-BA), lard-based HFD (HDF), or lard-based HFD supplemented with 0.1% CA and 0.1% CDCA (HFD-BA). In a previous mouse study, CORIO mice were found to have higher plasma cholesterol levels, regardless of diet. Furthermore, WAT mass doubled and leptin levels increased in CORIO mice fed a diet supplemented with primary BAs (Just 2017). In the present mouse experiment however, the CORIO strains did not colonise the mouse gut. Further investigations have pointed at the semi-synthetic control diet hindering the engraftment of CORIO strains in the gut. Due to this, only the data obtained for the SPF and GF mice is presented in the following paragraphs.

The anatomy of the gut showed some marked differences between GF and SPF mice. The weight of the caecum was significantly reduced in SPF mice regardless of diet (**Figure 13A**). The diet also influenced the caecum weight in GF mice: the caecum weight of GF mice fed the CD diet was significantly higher than that of the GF mice fed all other diets (enriched in fat and/or BAs). Whilst the colon length was not affected by colonisation or diet, the small intestinal length was significantly and markedly decreased in SPF mice, regardless of diet (**Figure 13B**). Histological analysis of H&E-stained transversal sections of the distal small intestine did not reveal differences in villi length or width due to colonisation (**Figure 13C**). The only significant alteration was thicker villi in GF mice fed HFD-BA compared to GF mice fed CD-BA.

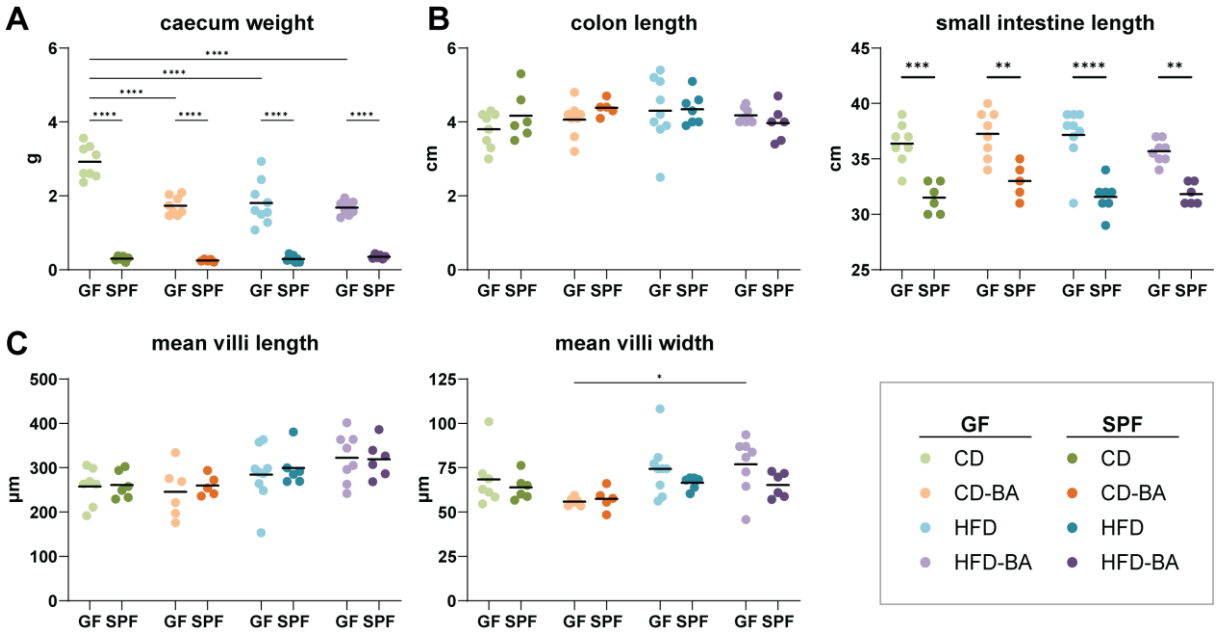

Figure 13: Differences in gut physiology of GF and SPF mice. A Weight of the caecum in g. **B** Length of the colon and small intestine in cm. **C** Mean villi length and width in µm measured from haematoxylin and eosin-stained sections of the distal small intestine. Five villi were measured per slide and one slide per mouse was analysed. Autolytic samples were excluded. In all figure panels, dots represent the values for individual mice and black bars indicate mean values. Statistics: * adj. $p < 0.05$, ** adj. $p < 0.01$, ***adj. $p < 0.001$, ****adj. $p < 0.0001$; two-way ANOVA followed by Tukey test; significant differences are only indicated for comparisons between the same colonisation or diet groups. Abbreviations: CD, control diet; CD-BA, control diet supplemented with 0.1% CA and 0.1% CDCA; HFD, lard-based high-fat diet with 48 kJ% fat; HFD-BA, high-fat diet supplemented with 0.1% CA and 0.1% CDCA.

Due to our previous results linking host metabolic phenotypes to gut colonisation with CORIO, an OGTT was conducted after 16 h fasting at the end of the experiment (12 weeks of feeding) prior to a µCT scan to quantify body fat volume. Regarding body weight before fasting, only SPF mice fed the lard-based HFD were significantly heavier than their GF counterparts (**Figure 14A**). In the other diet groups, no statistically significant differences of body weight before fasting were observed due to colonisation. Body weight was also significantly influenced by diet after the 12 weeks of experimental feeding. However, the changes observed were unexpected. In the GF groups, mice fed CD were heavier than those fed HFD or HFD-BA. Similarly, in the SPF groups, CD-fed mice had the highest body weight; it was significantly higher than the body weight of mice fed CD-BA or HFD-BA. All mice lost body weight during the 16h fasting, but the GF mice lost slightly more body weight then the SPF mice (12% vs. 9% mean body weight loss). After fasting, SPF mice fed the CD or HFD were significantly heavier than their respective GF counterparts. SPF mice fed the CD diet had a significantly higher body weight than SPF mice fed the CD-BA or HFD-BA. No significant differences of fasted body weight due to diet were observed in the GF group.

In contrast to the small differences in body weight due to colonisation (above), the percentage of subcutaneous and visceral fat was higher in SPF mice compared to GF mice for all diet groups, even though the values did not reach statistical significance in CD-BA mice (**Figure 14B**). In the SPF mice, visceral fat was increase in CD-fed compared to CD-BA-fed mice. Blood glucose levels over the course of the OGTT are plotted in **Figure 14C**. In general, blood glucose levels decreased faster in GF than in SPF mice. These observations were also confirmed by calculating the area under the curve (AUC), which was significantly higher for the SPF mice compared to the GF mice in all four diet groups, indicating a poorer glucose tolerance. No significant differences due to diet were observed for GF mice. For SPF mice, the AUC was significantly increased for mice fed HFD or HFD-BA compared to mice fed the CD or CD-BA diet, indicating that the high fat content of the diets resulted in impaired glucose tolerance.

The results of the µCT scans could also be used to quantify the lung volume and femur density of the mice (supplementary **Figure S1**). Lung volume was significantly increased in SPF compared to GF mice in all diet groups except HFD-BA. Some variation within the groups could be observed for femur density, with only one significant difference between GF mice fed CD-BA and HFD (higher in HFD-fed GF mice).

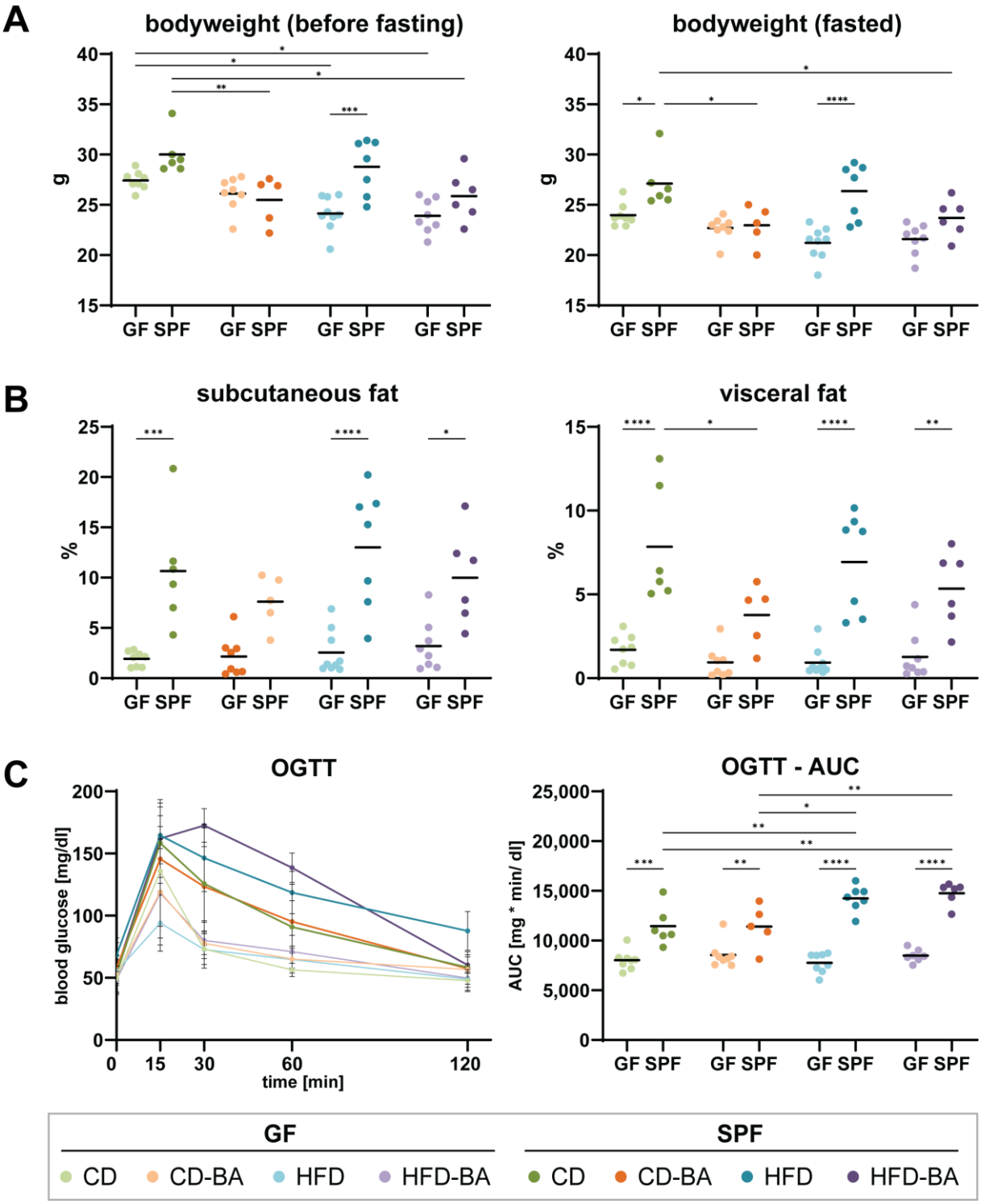

Figure 14: Effect of complex colonisation and diet on host metabolism. A Body weight measured at the end of the experiment before and after fasting of the mice. **B** Subcutaneous and visceral fat in % of the total body volume measured via µCT scans. **C** Blood glucose levels over the course of the OGTT shown as mean value for each colonisation/diet group. And the area under the curve (AUC) calculated for each mouse. In all figure panels, dots represent the values for individual mice and black bars indicate mean values. Statistics: * adj. $p < 0.05$, ** adj. $p < 0.01$, ***adj. $p < 0.001$, ****adj. $p < 0.0001$; two-way ANOVA followed by Tukey test; significant differences are only indicated for comparisons between the same colonisation or diet groups. Abbreviations: CD, control diet; CD-BA, control diet supplemented with 0.1% CA and 0.1% CDCA; HFD, lard-based high-fat diet with 48 kJ% fat; HFD-BA, high-fat diet supplemented with 0.1% CA and 0.1% CDCA.

As small intestine shortening occurred in all SPF mice, no matter which diet they were fed, we aimed to characterise their microbiota to assess the spectrum of microbial diversity and composition associated with the phenotype. Colonisation profiles in the caecum of the SPF mice were investigated by high-throughput 16S rRNA gene amplicon sequencing. An average of 36,431 ± 12,595 high-quality, assembled sequences were obtained per sample. The microbiota of the HFD-BA-fed mice were less diverse compared to the other diet groups, both in terms of richness and Shannon effective counts (**Figure 15A**). *Beta*-diversity analysis based on generalised UniFrac distances showed that the microbial communities differed significantly due to diet (p-value = 0.001, PERMANOVA) (**Figure 15B**). All six possible pairwise comparisons between the diet groups revealed statistically significant differences in microbiota profiles (adj. p-value <0.05, PERMANOVA). The following five phyla were detected, in descending ranking of relative abundances without significant changes between the diet groups: *Firmicutes* (current valid name: *Bacillota*), *Bacteroidota*, *Desulfobacterota* (current valid name: *Pseudomonadota*), *Deferribacterota*, and *Proteobacteria* (current valid name: *Pseudomonadota*) (**Figure 15C**). At the family level however, four families with minor significant differences were identified (**Figure 15D**). *Oscillospiraceae*, *Marinifilaceae* (other taxonomic placement: *Odoribacteraceae*), and *Ruminococcaceae* had the highest relative abundance in mice fed the CD-BA diet, while *Tannerellaceae* had the highest relative abundance in the HFD-BA group.

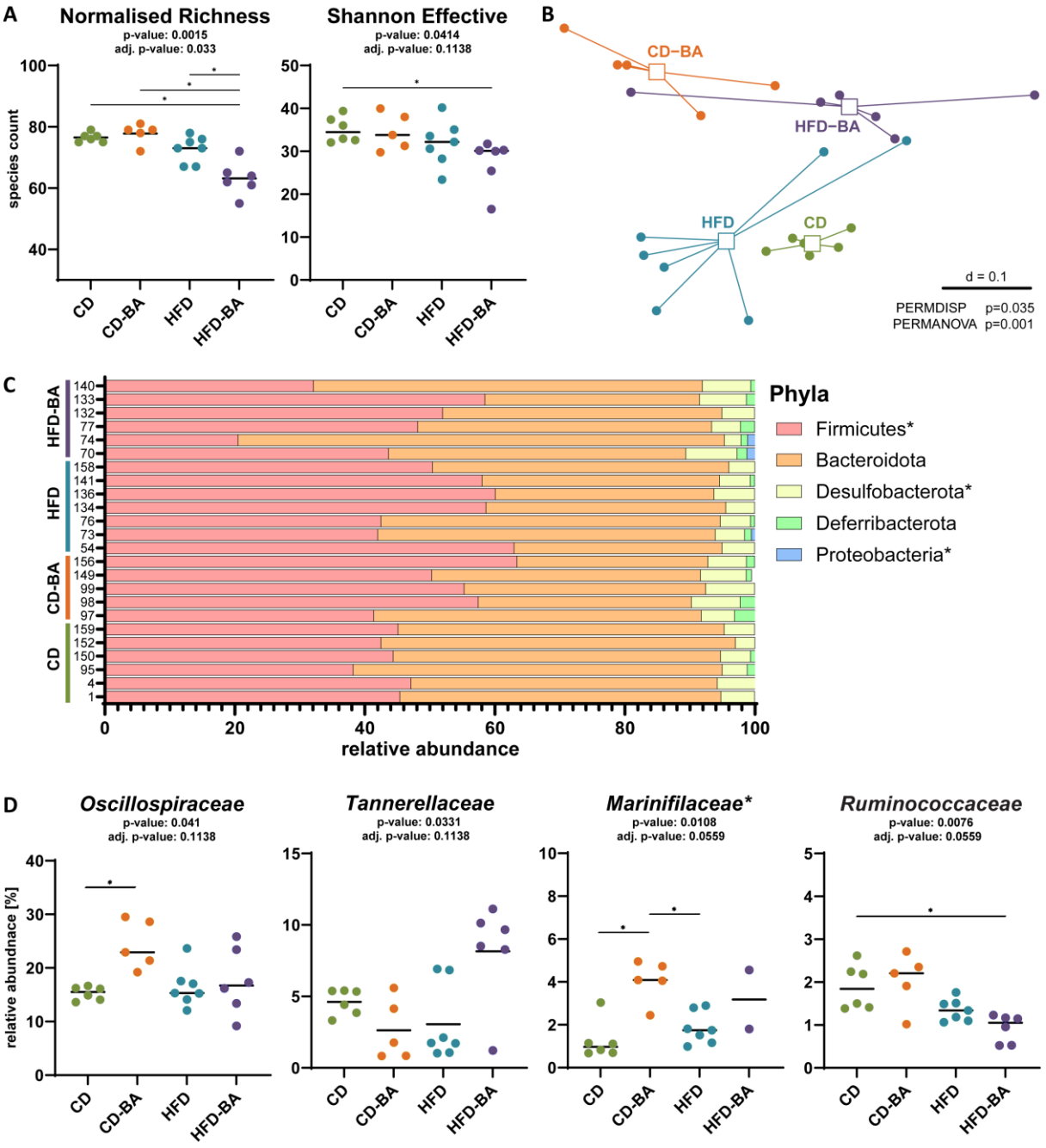

Figure 15: Caecal colonisation profiles in SPF mice fed different diets as analysed by 16S rRNA gene amplicon sequencing. **A** *Alpha*-diversity shown as normalised richness and Shannon effective counts. Dots represent individual mice, and black bars indicate median values. Results of Kruskal–Wallis test with and without Benjamini-Hochberg correction are stated on top of the graphs. Pairwise comparison was done by Mann-Whitney tests and significant results are indicated by stars (* adj. p < 0.05). **B** *Beta*-diversity analysis of diet groups shown as a multidimensional scaling plot of generalised UniFrac distances. **C** Stacked bar plots for phyla that were detected with a minimum prevalence of 30% mice in at least one group and a minimum relative abundance of 0.5%. Phyla names marked with stars are not validly published. The current valid names are: *Bacillota* (synonym *Firmicutes*); *Pseudomonadota* (synonym *Desulfobacterota*); *Pseudomonadota* (synonym *Proteobacteria*). **D** Families with significant alterations between the diet groups. Data visualisation and statistical analysis are as in panel A. The family name *Marinifilaceae* is marked with a star as the correct taxonomic classification is *Odoribacteraceae.* Abbreviations: CD, control diet; CD-BA, control diet supplemented with 0.1% CA and 0.1% CDCA; HFD, lard-based high-fat diet with 48 kJ% fat; HFD-BA, high-fat diet supplemented with 0.1% CA and 0.1% CDCA.

In summary, due to the lack of colonisation of the CORIO strains, only the GF and SPF control mice were compared in this experiment. The small intestine was significantly elongated in GF mice compared to SPF mice regardless of diet and varying microbiota profiles in the SPF mice. The percentage of subcutaneous and visceral fat was increased in SPF mice, and OGTT results indicated a poorer glucose tolerance in SPF mice, particularly in the HFD groups, compared to GF mice.

4.3 Influence of *Collinsella aerofaciens* on lipid absorption

This chapter presents the results of experiments conducted to specifically investigate the influence of the lipase-positive *Coriobacteriia* species, *C. aerofaciens,* on lipid absorption in the gut. Following an examination of 14 in-house *C. aerofaciens* isolates and the type strain regarding lipase activity and their ability to metabolise CA, two gnotobiotic mouse experiments were conducted to study the effect of *C. aerofaciens* DSM 3979^T on lipid absorption *in vivo*.

C. aerofaciens strains isolated from human faecal samples (n = 14) and the type strain (DSM 3979^T) were analysed to test for differences in their lipolytic activity. **Figure 16** shows a phylogenetic tree with all isolates analysed together with additional *Collinsella* genomes from the literature. Only one isolate per faecal sample was included unless a clear difference in colony morphology or growth features in liquid culture was observed between two strains isolated from the same donor. All 14 in-house isolates and the type strain showed lipolytic activity *in vitro* using the rhodamine B plate assay with olive oil. Exemplary results are presented in **Figure 17A**. It was further tested whether the lipolytic activity could be detected in the supernatant or pellet of bacterial cultures grown in BHI medium with olive oil. All isolates showed lipolytic activity in the pellets (also when washed), whereas no activity was observed in the supernatant (**Figure 17B** and **C**). This may indicate that the lipolytic activity is cell-bound. For the type strain, five potential lipase genes had previously been predicted *in silico* by Streidl and Hitch (Streidl 2021). To determine whether the isolates also encoded for these genes, a protein BLAST was performed to search for matches between the five protein sequences and genes within the isolate's genomes. The potential lipase genes #1 and #3 had positive matches for only a few isolates, whereas lipase genes #2, #4 and #5 were identified in all isolates. Submission of the five potential lipase genes sequences to the transmembrane helices prediction tool TMHMM indicated that only gene #5 had a high probability of containing a transmembrane region, which could be a reason for the observed cell-bound lipase activity.

Due to *C. aerofaciens* DSM 3979^T being also able to metabolise BAs, conversion of the primary BA CA was also tested. The reduction in CA concentration in the medium was quantified after 48 hours of incubation in anaerobic BHI broth containing 50 µM CA. The concentration of CA was decreased in all cultures, yet variations in the efficacy of conversion were observed. The lowest decrease in CA concentration occurred with strain CLA-ER-H9 (1%), while the greatest decrease was observed for strain CLA-AA-H167 (40%). Most of the isolates exhibited a CA decrease between 10 and 20%.

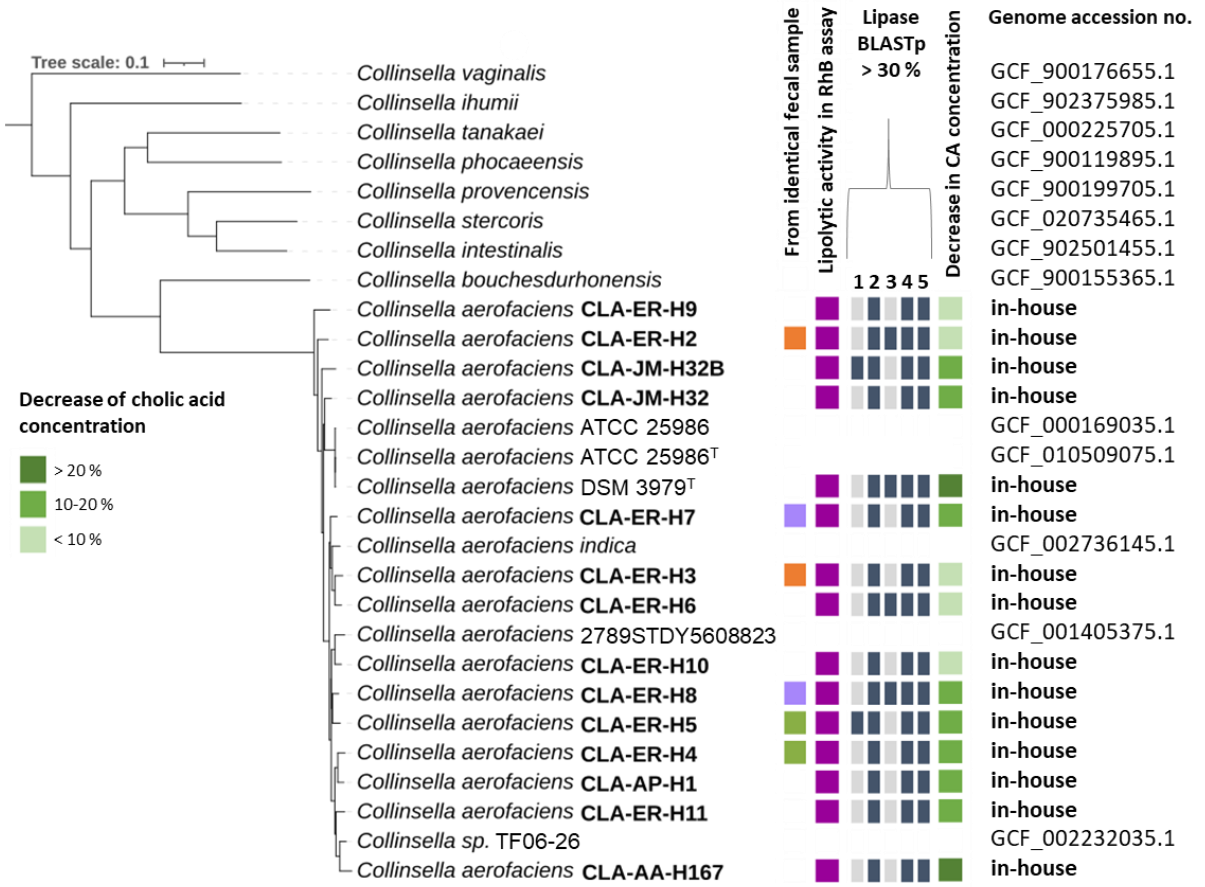

Figure 16: Genome-based phylogenetic tree of the *C. aerofaciens* isolates and additional *Collinsella* genomes. The tree (maximum likelihood method) was created with Phylophlan and visualised in iTOL. The tree is rooted to *Coriobacterium glomerans* (genome accession GFC_000195315.1). In-house strains isolated from the same individual have the same color in row 1. All in-house isolates showed *in vitro* lipolytic activity in the rhodamine B (RhB) plate assay (violet boxes in row 2). BLASTp matches to protein sequences of predicted lipases 1-5 are displayed in dark grey boxes, while light grey boxes indicate negative results (row 3-7). The decrease in CA concentration after 48 hours incubation is indicated by a green colour gradient (row 8; see legend for the values).

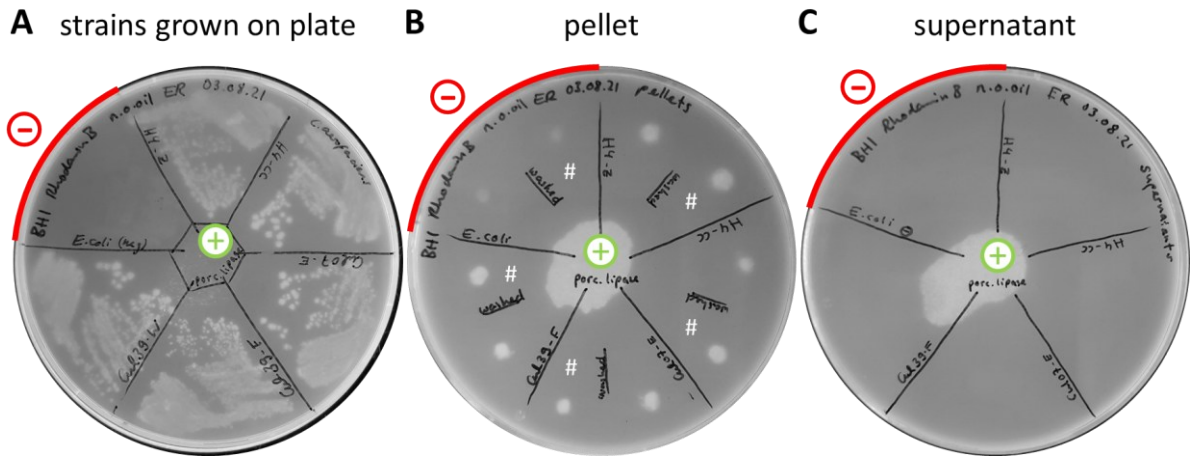

Figure 17: Lipolytic activity of exemplary *C. aerofaciens* isolates using the rhodamine B agar assay. Lipolytic activity indicated by fluorescence on rhodamine B plates with olive oil detected under UV light (302nm). Fluorescent areas appear white on the images of the agar plates, which otherwise have a grey background. *E. coli* used as negative control is marked with a red line with a minus symbol (-); 20 µL porcine pancreatic lipase [20 g/L] used as positive control is marked with a green plus symbol (+). **A** Exemplary *C. aerofaciens* isolates (CLA-ER-H4, CLA-ER-5, CLA-ER-6, CLA-ER-7, CLA-ER-H8) were grown on the plate. **B** Unwashed pellets and pellets washed in PBS (marked with # symbol) were applied to the plate for four exemplary *C. aerofaciens* strains (CLA-ER-H4, CLA-ER-5, CLA-ER-6, CLA-ER-7) and the negative *E. coli* control. **C** Corresponding culture supernatant was pipetted onto the plate, showing no lipolytic activity.

As no variation in the lipolytic activity of *C. aerofaciens* isolates could be observed, the two gnotobiotic mouse experiments were conducted with the type strain *C. aerofaciens* DSM 3979^T, which was also used in the previous mouse experiments (Chapter **4.2** and Just 2017). All mice were either colonised with *C. aerofaciens* DSM 3979^T, SPF gut microbiota, or remained GF and were fed with two different diets for a period of two weeks: chow diet supplemented with 0.1% CA and 0.1% CDCA (chow-BA), or chow diet with 20% palm oil (chow-HFD). At the end of the experiment, mice were gavage with deuterium-labelled lipids and subsequently sampled after one (chow-BA) or six (chow-HFD) hours to investigate the absorption of the isotope-labelled lipids. The time points were chosen due to previous experiments in the laboratory of our collaborator (AG Ecker; personal communication). The gavage consisted of 100 µl of olive oil supplemented with a mixture of D5-palmitic acid and D93-tripalmitin. While D5-palmitic acid can be absorbed directly by the enterocytes, D93-tripalmitin must be hydrolysed by lipases before the resulting D31-palmitic acid can be absorbed. Due to the different number of deuterium atoms (D5 vs. D31), mass spectrometric methods can be used to determine whether the absorbed and metabolised palmitic acid molecules originate from the free FA or the triglyceride. In this way, both the absorption of FAs and the influence of lipases can be analysed.

The combined results of the two mouse experiments are presented below. The main differences between the experiments were: (i) the first experiment was carried out with both, male and female mice, whilst the second experiment included only male mice; (ii) mice in the second experiment were obtained from Charles River rather than our own GF breeding colony (due to a contamination) and

they were slightly older at the start of the experiment (six vs. five week of age); (iii) more diet-time point combinations were investigated in the first mouse experiment (three diets with two time points each), whilst the second experiment included only the most interesting groups (chow-BA sampled one hour after gavage, and chow-HFD sampled six hours after gavage).

Prior to analysing lipid absorption, it was important to assess the colonisation status of the mice. To quantify *C. aerofaciens* colonisation in the different gut regions, the number of CFUs was calculated for three mice per diet group (**Figure 18A**). *C. aerofaciens* was detected in all gut regions. The number of CFUs was expectedly lower in the small intestine than in the caecum and colon. When comparing the mice fed the chow-BA and chow-HFD diets (experiment 2), a higher count of CFUs was observed in the caecum and colon of the mice due to a higher fat content in chow-HFD. In addition, the caecum content of *C. aerofaciens*-monocolonised mice was analysed by 16S rRNA gene amplicon sequencing. Only one OTU with 100% similarity to *C. aerofaciens* DSM 3979^{T} and no other contaminants were detected (data not shown). Also, colonisation profiles in the caecum of SPF mice from experiment 2 were analysed using 16S rRNA gene amplicon sequencing to investigate whether the different diets led to large differences in the microbiota profiles of the SPF mice, which could possibly influence lipid absorption. The mean number of high-quality, assembled sequences obtained per sample was 27,442 ± 6,060. *Beta*-diversity analysis based on generalised UniFrac distances revealed a significant separation between the microbiota profiles of the two diet groups (chow-BA and chow-HFD, PERMANOVA p=0.009, **Figure 18B**). Mice fed the chow-HFD had a significantly higher richness compared to the mice fed chow-BA (**Figure 18C**). Among the phyla with significant differences between the two diet groups, *Bacteroidota* and *Proteobacteria* (current valid name: *Pseudomonadota*) were increased in the chow-BA group, while *Firmicutes* (current valid name: *Bacillota*) was decreased (**Figure 18D**). At the family level, *Muribaculaceae* and *Tannerellaceae* (both phylum *Bacteroidota*) were increased in the chow-BA group, while *Lachnospiraceae* (phylum *Firmicutes*) and *Rikenellaceae* (phylum *Bacteroidota*) were decreased (**Figure 18E**).

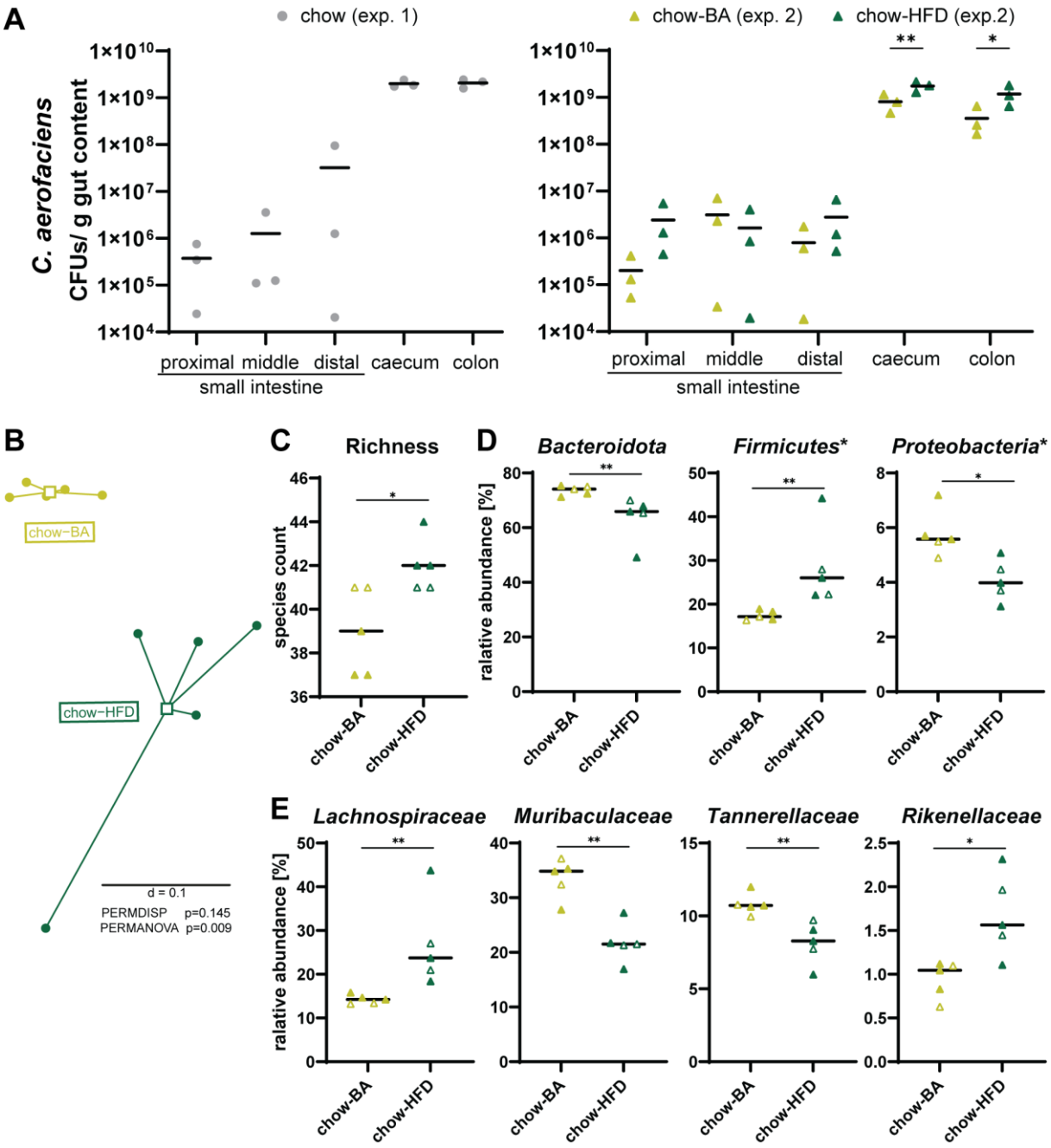

Figure 18: Colonisation of *C. aerofaciens*-monocolonised and SPF mice. A Colony forming units (CFUs) per gram of gut content from *C. aerofaciens*-monocolonised mice in different gut regions. Data for experiment 1 (chow, female mice) and 2 (chow-BA and chow-HFD, male mice) are shown separately. Symbols represent individual mice, and black bars indicate mean values. Stars indicate significant results using two-way ANOVA followed by Tukey test for comparisons between diet groups within the same gut region (* adj. $p < 0.05$, ** adj. $p < 0.01$). **B-E** Caecal colonisation profiles in SPF mice in experiment 2 as analysed by 16S rRNA gene amplicon sequencing. **B** *Beta*-diversity analysis of diet groups shown as a multidimensional scaling plot of generalised UniFrac distances. **C** Richness. Symbols represent individual mice, filled and non-filled triangles represent different cages (male mice only). Black bars indicate median values. Significant results of Mann-Whitney tests are indicated by stars (* adj. $p < 0.05$, ** adj. $p < 0.01$). **D** Phyla with significant changes between the diet groups. Phyla names marked with stars are not validly published. The current valid names are: *Bacillota* (synonym *Firmicutes*) and *Pseudomonadota* (synonym *Proteobacteria*). Data visualisation and statistical analysis are as in panel C. **E** Families with significant changes between the diet groups. Data visualisation and statistical analysis are as in panel C. Abbreviations: chow-BA, chow diet supplemented with 0.1% CA and 0.1% CDCA; chow-HFD, chow with 20% palm oil.

To study the effect of *C. aerofaciens* and diet on lipid absorption, the FA profiles in the plasma of the mice were measured (combined data from experiment 1 and 2). PCA showed that the combination of diet and timepoint (**Figure 19A**), but not colonisation (**Figure 19B**), influenced the overall FA profiles. Furthermore, no separation was observed between colonisation groups when analysing each diet group separately (**Figure 19C-D**).

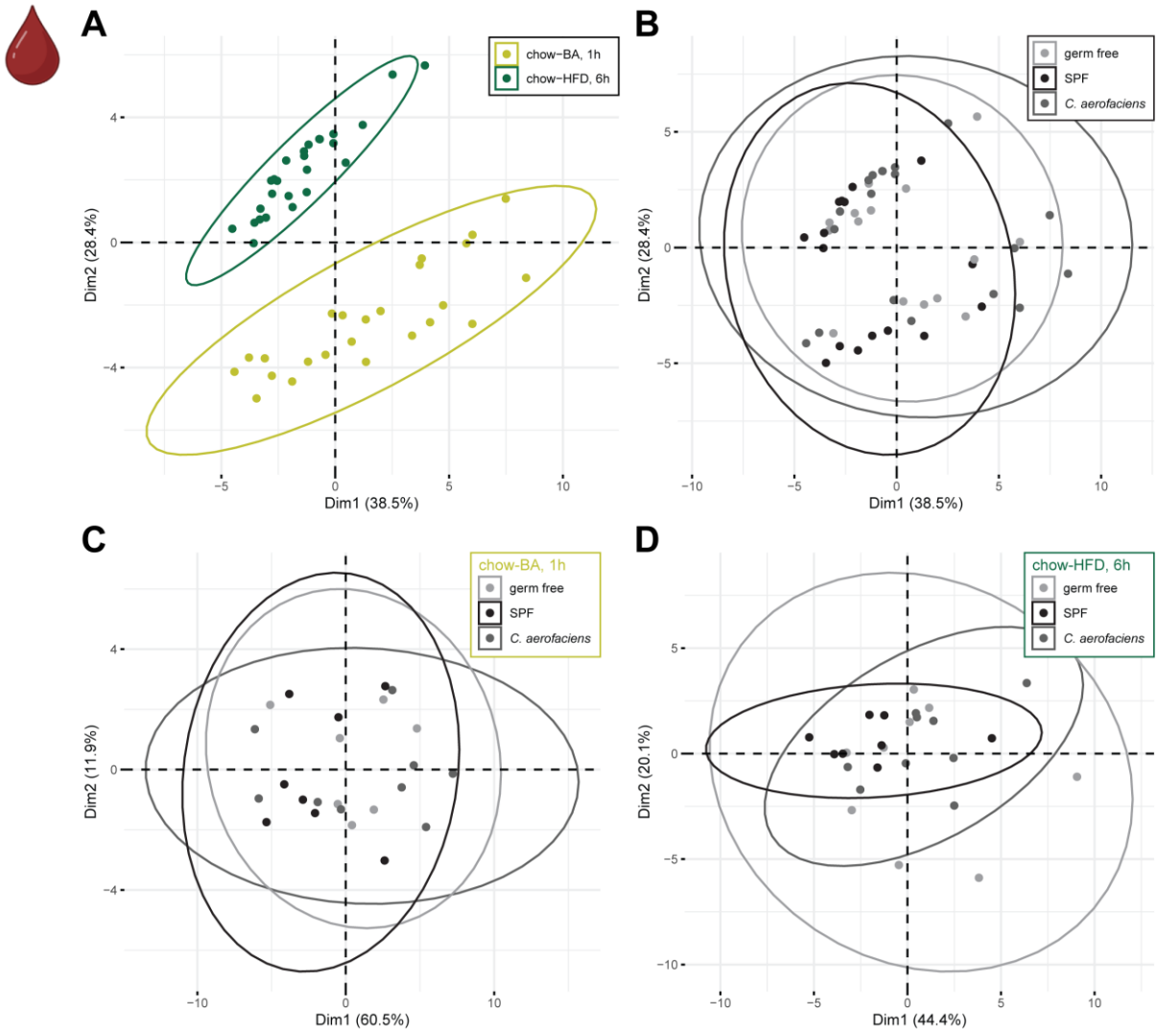

Figure 19: Effects of *C. aerofaciens*-monocolonisation and diet on fatty acid profiles in the plasma of gnotobiotic mice. Principal component analysis (PCA) of all measured fatty acids (FAs) for mice fed with chow-BA, sampled after one hour, and those fed chow-HFD, sampled after six hours. The combined data set was derived from experiments 1 and 2. **A** PCA according to diet. **B** PCA according to colonisation. **C** PCA only for mice fed with chow-BA, sampled after one hour, according to colonisation status. **D** PCA only for mice fed chow-HFD, sampled after six hours, according to colonisation. Abbreviations: chow-BA, chow diet supplemented with 0.1% CA and 0.1% CDCA; chow-HFD, chow with 20% palm oil.

We then investigated the occurrence of FA categories and single FAs, especially those labelled with stable isotopes, in the plasma of the mice. The median concentrations of total FAs, saturated FAs

(SAFAs), monounsaturated FAs (MUFAs), and polyunsaturated FAs (PUFAs) were highest for *C. aerofaciens* mice and lowest for SPF mice, with the exception of the MUFA concentration in mice fed the HFD, which exhibited the highest median concentration in GF mice (**Figure 20A**). However, nearly all comparisons did not reach statistical significance, likely due to marked inter-individual differences, with the exception of SAFA concentrations, which were significantly increased in the plasma of *C. aerofaciens* vs. SPF mice fed the HFD and sampled six hours after gavage with the labelled lipids. A similar trend (highest concentrations in the blood of *C. aerofaciens*-monocolonised mice) was observed for the concentrations of deuterium-labelled FAs from the gavage solution (**Figure 20B**). However, results did not reach statistical significance for the mice fed the chow-BA diet sampled one hour after gavage. In the plasma of the mice fed the chow-HFD and sampled after six hours, the D5-palmitic acid concentration was significantly increased in both the *C. aerofaciens*-monocolonised and GF mice compared to the SPF mice. Similarly, the D31-palmitic acid concentration was significantly elevated in the *C. aerofaciens*-monocolonised mice compared to the SPF mice. To assess the role of lipase in the absorption of the deuterium-labelled lipids, the log2 of the ratio between D31-palmitic acid, which originates from D93-tripalmitin hydrolysed by lipases, and free D5-palmitic acid was calculated (**Figure 20C**). For the mice fed the chow-BA diet and sampled one hour after gavage, all median values were <0, indicating that there was more uptake from the free FA D5-palmitic acid. In contrast, the median values for the mice fed the chow-HFD and sampled six hours after gavage were all >0, indicating a greater uptake of FAs originating from the triglyceride D93-tripalmitin than from the already free FA D5-palmitic acid. No significant differences were observed between the colonisation groups.

In general, the data from experiments 1 and 2 were comparable and merged (as illustrated by lighter and darker colour of the symbols in **Figure 20**). In the initial experiment, sex differences were observed, particularly for the concentration of D5- and D31 palmitic acid in the plasma of *C. aerofaciens*-monocolonised mice fed the chow-BA diet and sampled after one hour (dots in the lighter colour represent female mice and triangles in the lighter colour represent the male mice in experiment 1 in **Figure 20**). The data from experiment 2, which was conducted only with male mice, tended to cluster together with the data of the female mice, rather than with the high value of male mice in experiment 1.

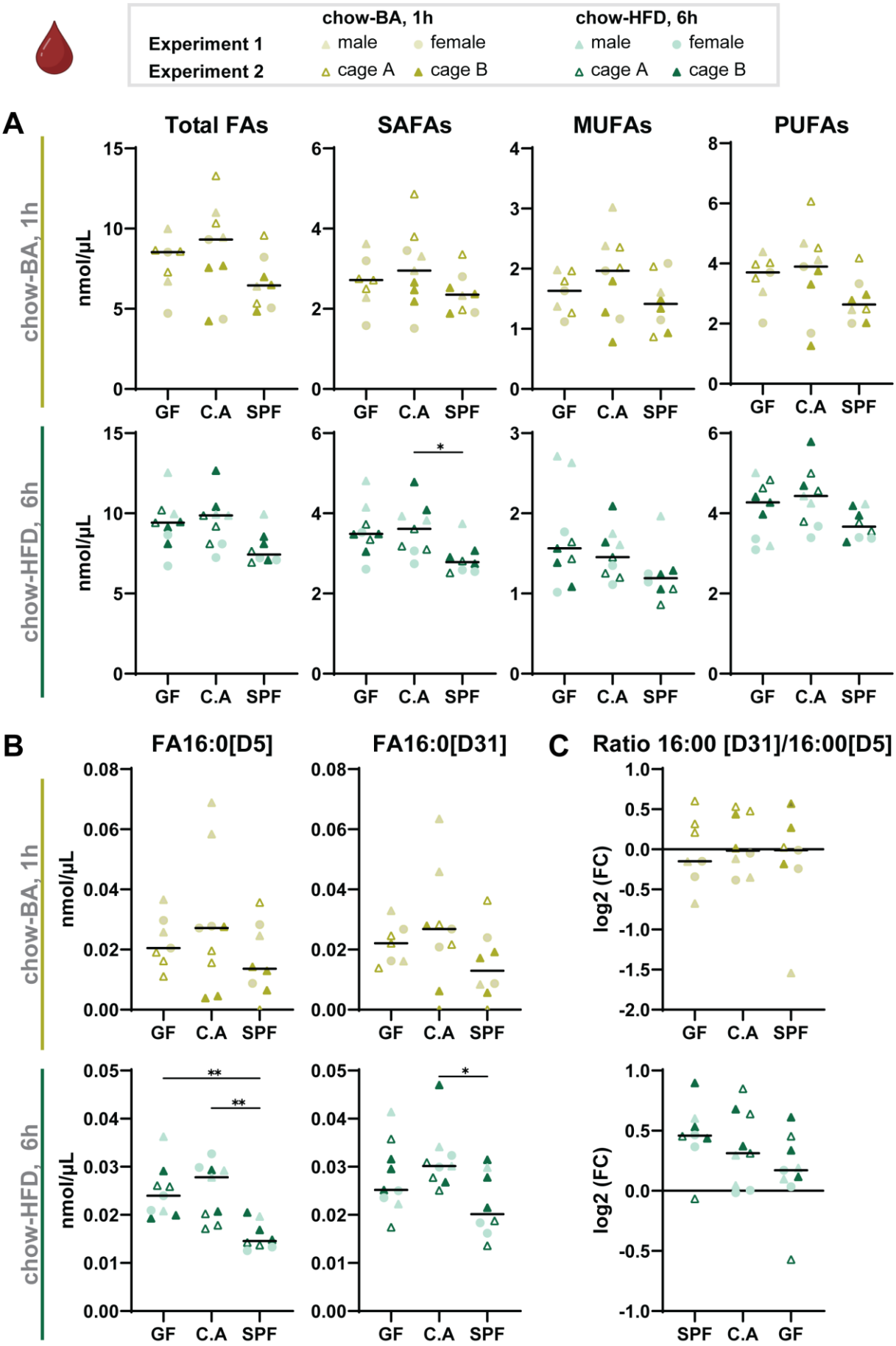
chow-BA, 1h
chow-HFD, 6h
Experiment 1
Experiment 2
male
female
cage A
cage B
A
Total FAs
SAFAs
MUFAs
PUFAs
nmol/µL
GF
C.A
SPF
*
B
FA16:0[D5]
FA16:0[D31]
**
C
Ratio 16:00 [D31]/16:00[D5]
log2 (FC)

Figure 20: Effects of *C. aerofaciens*-monocolonisation on fatty acids composition and absorption of isotope-labelled fatty acids measured in plasma. Fatty acids (FAs) measured in plasma of mice fed with a chow-BA, sampled after one hour, and mice fed a chow-HFD, sampled after six hours. The combined data set was derived from experiments 1 and 2, symbols in lighter and darker colour, respectively. Dots represent female mice and triangles represent male mice. Filled and non-filled triangles in the darker colour represent different cages in experiment 2. Black bars indicate median values. Statistics: Kruskal-Wallis followed by posthoc Dunn test for pairwise comparisons (* adj. $p < 0.05$, ** adj. $p < 0.01$). **A** General FA composition in plasma**:** total FAs, saturated FAs (SAFAs), monounsaturated FAs (MUFAs), and polyunsaturated FAs (PUFAs). **B** Deuterium-labelled FAs that were absorbed from the gavage solution: palmitic acid labelled with 5 deuterium atoms (FA16:0[D5]), and palmitic acid labelled with 31 deuterium atoms (FA16:0[D31]) originating from the labelled triglyceride. **C** Ratio of FA16:0[D31] to FA16:0[D5]. Abbreviations: GF, germfree mice; C.A, *C. aerofaciens*-monocolonised mice; SPF, mice colonised with microbiota from SPF mice; chow-BA, chow diet supplemented with 0.1% CA and 0.1% CDCA; chow-HFD, chow with 20% palm oil.

The FA profiles were also measured in colon tissue from the mice in experiment 2 fed the chow-HFD and sampled six hours after the gavage (**Figure 21**). The colon tissue of mice fed the chow-BA diet and sampled one hour after gavage was not analysed, as it was not expected to detect any of the labelled lipids in the colon tissue within only one hour after the gavage. In the colon tissue of mice fed the chow-HFD, the concentrations of total FAs, SAFAs, MUFAs and PUFAs were all lowest in *C. aerofaciens*-monocolonised mice and highest in SPF mice, although the differences reached statistical significance only in the case of MUFA concentrations (**Figure 21A**). The deuterium-labelled FAs D5- and D31-palmitic acid had also the lowest concentrations in the colon of *C. aerofaciens*-monocolonised mice, though the differences were not statistically significant (**Figure 21B**). The values for the log2 of the ratio between D31-palmitic acid and D5-palmitic acid also exhibited no significant differences between the colonisation groups (**Figure 21C**). The median value for the *C. aerofaciens* mice was close to 0, while the median values for GF and SPF mice were observed to be >0, indicating equal or higher uptake of D31- vs. D5-palmitic acid, respectively.

The FA profiles were also measured in liver tissue of the mice from experiment 1 and in the epididymal WAT of chow-HFD fed mice from experiment 2 (data not shown). No statistically significant differences were observed between the colonisation groups regarding the concentrations of the deuterium-labelled FAs.

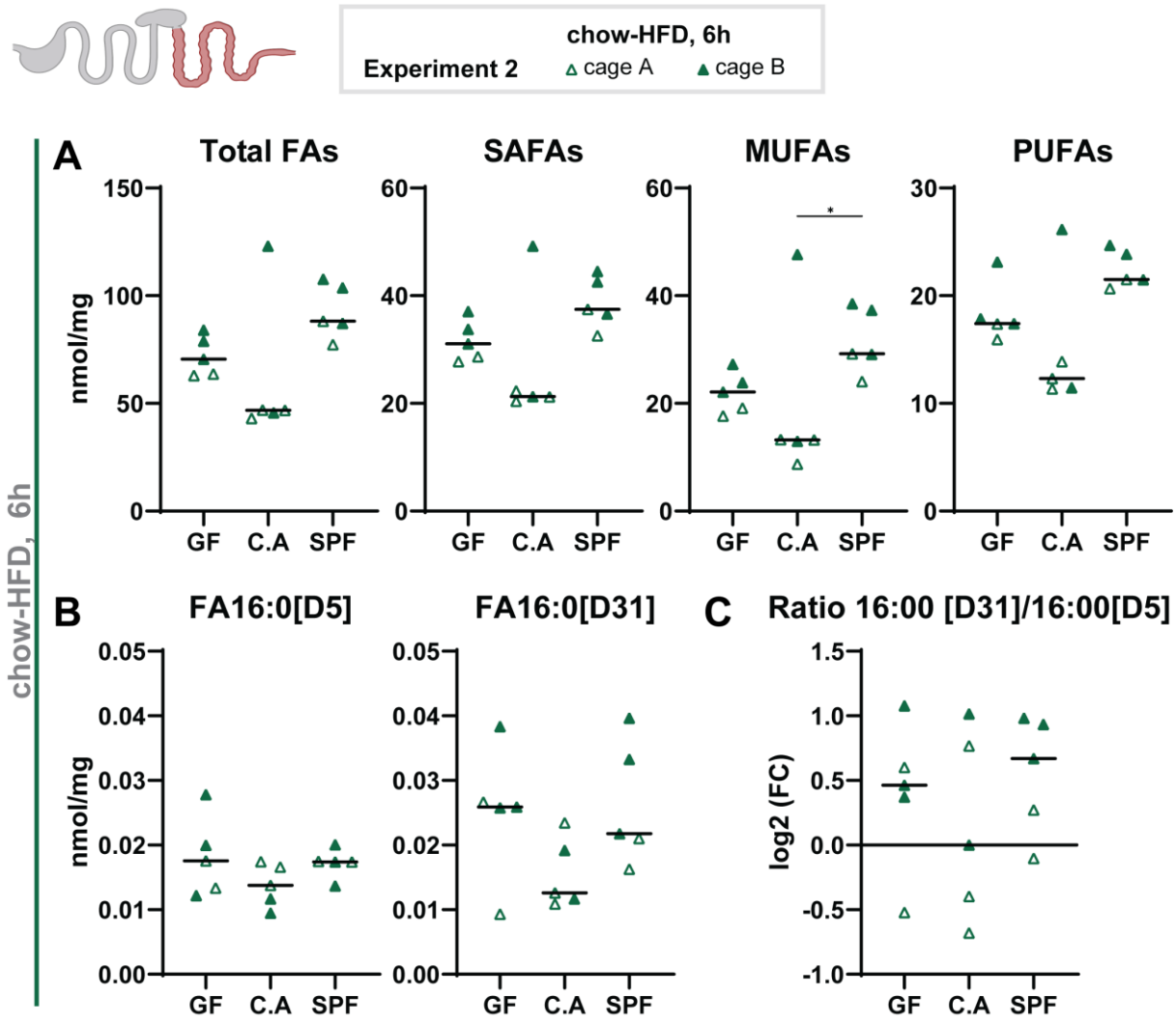

Figure 21: Effects of *C. aerofaciens*-monocolonisation on fatty acids composition and absorption of labelled fatty acids measured in colon tissue. Fatty acids (FAs) measured in colon tissue of mice from experiment 2 fed a chow-HFD, sampled after six hours. Filled and non-filled triangles in the darker colour represent different cages. Black bars indicate median values, and symbols individual mice. Statistics: Kruskal-Wallis followed by posthoc Dunn test for pairwise comparisons (* adj. $p < 0.05$). **A** General FA composition in colon tissue**:** total FAs, saturated FAs (SAFAs), monounsaturated FAs (MUFAs), and polyunsaturated (PUFAs). **B** Deuterium-labelled FAs that were absorbed from the gavage solution: palmitic acid labelled with 5 deuterium atoms (FA16:0[D5]), and palmitic acid labelled with 31 deuterium atoms (FA16:0[D31]) originating from the labelled triglyceride. **C** Ratio of FA16:0[D31] to FA16:0[D5]. Abbreviations: GF, germfree mice; C.A, *C. aerofaciens*-monocolonised mice; SPF, mice colonised with microbiota from SPF mice; chow-HFD, chow with 20% palm oil.

In summary, all 14 in-house *C. aerofaciens* isolates analysed possessed cell-bound lipolytic activity and were able to metabolise CA (albeit with different efficacy in the latter case). In the gnotobiotic experiments performed to study lipid absorption in the gut, the *C. aerofaciens* type strain colonised all regions of the gut, with higher cell densities in the caecum and colon. In mice fed chow-BA and sampled one hour after gavage, and in mice fed chow-HFD and sampled six hours after gavage, the median levels of total FAs and deuterium-labelled FAs were highest in the blood of *C. aerofaciens*-monocolonised mice, with statistical significance only for chow-HFD fed mice sampled six hours after gavage compared to SPF mice.

4.4 Occurrence of lipase-positive bacteria in human stool from a population study

In this chapter, a nested cohort (n = 348) of the KORA population study (Cooperative Health Research in the Region of Augsburg) was analysed to investigate whether the presence of lipase-positive bacteria in human stool, including *C. aerofaciens*, was associated with host metabolic parameters.

The KORA cohort is a population-based study in the Augsburg region (Germany), focusing on diabetes, cardiovascular diseases, health in old age, allergies and the environment (Bamberg *et al.* 2017; Holle *et al.* 2005). In total, 17,602 participants are included in KORA (baseline surveys from 1984 to 2001), but for this analysis, 338 participants with available faecal microbiota profiles and body composition data from MRI scans were examined. Participants taking antibiotics were excluded from the analysis. All participants were adults aged between 39 and 73 years, with the majority being 40-69 years of age (**Figure 22A**). The cohort was slightly skewed towards males (58%) (**Figure 22A**). According to BMI classification, only one participant was underweight (BMI <18.5), 27% were in the normal range (BMI ≥18.5 - <25), 42% were overweight (BMI ≥25 - <30), and 31% were obese (BMI ≥30) (**Figure 22A**).

Faecal colonisation profiles were analysed by 16S rRNA gene amplicon sequencing. Samples with less than 5,000 reads per sample were excluded from the analysis. The mean number of high-quality, assembled reads obtained per sample was 35,994 ± 17,846. The median normalised richness for all participants was 71.5 (**Figure 22B**). The top five detected phyla were as follows (**Figure 22C**): *Firmicutes* (current valid name: *Bacillota*) was the most abundant phylum with a median relative abundance of 73%, followed by *Bacteroidota* (16%), *Actinobacteriota* (current valid name: *Actinomycetota*) (6%), *Proteobacteria* (current valid name: *Pseudomonadota*) (0.9%), and *Verrucomicrobiota* (0.1%). To identify potential confounding variables that were influenced by microbiota profiles, *de novo* clustering was applied, identifying three native microbiota clusters (**Figure 22D**), which differed in their relative abundance of the genera *Prevotella/Segatella* (cluster 3)*, Bacteroides* (cluster 2)*,* and *Ruminococcus* (cluster 1) (**Figure 22E**). One-way ANOVA analysis was then performed to identify variables (i.e., host parameters) with significant differences between the three clusters. After correction for multiple testing using the Benjamini-Hochberg test, none of the tested variable showed statistically significant differences between the clusters. Descriptive statistics and the results of the one-way ANOVA are shown in supplemental **Table S1**. In addition, a Chi^2 test was performed to test for differences between the microbiota clusters for categorical variables, such as the intake of antidiabetic medication (test was performed separately for cluster 1 vs. 2, 1 vs. 3, and 2 vs.3). Again, all adjusted p-values (Benjamini-Hochberg) were >0.05. As no confounders associated with the microbiome could be identified with this method, the results of regression analysis were corrected only for the standard confounding factors age and sex.

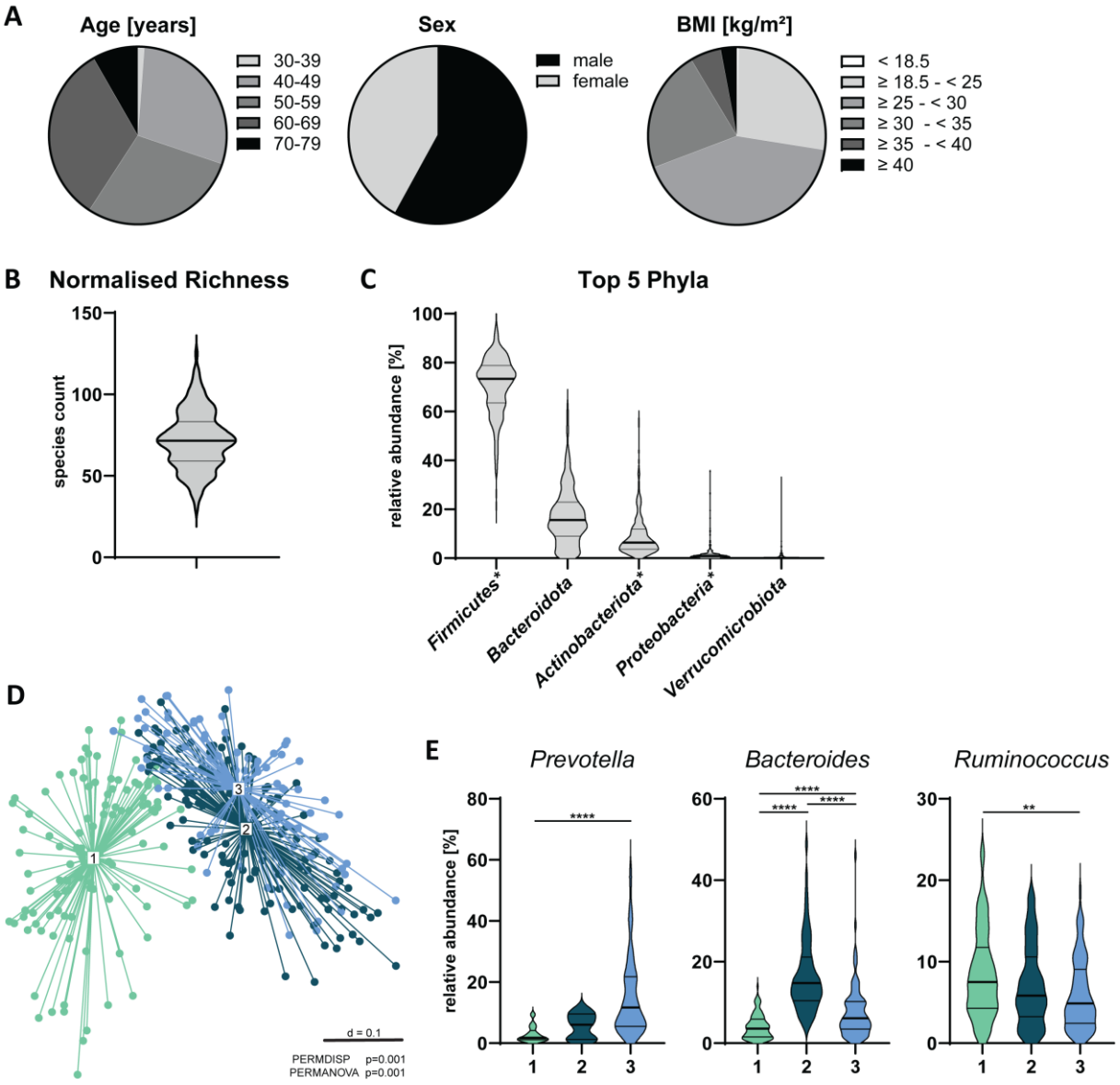

Figure 22: Description of the nested KORA cohort analysed in this work. A Pie charts displaying the distribution of age, sex and BMI of the 338 participants. **B-E** Faecal colonisation profiles analysed by 16S rRNA gene amplicon sequencing. Thick black lines in the violin plot indicate the median, and thin black lines the quartiles. **B** *Alpha*-diversity shown as normalised richness. **C** Relative abundance of the top five phyla. Phyla names marked with stars are not validly published. The current valid names are: *Bacillota* (synonym *Firmicutes*); *Actinomycetota* (synonym *Actinobacteriota*); *and Pseudomonadota* (synonym *Proteobacteria*). **D** *Beta*-diversity analysis of three *de novo* clusters (cluster 1, n = 109; cluster 2, n = 140; cluster 3, n = 89) shown as a multidimensional scaling plot of generalised UniFrac distances. **E** Relative abundances of the genera *Prevotella/Segatella*, *Bacteroides,* and *Ruminococcus* for the three *de novo* clusters. Significant results of Mann-Whitney tests are indicated by stars (** adj. p < 0.01, **** adj. p < 0.0001).

To calculate the cumulative relative abundance of lipase-positive bacteria, the results of an *in vitro* screening of human gut bacteria (www.hibc.rwth-aachen.de) for lipolytic activity in the rhodamine B plate assay were used. This screening resulted in 15 lipase-positive strains, including *C. aerofaciens*. The cumulative relative abundance of all OTUs with >97% identity to these lipase-positive strains was calculated and is referred to as the lipase-positive fraction (see material and methods section **3.5.3** for details).

The relative abundance of the lipase-positive fraction in the stool of all 338 participants ranged from 2.8% to a maximum of 65.1% with a median value of 25.7% (**Figure 23A**). The lipase-positive fraction was significantly higher in male compared to female participants. No significant correlation was observed between participants age and the lipase-positive fraction (**Figure 23B**). The baseline characteristics of the analysed 338 participants stratified by quartiles of the lipase-positive fractions are listed in **Table S2** for all categorical variables and **Table S3** for all continuous variables.

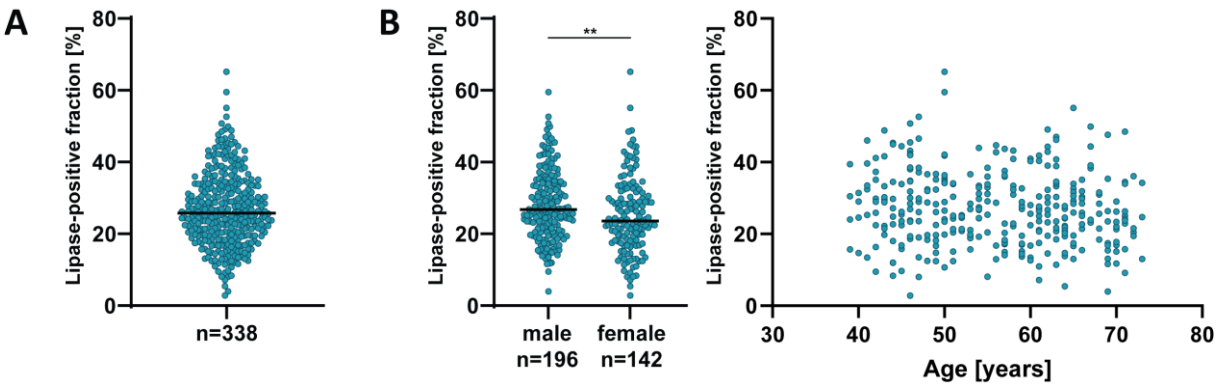

Figure 23: Distribution of the lipase-positive fraction of bacteria in human stool. A Relative abundance of the lipase-positive fraction for all 338 analysed KORA participants. **B** Plots of the potential confounders sex and age in relation to the lipase-positive fraction [%]. Dots represent individual participants, and the black bars mark the median. Significant results of Mann-Whitney test are indicated by stars (** $p < 0.01$).

To investigate whether the lipase-positive fraction in faecal microbiota of the KORA participants was associated with metabolic parameters, a multiple linear regression analysis was performed. As mentioned above, the regression analysis was corrected for the standard confounders age and sex, as no microbiome related confounders were identified when comparing the three *de novo* clusters. The p-value of the lipase-positive fraction corrected for age and sex, was < 0.05 for eleven of the dependent variables (**Table 3** and **Figure 24**). The most significant results were observed for the visceral fat at the level of the naval (p-value < 0.001); blood triglyceride levels were also highly significant (p-value = 0.002). The remaining dependent variables with statistically significant results (p-values between 0.018 and 0.045) were: fat content of the right liver lobe, insulin levels measured two hours after an OGTT, total fat from femoral head to cardiac apex, dietary fibre intake, visceral fat from femoral head to cardiac apex, fat content of the left liver lobe, mean fat content at the level of the portal vein, BMI, and LDL cholesterol. For ten of the eleven variables with a significant result, a positive relationship to the lipase-positive fraction was observed. Fibre intake was the only variable negatively associated with the lipase-positive fraction (i.e., higher fibre intake was linked to lower lipolytic fraction). **Figure 24**

depicts the relationship between the aforementioned variables and the lipase-positive fraction in dot plots.

Table 3: Multiple linear regression analysis for the lipase-positive fraction of bacteria in stool corrected for age and sex. Results are shown for dependent variables with significant results. The regression coefficient B and the p value corrected for age and sex are shown. Results are sorted by p value.

Dependent variable	Regression coefficient B	p value
Visceral fat at the level of the navel [cm^2]	1.428	< 0.001
Triglycerides (mg/dl)	1.383	0.002
Right liver lobe fat content, HISTO measurement [%]	0.107	0.018
Total fat from femoral head to cardiac apex [l]	0.068	0.020
Insulin (mU/l) 2h after OGTT	0.879	0.020
Dietary fibre [mg/d]	-58.556	0.023
Visceral fat from femoral head to cardiac apex [l]	0.027	0.024
Left liver lobe fat content, HISTO measurement [%]	0.088	0.031
Mean fat content of the liver at the level of the portal vein [%]	0.093	0.035
Body Mass Index (kg/m2)	0.053	0.044
LDL cholesterol (mg/dl)	0.357	0.045

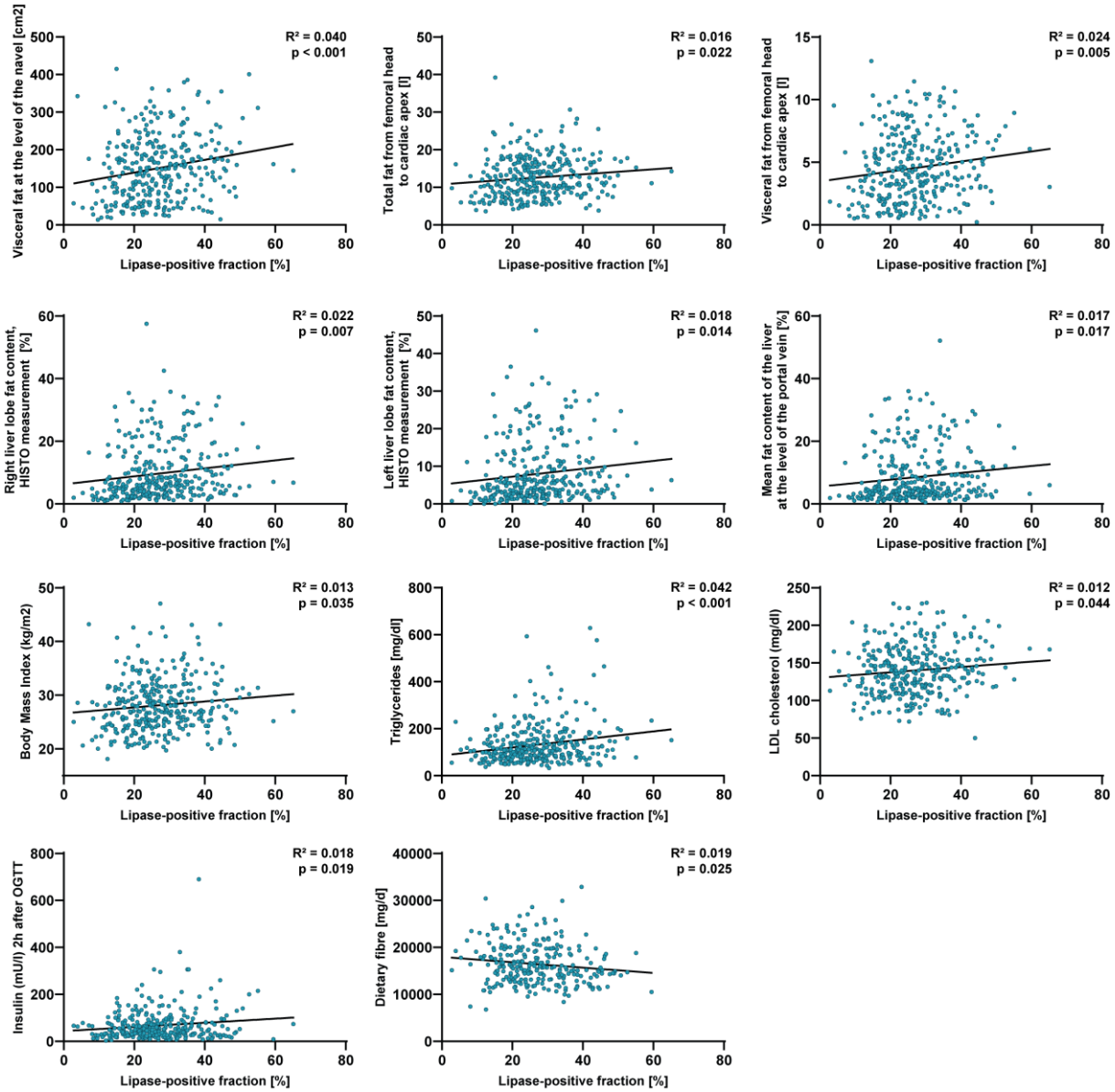

Figure 24: Visualisation of the regression analysis for the lipase-positive fraction of bacteria in human stool. Dot plots with regression line for the lipase-positive fraction [%] and the variables with a significant result in the linear regression analysis corrected for age and sex (**Table 3**). R^2 and p-value are given for the results of a simple linear regression analysis (without correction for sex and age).

In summary, the relative abundance of lipase-positive bacteria in human stool was positively associated with several metabolic parameters, especially higher body fat content and blood lipids.

5. Discussion

5.1 Influence of *Eggerthella lenta* on liver proteome and gut metabolome

Gnotobiotic mice were gavaged with OMM12 and four *Coriobacteriia* strains. It was repeatedly shown that the OMM12 community is permissive to colonisation with additional bacterial species (Herp *et al.* 2019; Marion *et al.* 2020; Streidl *et al.* 2021; Studer *et al.* 2016). However, out of the four *Coriobacteriia* species, only *E. lenta* successfully colonised the gut of the gnotobiotic mice as a dominant member of the community. *A. mucosicola*, *C. aerofaciens*, and *L. parvula* were not detected by 16S rRNA gene amplicon sequencing. As the *C. aerofaciens* type strain originates from the human gut, its origin may have hampered colonisation in the mouse gut, which has been shown to be influenced by the host origin of bacterial strains (Frese *et al.* 2013; Seedorf *et al.* 2014). However, colonisation with the same strain was successful in other studies (Desai *et al.* 2016; Kasahara *et al.* 2018; Kovatcheva-Datchary *et al.* 2019) and the *E. lenta* type strain, which successfully colonised the mouse gut in this experiment, also originated from the human gut. *A. mucosicola* has also been shown to colonise the murine gut as part of an extended version of OMM with 19 strains, though at low relative abundance (Afrizal *et al.* 2022). The reasons for unsuccessful colonisation in this work are not known and it cannot be excluded that the three strains colonised as members of subdominant populations, which could not be detected by high-throughput 16S rRNA gene amplicon sequencing. Despite this, as *E. lenta* colonised as a dominant member of the community, the two colonisation groups with different community profiles allowed us to investigate the effects of the presence of *E. lenta* on the liver proteome and gut metabolome.

Although *E. lenta* has important metabolic functions and colonised at high relative abundance, liver proteomic data did not indicate *E. lenta*-induced changes in liver function. In contrast, diet had significant effects on the liver proteomes, especially the addition of fat. Five proteins, which are involved in lipid and amino acid metabolism, were constantly under the top 10 differentially expressed proteins in the liver of mice fed low- vs. high-fat. Similar effects of HFD feeding on the liver proteome have been reported in other studies (Benard *et al.* 2016; Kirpich *et al.* 2011). The addition of primary BA to the diet also induced significant changes in the liver proteomes, albeit not as pronounced as the effects of fat.

Non-targeted metabolomics analysis of colon contents revealed significant changes due to both *E. lenta*-colonisation and diet. It is noteworthy that colonisation with *E. lenta* consistently altered the levels of five metabolites in at least three of the four diet groups. Latifolicinin C acid was elevated, while creatine, sarcosine, N,N-dimethylarginine, and N-Acetyl-DL-methionine were decreased in the *E. lenta*-colonised OMM12 mice. The elevated levels of latifolicinin C acid could be explained by the

ability of multiple gut bacteria, including *E. lenta*, to metabolise tyrosin to latifolicinin C acid (Beloborodova *et al.* 2012; Beloborodova *et al.* 2009). The reduced levels of the metabolites creatine, sarcosine, N,N-dimethylarginine, and N-Acetyl-DL-methionine indicate the capacity of *E. lenta* to degrade them. It has been reported that gut bacteria express enzymes involved in creatinine and creatine degradation (Wyss *et al.* 2000) and the gene encoding for creatininase, which catalyses the reversible conversion of creatinine to creatine, was detected in the *E. lenta* genome (GCA_000024265.1_01172, WP_009304706.1). The enzyme creatinase facilitates the further transformation of creatine to urea and sarcosine, which can then be degraded to glycine by sarcosine oxidase or sarcosine dehydrogenase. Sarcosine levels were also found to be significantly decreased in *E. lenta*-colonised mice, but the genes catalysing these reactions were not detected in the genome of *E. lenta*. Another significantly reduced metabolite was N,N-dimethylarginine, which is an analogue of L-arginine, a known substrate of *E. lenta* (Sperry *et al.* 1976). Increased N,N-dimethylarginine levels have been observed in plasma of humans with hypercholesterolemia (Boger *et al.* 1998), diabetes mellitus (Abbasi *et al.* 2001), atherosclerosis (Miyazaki *et al.* 1999), hypertension (Surdacki *et al.* 1999), chronic heart failure (Zairis *et al.* 2012), and chronic renal failure (Jacobi *et al.* 2008). N,N-dimethylarginine can be metabolised to dimethylamine and L-citrulline by dimethylarginine dimethylaminohydrolase (DDAH) (Santa Maria *et al.* 1999), and the gene encoding for DDAH was found in the genome of *E. lenta* (GCA_000024265.1_02955). Citrulline was reported to be produced (Noecker *et al.* 2023) and further metabolised (Sperry *et al.* 1976) by *E. lenta*, however, in this experiment no significant differences were observed for citrulline levels between the colonisation groups.

5.2 Comparison of gut physiology and metabolism in germfree and SPF mice on different diets

In this experiment mice were gavaged with the four *Coriobacteriia* strains *A. mucosicola*, *C. aerofaciens*, *E. lenta* and *L. parvula*, but none of them successfully colonised the intestine of the GF mice. It was shown that the colonisation ability is influenced by the host origin of bacterial strains (Seedorf et al. 2014; Frese et al. 2013) and only *A. mucosicola* was originally isolated from the mouse microbiome. However, colonisation has been successful in previous gnotobiotic experiments with a very similar experimental setup (Just 2017). The diet used may also play a role in successful bacterial colonisation. For instance, it was shown that different diets, e.g. with varying fibre contents, influenced microbiota profiles in gnotobiotic mice (Faith *et al.* 2011; Kovatcheva-Datchary *et al.* 2019; Weitkunat *et al.* 2015). Furthermore, in a diet intervention study with 14 overweight men, the relative abundance of *C. aerofaciens* was significantly decreased when volunteers were on a low carbohydrate diet compared to diets rich in complex plant polysaccharides (Walker *et al.* 2011). In the experiments discussed in this chapter, the feeding of semi-synthetic experimental diets was started immediately in the week following initial colonisation by gavage. In the original experiment with successful colonisation of the four *Coriobacteriia* strains (Just 2017), the mice were fed with a chow diet for 2 weeks after initial association with the consortium, before being switched to the semi-synthetic experimental diets. The prolonged feeding with chow may have supported an initial stable colonisation. In addition, at least for monocolonisation with *C. aerofaciens* in the lipid absorption experiments, successful colonisation of mice fed with chow-based diets was achieved (see **4.3**). These results may suggest that feeding a chow diet with a higher fraction of undefined fibres is more likely to promote successful colonisation with the *Coriobacteriia* strains than feeding a synthetic experimental diet, but further experiments are needed to prove this.

The influence of colonisation on gut physiology was investigated by comparing the SPF to GF mice on the different diets. As expected, the caecum weight was significantly increased in the GF mice. An enlarged caecum in GF mice is normal and happens because undegraded mucopolysaccharides attract water into the caecal lumen (Basic *et al.* 2019; Wostmann 1981). The colon length, which is often used as an indication for colonic inflammation and injury, was not affected by colonisation. However, a significantly elongated small intestine was observed in the GF mice, independent of the diet used. Histological analysis of the distal small intestine did not indicate differences in villi length or width due to colonisation. It cannot be excluded that differences could have been observed in more proximal parts of the small intestine, however, no further tissue samples for histological analysis had been sampled. The small intestine was markedly and significantly shortened in SPF mice of all diet groups, although the caecal microbiota profiles analysed via 16S rRNA gene amplicon sequencing were significantly different between the four diet groups. Complex colonisation seems to be sufficient for

shortening of the small intestine, even if microbiota profiles vary. The elongated small intestine in GF mice has also been reported by others. Some studies showed that colonisation with synthetic communities can be sufficient to reduce small intestinal length. For example, van Tilburg Bernardes *et al.* (2020) reported that colonisation of C57Bl/6J mice with the OMM12 community resulted in a significantly decreased small intestinal length compared to GF mice (mean of 45.5 cm vs. 41.9 cm; 10 weeks old, colonised from birth); however, colonisation with five yeast strains was not sufficient to shorten the small intestine. Slezak *et al.* (2014) reported similar results: Colonisation of GF PRM/Alf and C3H/He mice with the simplified human microbiota (SIHUMI) community shortened the small intestine in comparison to GF mice (16.4% for PRM/Alf and 9.7% for C3H/He mice; 8 weeks old, colonised from birth). The reasons for the small intestinal shortening in GF mice are still unclear; the increased surface area may improve nutrient absorption, or bacterial metabolites or the immune system could play a role. Further studies are needed to study the mechanisms underlying this phenotype.

The effect of microbiota colonisation and diet on the mouse metabolism was also studied. The subcutaneous and visceral fat volume measured by whole body imaging were increased in SPF mice compared to GF mice in all diet groups but CD-BA, although, the body weight (after 16h fasting) was only significantly increased for SPF mice fed the CD and HFD compared to their GF counterparts. The results of the OGTT revealed a reduced glucose tolerance in SPF compared to GF mice in all diet groups, which agrees with previous results reported by Just *et al.* (2018) and Rabot *et al.* (2010). In addition to the effects of microbiota colonisation, HFD feeding also influenced the metabolism of the mice. Feeding of the HFDs for twelve weeks to the GF mice did not lead to increased body weight or fat volume, which is consistent with data from Kübeck *et al.* (2016) who showed that GF mice are protected from lard-based HFD induced obesity. However, it was surprising that the SPF mice fed the HFD did not show a significant increase in body weight or fat volume. In other studies, increased body weights were already observed after similar (8 weeks) or shorter feeding periods (Kübeck *et al.* 2016; Rabot *et al.* 2010). Nevertheless, a significant impairment of glucose tolerance was observed in the OGTT as an effect of both HFDs on the SPF mice. For the fat volume of SPF mice, marked inter-individual differences were observed. The split between HFD-BA fed SPF mice was linked to cage effects, but it was only partially the case for the HFD fed SPF mice. However, the mice with the higher fat volume and body weight in both groups had to be separated into individual cages due to severe fighting behaviour, which could have led to better feed access or less movement.

5.3 Influence of *Collinsella aerofaciens* on lipid absorption

C. aerofaciens has previously been reported to have lipolytic activity *in vitro* (Just 2017; Streidl 2021; Thorasin *et al.* 2015), and it has been observed that genomic diversity within the species *C. aerofaciens* is high (Lin *et al.* 2023). To identify potential differences between *C. aerofaciens* strains with respect to lipolytic activity, 14 in-house isolates with available draft genomes and the type strain were analysed. All strains showed *in vitro* cell-bound lipolytic activity. As the rhodamine B plate assay used is not quantitative, it cannot be excluded that the strength of lipolytic activity varies between the strains. Five potential lipase genes were previously predicted in the genome of *C. aerofaciens* DSM 3979^T by Steidl and Hitch (Streidl 2021). But only the potential lipase gene #5 had a predicted transmembrane region and was identified in all analysed strains, making it the most likely candidate gene responsible for the lipolytic activity. However, further tests such as the heterologous expression of the potential lipase gene in a lipase-negative strain, or a knockout of the gene in *C. aerofaciens* would be required to prove this. As *C. aerofaciens* has been reported to express BA-modifying enzymes, including 3α-, 7α-, 7β- and 12α-HSDH (Liu *et al.* 2011; Lucas *et al.* 2021; Wegner *et al.* 2017), the ability of the analysed strains to convert the primary BA CA was also tested. All strains were able to reduce the CA concentration after 48 hours of incubation, but variations in the efficacy of conversion were observed (1-40% reduction in CA concentration). CA was probably metabolised to 3-oxoCA, 7-oxoDCA, 7-epiCA, or 12-oxoCDCA by HSDH enzymes; however, it was not possible for us to measure these secondary BAs with the analytics available.

To study the influence of *C. aerofaciens* on lipid absorption, mice were monocolonised with *C. aerofaciens* DSM 3979^T and compared with GF and SPF mice. They were fed with chow-BA or chow-HFD for two weeks and, at the end of the experiments, they were gavaged with a mixture of deuterium-labelled palmitic acid and tripalmitin and sampled one (chow-BA) or six hours (chow-HFD) after the gavage.

To quantify *C. aerofaciens* colonisation along the gut regions of the monocolonised mice, the number of CFUs per g of gut content was determined. As expected, the highest numbers of *C. aerofaciens* were observed in the caecum and colon. HFD feeding led to a significantly increased CFU count, which is in accordance with other studies observing an increased relative abundance of *Coriobacteriia* in HFD fed mice (Chen *et al.* 2018; Feng *et al.* 2024; Just 2017; Lin *et al.* 2023; Park *et al.* 2020; Tang *et al.* 2024). Although at lower density, *C. aerofaciens* also colonised the small intestine of the monocolonised mice, where lipid absorption mainly occurs.

No major difference in the overall plasma FA profiles due to colonisation were observed between chow-BA fed mice one hour after gavage and chow-HFD fed mice six hours after gavage. In contrast, some differences were observed for the labelled lipids. In the GF mice, higher levels of the absorbed

labelled lipids were observed compared to SPF mice, however differences were only significant for D5-palmitic acid concentration measured in HFD fed mice six hours after gavage. These results hint at a decreased lipid absorption due to complex microbial colonisation in SPF mice. Similar results were found by Plagge (2023), who reported an reduced uptake of the same deuterium-labelled lipids (D5-palmitic acid and D93-tripalmitin) in plasma and epididymal WAT of SPF and OMM12 compared to GF mice. Their results indicate that higher TCA levels in colonised mice lead to enhanced phospholipase A1 activity in the bile, resulting in increased phosphatidylcholine degradation and thus reduced fat absorption in the intestine. However, Martinez-Guryn *et al.* (2018) reported contrary results. They observed an increased absorption of the radiolabelled lipids triolein and cholesterol in SPF compared to GF mice, and that HFD feeding further increased absorption in SPF mice, but not in GF mice. The median plasma levels of the labelled FAs were highest in *C. aerofaciens*-monocolonised mice, indicating increased lipid absorption due to *C. aerofaciens* colonisation. However, results reached statistical significance only for *C. aerofaciens*-monocolonised compared to SPF mice fed the HFD and sampled six hours after gavage. As the differences between GF and *C. aerofaciens*-monocolonised mice were not significant, further experiments with more mice would be needed to validate the potential effects of *C. aerofaciens* colonisation on lipid absorption.

As described in section **1.2** of the introduction, there is evidence from studies in the 1960s and 1970s that lipids can also be absorbed in distal regions of the gut, especially when large amounts of fat are available (Ammon *et al.* 1973; Booth *et al.* 1961; Snipes 1977). Because the high bacterial density in the colon could potentially lead to differences in the uptake of FA into epithelial cells, FAs were also measured in colon tissue for the mice fed with chow-HFD and sampled six hours after gavage with the labelled lipids. However, we observed only a trend towards lowest levels in *C. aerofaciens*-monocolonised mice (the opposite of the trend towards highest levels of labelled lipids in the plasma of these mice) without statistical significance. Faster systemic absorption of lipids in the colon of *C. aerofaciens*-monocolonised mice could explain these observations. To draw definitive conclusions, it would have been necessary to extend the measurements of lipids to additional time points in colon tissue and other compartments.

To study the influence of *C. aerofaciens* on lipid absorption, the results of two gnotobiotic experiments were combined. In the first experiment a separation of measured FA levels due to sex was observed in some groups, therefore the second experiment was done with male mice only. Especially for D5-palmitic acid and D31-palmitic acid measured in plasma of *C. aerofaciens*-monocolonised mice fed chow-BA diet and sampled one hour after gavage, a clear separation of data from male and female mice was observed in experiment 1. However, when combining the results of both experiments, the values of the male mice in experiment 2 clustered together with the values of the female mice in experiment 1, suggesting a cage rather than a sex effect, despite considering litter and cage effects

during experimental planning. In general, some inter-individual variation was observed, but the measured FA values from experiment 1 and 2 clustered well together, confirming the accuracy of the measurements.

5.4 Occurrence of lipase-positive bacteria in human stool from a population study

Associations between the occurrence of lipase-positive bacteria in human stool and host metabolic parameters were analysed using data from 338 participants of the KORA population study. The analysed participants were aged between 39 and 73 years old, slightly dominated by men (58%), and more than 70% were obese or overweight. Faecal microbiota profiles were determined using 16S rRNA gene amplicon sequencing, and individuals taking antibiotics were excluded to avoid confounding effects. Use of the antidiabetic drug metformin is also known to alter the gut microbiota composition and may be a potential confounding factor, especially in studies involving T2D (de la Cuesta-Zuluaga *et al.* 2017; Forslund *et al.* 2015). However, in this analysis no significant difference between the three microbiome *de novo* clusters and metformin intake was found. Therefore, metformin intake was not considered a confounding factor. Also, no other confounders influenced by the microbiota profiles were identified, and the regression analysis was only corrected for the standard confounding factors age and sex.

The overall relative abundance of lipase-positive bacteria ranged from 2.8% to a maximum of 65.1% with a median value of 25.7%. This potentially high lipase-positive fraction of the microbiota highlights the importance of studying their effect on host metabolism. Linear regression analysis revealed highly significant positive associations between the relative abundance of lipase-positive bacteria and visceral fat at the level of the naval and blood triglyceride levels. Significant positive associations were also identified for other visceral and total fat mass variables, fat content in the liver, BHI, and the blood parameters LDL cholesterol and insulin levels two hours after OGTT. Previous studies have already found links between changes in the microbiota profiles and body weight, BMI, or blood parameters associated with lipid metabolism, but the potential role of lipase-positive bacteria in this was not studied. For example, Fu *et al.* (2015) studied participants of the LifeLines-DEEP population cohort (n = 893) and found that that the gut microbiota explains 4.5% of the variance in BMI, 6% in triglycerides and 4% in HDL, independent of age, sex, and host genetics. Also, Yun *et al.* (2020) found significant associations between gut microbiota diversity and composition and triglyceride levels (n = 1,141). Interestingly, fibre intake was the only variable negatively associated with the lipase-positive fraction in our analysis, suggesting a potential dietary influence on gut microbial composition and lipolytic activity. Dietary fibre is known to impact gut microbiota ecology, host physiology and health (Makki *et al.* 2018). Our results indicate that a fibre-rich diet could antagonize lipase-positive bacteria or enhance the growth of lipase-negative bacteria, however, further investigations would be needed to confirm this assumption. The overall results indicate a link between the relative abundance of lipase-positive bacteria in stool and host metabolic parameters, related to body composition (e.g., visceral fat and liver fat content) and lipid metabolism-related blood parameters. The occurrence of lipase-positive bacteria could possibly lead to a modulation of lipid digestion and absorption in the

intestine by modulating the amount of available free FAs in the intestinal lumen. Alternatively indirect effects could play a role, or the relative abundance of lipase-positive bacteria could be only a proxy for different microbiota profiles affecting lipid metabolism through unknown mechanisms.

While the findings are promising, the analysis has some limitations. The faecal microbiota profiles were analysed by 16S rRNA gene amplicon sequencing, with subsequent BLAST searches at a 97% cutoff for species identification. This approach, however, offers only limited taxonomic resolution. The use of shotgun metagenomic sequencing would enable the analysis of community composition at the strain level and the analysis of the functional potential of the microbiota, which could provide additional and more precise information on the relative abundance of lipase-positive bacteria. Furthermore, the way to calculate the relative abundance of the lipase-positive fraction is relying on the assumption that all OTUs with 97% identity to known lipase-positive bacteria (V3-V4 region of the 16S rRNA gene) are also lipase-positive. On the one hand, this assumption could overestimate the number of lipase-positive bacteria, as it is not clear whether all bacteria with 97% identity in the 16S rRNA gene actually have lipase activity. On the other hand, the calculation is based on a screening of a limited number of isolates for lipase activity, which could lead to an underestimation of the lipase-positive bacteria.

6. Conclusion and outlook

The aim of my PhD thesis was to understand whether and how *Coriobacteriia* have causal effects on host metabolism. In the four parts of this thesis, I explored the complex interactions between gut microbiota, lipid metabolism and absorption, and host physiology, with a particular focus on the *Coriobacteriia* species *E. lenta* and *C. aerofaciens*.

The addition of *E. lenta* to the synthetic community OMM12 triggered significant changes in the colon metabolome of mice. The observed increase in latifolicinin C acid levels and reductions in creatine, sarcosine, N,N-dimethylarginine, and N-Acetyl-DL-methionine suggest that *E. lenta* possesses unique enzymatic capacities that could have implications for host metabolism and health. However, further proof is needed and the mechanisms are unclear. The liver proteome was not affected by *E. lenta* colonisation. However, the different diets had a significant effect on both colon metabolome and liver proteome. These findings highlight the complexity of host-microbe interactions, with diet having a key influence on metabolic outcomes. Genetic tools and phages available for targeted manipulation of *E. lenta* could help to accelerate future research into its role in gut microbiome-host interactions (Bisanz *et al.* 2020; Dong *et al.* 2022; Sprotte *et al.* 2022).

The colonisation experiments performed with *A. mucosicola*, *C. aerofaciens*, *E. lenta*, and *L. parvula* highlighted the challenges associated with colonising GF mice with *Coriobacteriia*. Despite previous successes in similar experimental setups, none of the four strains were able to successfully engraft in the gut. Factors such as the host origin of the bacterial strains and dietary composition may influence the success of colonisation. Additional investigations would be needed to determine why the strains failed to colonise the mice and to identify alternative strategies that might improve colonisation. Although colonisation with four *Coriobacteriia* strains was unsuccessful, the differences between GF and SPF mice in terms of intestinal physiology and metabolism could be investigated. Most interestingly, small intestinal length was reduced by complex colonisation regardless of diet groups, which were associated with significantly different colonisation profiles. However, the reason and underlying mechanisms for this phenotype remain unclear and further work is needed. For instance, GF mice could be treated with filtered faecal water to investigate whether bacterial metabolites are sufficient to induce the small intestinal shortening.

C. aerofaciens has *in vitro* lipolytic activity. To investigate whether it influences intestinal lipid absorption in combination with diets high in fat or supplemented with primary BAs, deuterium-labelled lipids were gavaged to monocolonised mice and their levels in plasma and other tissues were measured after one or six hours. Although a trend towards increased lipid absorption was observed, statistical significance was not achieved compared to GF mice. Further studies with more animals

would be needed to validate the potential effect of *C. aerofaciens* on lipid absorption. In addition, to analyse the specific role of bacterial lipolytic activity, genetic engineering to knockout or overexpress the *C. aerofaciens* lipase gene would be required. Although this study has not definitively proven that *C. aerofaciens* plays a role in improving lipid absorption, it provides a foundation for further research in this direction.

To elucidate the potential clinical relevance of dominant lipase-positive bacteria, including *C. aerofaciens*, their relative abundance in human stool was studied in 338 participants from the KORA cohort in relation to host body parameters. There was an association between the lipase-positive fraction of faecal microbiota and several metabolic parameters related to fat distribution and lipid metabolism. However, further research is needed to confirm these associations across larger cohorts and to investigate the underlying mechanisms. The results of this analysis highlight the importance of the gut microbiota for metabolic health and lay the groundwork for future research. Understanding these relationships may in the future open new avenues for interventions targeting the intestinal microbiota to modulate lipid metabolism and improve metabolic health.

In summary, multiple gnotobiotic mouse experiments and the analysis of data from a human cohort were conducted to investigate the influence of intestinal *Coriobacteriia*, which can metabolise BAs and express lipases, on host metabolism. One major challenge was the difficulty to colonise GF mice with these bacteria. Our findings indicate that *E. lenta* colonisation can affect metabolites in the gut. Trends related to changes in lipid absorption due to *C. aerofaciens* require additional validation. The analysis of the occurrence of dominant lipase-positive bacteria within human stool revealed associations with metabolic body parameters, underscoring their relevance to human health. Overall, the results of this this PhD thesis provide further evidence for the role of *Coriobacteriia* in metabolic health.

Supplement

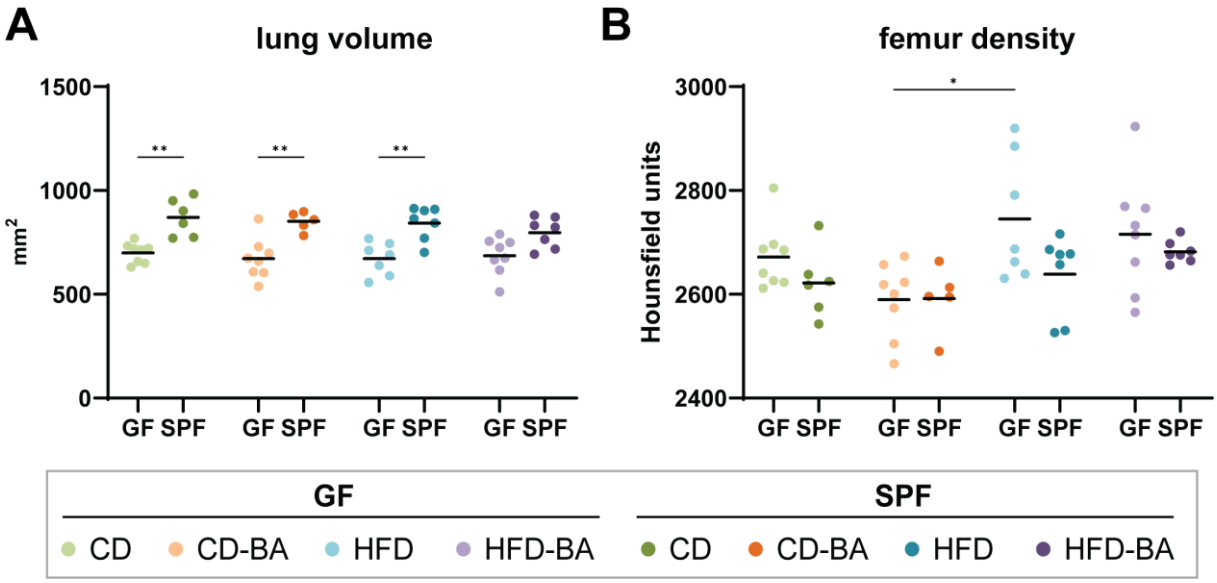

Figure S1: Effect of complex colonisation and diet on lung volume and femur density. A Lung volume in mm^2 measured via µCT scans. **B** Femur density in Hounsfield units measured via µCT scans. In all figure panels, dots represent the values for individual mice and black bars indicate mean values. Statistics: * adj. $p < 0.05$, ** adj. $p < 0.01$; two-way ANOVA followed by Tukey test; significant differences are only indicated for comparisons between the same colonisation or diet groups. Abbreviations: CD, control diet; CD-BA, control diet supplemented with 0.1% CA and 0.1% CDCA; HFD, lard-based high-fat diet with 48 kJ% fat; HFD-BA, high-fat diet supplemented with 0.1% CA and 0.1% CDCA.

Table S1: Descriptive statistics and results of one-way ANOVA for the analysed KORA sub-cohort by three *de novo* clusters of the faecal colonisation profiles. Faecal colonisation profiles were analysed by 16S rRNA gene amplicon sequencing and *de novo* clustering was applied, identifying three native microbiota clusters. The first columns show the descriptive statistics for the three clusters, including the number of participants (n), the mean, and the standard deviation. The last two columns show the results of the one-way ANOVA with Benjamini-Hochberg adjustment, performed to identify variables with significant differences between the three clusters.

variable	descriptive statistics									one-way ANOVA	
	cluster 1			cluster 2			cluster 3				
	n	mean	standard deviation	n	mean	standard deviation	n	mean	standard deviation	p-value	adjusted p-value
Appendicular muscle mass index [kg/m2] (Kyle)	109	7.65	1.12	140	7.92	1.27	89	8.09	1.36	0.040	0.461
HOMA-IR (homoeostasis model assessment of insulin resistance)	100	2.52	1.66	129	2.82	2.01	84	3.30	2.66	0.045	0.461
Lean Body Mass Index [kg/m2] (Kyle)	109	18.39	2.27	140	18.93	2.57	89	19.30	2.75	0.037	0.461
Physical Activity in Categories	109	2.11	1.07	140	2.45	1.14	89	2.53	1.23	0.019	0.461
Fasting Insulin in Serum (mU/l)	109	10.47	6.78	139	10.81	6.71	89	12.86	9.32	0.057	0.467
Waist-Hip-Ratio	109	0.90	0.09	140	0.92	0.09	89	0.93	0.09	0.086	0.588
Body Mass Index (kg/m2)	109	27.37	4.84	140	28.25	4.69	89	28.73	5.19	0.133	0.723
Insulin in Serum (2h after OGTT)	99	59.82	51.07	128	65.89	74.33	80	79.75	74.76	0.141	0.723
Alcohol onsumption (g/day)	109	18.12	22.35	140	16.78	25.37	89	20.33	23.91	0.553	0.742
Age [years]	109	56.07	8.63	140	55.11	9.19	89	57.25	10.15	0.235	0.742
Dietary Cholesterol [mg/day]	87	285.65	66.09	111	294.03	69.35	72	296.58	64.82	0.546	0.742
Dietary MUFAs [mg/day]	87	26459.42	5409.96	111	27655.99	6507.82	72	27489.25	5709.03	0.342	0.742
Energy (kilojoule) [kJ/d]	87	7530.57	1494.68	111	7798.68	1880.11	72	7772.98	1562.05	0.498	0.742
Energy (kilocalories) [kcal/day]	87	1797.83	356.73	111	1862.23	449.19	72	1855.71	373.24	0.495	0.742
Dietary Fat [mg/day]	87	74788.54	14843.10	111	78200.71	17373.06	72	77856.11	14900.35	0.287	0.742
Left liver lobe fat content, HISTO measurement [%]	107	7.09	6.72	135	8.29	8.44	86	8.62	8.38	0.348	0.742
Right liver lobe fat content, HISTO measurement [%]	107	8.68	7.33	136	10.13	9.73	86	10.28	8.99	0.346	0.742
Fat Mass Index [kg/m2] (Kyle)	109	8.99	3.49	140	9.33	3.09	89	9.43	3.40	0.601	0.742
Pack Years	108	13.08	18.60	133	14.15	20.39	88	11.48	17.88	0.598	0.742
Total Cholesterol (mg/dl)	109	221.00	38.04	140	216.71	35.03	89	217.21	34.25	0.615	0.742

Total fat from femoral head to cardiac apex [l]	105	12.01	5.03	136	12.85	5.27	84	12.95	5.77	0.379	0.742
Dieraty SAFAs [mg/day]	87	33703.23	7138.14	111	35444.88	7967.81	72	35166.42	6644.91	0.230	0.742
HDL cholesterol (mg/dl)	109	63.77	17.65	140	61.59	18.04	89	60.99	17.05	0.488	0.742
HOMA-beta (homoeostasis model assessment of beta-cell function) in %	100	105.02	56.25	129	109.64	56.32	84	118.13	66.20	0.320	0.742
hs C-reactive protein (EDTA plasma) in mg/L	107	2.53	3.83	139	1.98	2.46	89	2.40	3.58	0.380	0.742
Dietary Carbohydrates, absorbable [mg/day]	87	186144.69	40336.16	111	196870.65	58597.64	72	195702.43	47784.94	0.293	0.742
Dietary PUFAs [mg/day]	87	9624.31	2331.65	111	10021.12	2562.18	72	9996.90	2545.89	0.489	0.742
Mean fat content of the liver at the level of the portal vein [%]	107	7.56	7.16	136	8.75	9.11	84	9.33	8.82	0.326	0.742
Dietary Omega-3 fatty acids [mg/day]	87	1542.10	494.43	111	1490.78	389.15	72	1555.32	467.57	0.574	0.742
Dietary Omega-6 fatty acids [mg/day]	87	8072.81	2028.22	111	8520.57	2273.30	72	8432.27	2180.95	0.334	0.742
subcutaneous fat at the level of the navel [cm^2]	106	271.72	114.74	137	291.11	113.17	85	281.72	119.74	0.430	0.742
subcutaneous fat from femoral head to cardiac apex [l]	105	7.73	3.44	136	8.36	3.52	84	8.18	4.18	0.413	0.742
Visceral fat at the level of the navel [cm^2]	107	146.29	87.00	138	149.63	86.63	85	158.40	83.02	0.611	0.742
Visceral fat from femoral head to cardiac apex [l]	107	4.31	2.63	138	4.55	2.72	85	4.82	2.59	0.417	0.742
Dietary Fibre [mg/day]	87	16724.16	4380.97	111	16240.05	4314.91	72	16408.94	4097.91	0.730	0.828
Glucose value 2 in serum (after OGTT) (mg/dl)	100	113.82	34.18	128	112.98	42.35	80	117.41	42.39	0.726	0.828
LDL cholesterol (mg/dl)	109	141.37	34.80	140	138.51	32.79	89	140.53	31.42	0.782	0.828
Fasting Glucose in Serum (mg/dl)	109	104.67	30.14	139	102.76	17.29	89	104.03	16.75	0.788	0.828
Triglycerides (mg/dl)	109	126.96	93.15	140	134.53	88.94	89	132.51	68.12	0.780	0.828
Dietary Protein [mg/day]	87	69234.04	14265.69	111	70343.61	14641.99	72	69699.25	14216.43	0.863	0.863
Body Fat Percentage [%] (Kyle)	109	31.94	7.37	140	32.42	6.65	89	32.11	6.74	0.857	0.863

Table S2: Baseline characteristics of the analysed KORA sub-cohort by quartiles of the lipase-positive fractions for categorical variables. The total number of participants with available data and the number of participants in each category are shown in the first column (N). Following, the percentage of participants in each category are shown for each quartile of the lipase-positive fraction (Q1-4).

Characteristics	N	Q1	Q2	Q3	Q4
Sex	**338**				
male	196	48.8	56.5	58.8	67.9
female	142	51.2	43.5	41.2	32.1
Physical activity in categories	**338**				
regularly more than 2 hours per week	98	32.1	28.2	24.7	31.0
regularly approx. 1 hour per week	106	31.0	31.8	43.5	19.0
irregularly approx. 1 hour per week	48	9.5	16.5	12.9	17.9
almost no or no sporting activity	86	27.4	23.5	18.8	32.1
Smoking behaviour	**338**				
regular smoker	57	17.9	21.2	10.6	17.9
irregular smoker	10	3.6	2.4	2.4	3.6
ex-smoker	148	41.7	38.8	49.4	45.2
never smoker	123	36.9	37.6	37.6	33.3
Metabolic Syndrome	**338**				
yes	125	34.5	32.9	31.8	48.8
no	213	65.5	67.1	68.2	51.2
Myocardial infarction treated as an inpatient	**338**				
yes	0	0.0	0.0	0.0	0.0
no	338	100.0	100.0	100.0	100.0
Angina Pectoris	**336**				
yes	18	6.0	4.8	4.7	6.0
no	318	94.0	95.2	95.3	94.0
Stroke treated as an inpatient	**338**				
yes	0	0.0	0.0	0.0	0.0
no	338	100.0	100.0	100.0	100.0
Metformin Intake	**338**				
yes	23	8.3	3.5	8.2	7.1
no	315	91.7	96.5	91.8	92.9
Intake of digestives	**338**				
yes	1	0.0	0.0	1.2	0.0
no	337	100.0	100.0	98.8	100.0
Intake of medication for neurological diseases	**338**				
yes	21	7.1	4.7	5.9	7.1
no	317	92.9	95.3	94.1	92.9
Medication intake in the last 7 days	**338**				
yes	253	73.8	74.1	70.6	81.0
no	85	26.2	25.9	29.4	19.0
Antidiabetic medication	**338**				
yes	25	9.5	4.7	8.2	7.1
no	313	90.5	95.3	91.8	92.9
Intake of proton pump inhibitors	**338**				

yes	20	2.4	7.1	5.9	8.3
no	318	97.6	92.9	94.1	91.7
Intake of antihypertensives	**338**				
yes	85	29.8	22.4	21.2	27.4
no	253	70.2	77.6	78.8	72.6
Intake of lipid-lowering agents including herbal substances	**338**				
yes	37	11.9	11.8	8.2	11.9
no	301	88.1	88.2	91.8	88.1
Intake of antidepressants	**338**				
yes	15	4.8	3.5	4.7	4.8
no	323	95.2	96.5	95.3	95.2
Antineoplastic and immunomodulating agents	**338**				
yes	5	0.0	2.4	3.5	0.0
no	333	100.0	97.6	96.5	100.0

Table S3: Baseline characteristics of the analysed KORA sub-cohort by quartiles of the lipase-positive fractions for continuous variables. The total number of participants with available data and the mean of the variables for each quartile of the lipase-positive fraction (Q1-4) is shown.

Characteristics	N	Q1	Q2	Q3	Q4
Age [years]	338	56.99	57.07	55.33	54.54
Body Mass Index (kg/m2)	338	27.09	28.15	27.99	29.15
Waist-Hip-Ratio	338	0.91	0.91	0.91	0.93
Body Fat Percentage [%] (Kyle)	338	32.32	32.39	31.59	32.46
Fat Mass Index [kg/m2] (Kyle)	338	8.96	9.30	9.03	9.69
Lean Body Mass Index [kg/m2] (Kyle)	338	18.13	18.86	18.96	19.46
Appendicular muscle mass index [kg/m2] (Kyle)	338	7.51	7.86	7.95	8.18
Pack Years	329	13.86	15.21	11.05	12.11
Alcohol consumption (g/day)	338	15.90	19.38	17.38	19.92
Fasting Glucose in Serum (mg/dl)	337	101.10	103.48	105.74	104.53
Glucose value 2 in serum (after OGTT) (mg/dl)	308	111.23	116.25	112.05	117.86
Fasting Insulin in Serum (mU/l)	337	10.14	11.64	10.90	12.31
Insulin in Serum (2h after OGTT)	307	56.69	66.13	64.49	82.48
HOMA-IR (homoeostasis model assessment of insulin resistance)	313	2.48	2.99	2.75	3.17
HOMA-beta (homoeostasis model assessment of beta-cell function) in %	313	104.93	112.11	108.72	115.79
Total fat from femoral head to cardiac apex [l]	325	11.63	12.74	12.11	13.93
Visceral fat from femoral head to cardiac apex [l]	330	4.00	4.57	4.38	5.22

subcutaneous fat from femoral head to cardiac apex [l]	325	7.72	8.18	7.75	8.82
Visceral fat at the level of the navel [cm^2]	330	128.98	151.75	143.30	179.09
subcutaneous fat at the level of the navel [cm^2]	328	266.17	285.14	273.19	305.22
Right liver lobe fat content, HISTO measurement [%]	329	7.79	10.09	8.74	12.07
Left liver lobe fat content, HISTO measurement [%]	328	6.65	7.94	7.54	9.74
Mean fat content of the liver at the level of the portal vein [%]	327	7.10	8.65	7.58	10.61
Total Cholesterol (mg/dl)	338	214.48	218.55	219.99	219.87
HDL cholesterol (mg/dl)	338	66.48	62.28	60.23	59.57
LDL cholesterol (mg/dl)	338	136.87	139.02	142.20	141.74
Triglycerides (mg/dl)	338	105.88	128.18	137.63	154.52
hs C-reactive protein (EDTA plasma) in mg/L	335	2.05	2.29	2.02	2.71
Dietary SAFAs [mg/day]	270	34108.08	33896.28	35742.68	35463.80
Dietary MUFAs [mg/day]	270	26609.03	26566.57	27903.10	27805.77
Dietary PUFAs [mg/day]	270	9701.22	9724.61	10249.59	9867.02
Dietary Omega-3 fatty acids [mg/day]	270	1581.51	1533.58	1514.10	1469.19
Dietary Omega-6 fatty acids [mg/day]	270	8110.45	8182.08	8725.52	8387.92
Dietary Cholesterol [mg/day]	270	288.23	288.91	302.61	288.20
Energy (kilocalories) [kcal/day]	270	1807.56	1796.95	1872.23	1880.96
Dietary Protein [mg/day]	270	69284.98	68842.83	71727.23	69373.39
Dietary Fat [mg/day]	270	75400.78	75195.45	79070.79	78316.99
Dietary Carbohydrates, absorbable [mg/day]	270	191165.43	188671.67	195687.61	196756.89
Dietary Fibre [mg/day]	270	17037.67	16383.19	16962.61	15379.14

Bibliography

Abbasi, F., Asagmi, T., Cooke, J. P., Lamendola, C., McLaughlin, T., Reaven, G. M., Stuehlinger, M., and Tsao, P. S. 2001. 'Plasma concentrations of asymmetric dimethylarginine are increased in patients with type 2 diabetes mellitus', *Am J Cardiol*, 88: 1201-3.

Abellan-Schneyder, I., Matchado, M. S., Reitmeier, S., Sommer, A., Sewald, Z., Baumbach, J., List, M., and Neuhaus, K. 2021. 'Primer, Pipelines, Parameters: Issues in 16S rRNA Gene Sequencing', *mSphere*, 6.

Afolayan, A. O., Adebusoye, L. A., Cadmus, E. O., and Ayeni, F. A. 2020. 'Insights into the gut microbiota of Nigerian elderly with type 2 diabetes and non-diabetic elderly persons', *Heliyon*, 6: e03971.

Afrizal, A., Jennings, S. A. V., Hitch, T. C. A., Riedel, T., Basic, M., Panyot, A., Treichel, N., Hager, F. T., Wong, E. O., Wolter, B., Viehof, A., von Strempel, A., Eberl, C., Buhl, E. M., Abt, B., Bleich, A., Tolba, R., Blank, L. M., Navarre, W. W., Kiessling, F., Horz, H. P., Torow, N., Cerovic, V., Stecher, B., Strowig, T., Overmann, J., and Clavel, T. 2022. 'Enhanced cultured diversity of the mouse gut microbiota enables custom-made synthetic communities', *Cell Host Microbe*, 30: 1630-45 e25.

Agans, R., Gordon, A., Kramer, D. L., Perez-Burillo, S., Rufian-Henares, J. A., and Paliy, O. 2018. 'Dietary Fatty Acids Sustain the Growth of the Human Gut Microbiota', *Appl Environ Microbiol*, 84.

Alexander, M., Ang, Q. Y., Nayak, R. R., Bustion, A. E., Sandy, M., Zhang, B., Upadhyay, V., Pollard, K. S., Lynch, S. V., and Turnbaugh, P. J. 2022. 'Human gut bacterial metabolism drives Th17 activation and colitis', *Cell Host Microbe*, 30: 17-30 e9.

Almeida, A., Mitchell, A. L., Boland, M., Forster, S. C., Gloor, G. B., Tarkowska, A., Lawley, T. D., and Finn, R. D. 2019. 'A new genomic blueprint of the human gut microbiota', *Nature*, 568: 499-504.

Almeida, A., Nayfach, S., Boland, M., Strozzi, F., Beracochea, M., Shi, Z. J., Pollard, K. S., Sakharova, E., Parks, D. H., Hugenholtz, P., Segata, N., Kyrpides, N. C., and Finn, R. D. 2021. 'A unified catalog of 204,938 reference genomes from the human gut microbiome', *Nat Biotechnol*, 39: 105-14.

Altmann, S. W., Davis, H. R., Jr., Zhu, L. J., Yao, X., Hoos, L. M., Tetzloff, G., Iyer, S. P., Maguire, M., Golovko, A., Zeng, M., Wang, L., Murgolo, N., and Graziano, M. P. 2004. 'Niemann-Pick C1 Like 1 protein is critical for intestinal cholesterol absorption', *Science*, 303: 1201-4.

Ammon, H. V., and Phillips, S. F. 1973. 'Inhibition of colonic water and electrolyte absorption by fatty acids in man', *Gastroenterology*, 65: 744-9.

Arank, A., Syed, S. A., Kenney, E. B., and Freter, R. 1969. 'Isolation of anaerobic bacteria from human gingiva and mouse cecum by means of a simplified glove box procedure', *Appl Microbiol*, 17: 568-76.

Araujo, J. R., Tazi, A., Burlen-Defranoux, O., Vichier-Guerre, S., Nigro, G., Licandro, H., Demignot, S., and Sansonetti, P. J. 2020. 'Fermentation Products of Commensal Bacteria Alter Enterocyte Lipid Metabolism', *Cell Host Microbe*, 27: 358-75 e7.

Arumugam, M., Raes, J., Pelletier, E., Le Paslier, D., Yamada, T., Mende, D. R., Fernandes, G. R., Tap, J., Bruls, T., Batto, J. M., Bertalan, M., Borruel, N., Casellas, F., Fernandez, L., Gautier, L., Hansen, T., Hattori, M., Hayashi, T., Kleerebezem, M., Kurokawa, K., Leclerc, M., Levenez, F., Manichanh, C., Nielsen, H. B., Nielsen, T., Pons, N., Poulain, J., Qin, J., Sicheritz-Ponten, T., Tims, S., Torrents, D., Ugarte, E., Zoetendal, E. G., Wang, J., Guarner, F., Pedersen, O., de Vos, W. M., Brunak, S., Dore, J., Meta, H. I. T. C., Antolin, M., Artiguenave, F., Blottiere, H. M., Almeida, M., Brechot, C., Cara, C., Chervaux, C., Cultrone, A., Delorme, C., Denariaz, G., Dervyn, R., Foerstner, K. U., Friss, C., van de Guchte, M., Guedon, E., Haimet, F., Huber, W., van Hylckama-Vlieg, J., Jamet, A., Juste, C., Kaci, G., Knol, J., Lakhdari, O., Layec, S., Le Roux, K., Maguin, E., Merieux, A., Melo Minardi, R., M'Rini, C., Muller, J., Oozeer, R., Parkhill, J., Renault, P., Rescigno, M., Sanchez, N., Sunagawa, S., Torrejon, A., Turner, K., Vandemeulebrouck, G., Varela, E., Winogradsky, Y., Zeller, G., Weissenbach, J., Ehrlich, S. D., and Bork, P. 2011. 'Enterotypes of the human gut microbiome', *Nature*, 473: 174-80.

Asnicar, F., Thomas, A. M., Beghini, F., Mengoni, C., Manara, S., Manghi, P., Zhu, Q., Bolzan, M., Cumbo, F., May, U., Sanders, J. G., Zolfo, M., Kopylova, E., Pasolli, E., Knight, R., Mirarab, S., Huttenhower, C., and Segata, N. 2020. 'Precise phylogenetic analysis of microbial isolates and genomes from metagenomes using PhyloPhlAn 3.0', *Nat Commun*, 11: 2500.

Ay, U., Lenicek, M., Classen, A., Olde Damink, S. W. M., Bolm, C., and Schaap, F. G. 2022. 'New Kids on the Block: Bile Salt Conjugates of Microbial Origin', *Metabolites*, 12.

Bäckhed, F., Manchester, J. K., Semenkovich, C. F., and Gordon, J. I. 2007. 'Mechanisms underlying the resistance to diet-induced obesity in germ-free mice', *Proc Natl Acad Sci U S A*, 104: 979-84.

Bamberg, F., Hetterich, H., Rospleszcz, S., Lorbeer, R., Auweter, S. D., Schlett, C. L., Schafnitzel, A., Bayerl, C., Schindler, A., Saam, T., Muller-Peltzer, K., Sommer, W., Zitzelsberger, T., Machann, J., Ingrisch, M., Selder, S., Rathmann, W., Heier, M., Linkohr, B., Meisinger, C., Weber, C., Ertl-Wagner, B., Massberg, S., Reiser, M. F., and Peters, A. 2017. 'Subclinical Disease Burden as Assessed by Whole-Body MRI in Subjects With Prediabetes, Subjects With Diabetes, and Normal Control Subjects From the General Population: The KORA-MRI Study', *Diabetes*, 66: 158-69.

Basic, M., and Bleich, A. 2019. 'Gnotobiotics: Past, present and future', *Lab Anim*, 53: 232-43.

Beloborodova, N., Bairamov, I., Olenin, A., Shubina, V., Teplova, V., and Fedotcheva, N. 2012. 'Effect of phenolic acids of microbial origin on production of reactive oxygen species in mitochondria and neutrophils', *J Biomed Sci*, 19: 89.

Beloborodova, N. V., Khodakova, A. S., Bairamov, I. T., and Olenin, A. Y. 2009. 'Microbial origin of phenylcarboxylic acids in the human body', *Biochemistry (Mosc)*, 74: 1350-5.

Benard, O., Lim, J., Apontes, P., Jing, X., Angeletti, R. H., and Chi, Y. 2016. 'Impact of high-fat diet on the proteome of mouse liver', *J Nutr Biochem*, 31: 10-9.

Berry, D., Ben Mahfoudh, K., Wagner, M., and Loy, A. 2011. 'Barcoded primers used in multiplex amplicon pyrosequencing bias amplification', *Appl Environ Microbiol*, 77: 7846-9.

Bess, E. N., Bisanz, J. E., Yarza, F., Bustion, A., Rich, B. E., Li, X., Kitamura, S., Waligurski, E., Ang, Q. Y., Alba, D. L., Spanogiannopoulos, P., Nayfach, S., Koliwad, S. K., Wolan, D. W., Franke, A. A., and Turnbaugh, P. J. 2020. 'Genetic basis for the cooperative bioactivation of plant lignans by *Eggerthella lenta* and other human gut bacteria', *Nat Microbiol*, 5: 56-66.

Bisanz, J. E., Soto-Perez, P., Noecker, C., Aksenov, A. A., Lam, K. N., Kenney, G. E., Bess, E. N., Haiser, H. J., Kyaw, T. S., Yu, F. B., Rekdal, V. M., Ha, C. W. Y., Devkota, S., Balskus, E. P., Dorrestein, P. C., Allen-Vercoe, E., and Turnbaugh, P. J. 2020. 'A Genomic Toolkit for the Mechanistic Dissection of Intractable Human Gut Bacteria', *Cell Host Microbe*, 27: 1001-13 e9.

Blaser, M. J., Devkota, S., McCoy, K. D., Relman, D. A., Yassour, M., and Young, V. B. 2021. 'Lessons learned from the prenatal microbiome controversy', *Microbiome*, 9: 8.

Boger, R. H., Bode-Boger, S. M., Szuba, A., Tsao, P. S., Chan, J. R., Tangphao, O., Blaschke, T. F., and Cooke, J. P. 1998. 'Asymmetric dimethylarginine (ADMA): a novel risk factor for endothelial dysfunction: its role in hypercholesterolemia', *Circulation*, 98: 1842-7.

Bokkenheuser, V. D., Winter, J., Dehazya, P., and Kelly, W. G. 1977. 'Isolation and characterization of human fecal bacteria capable of 21-dehydroxylating corticoids', *Appl Environ Microbiol*, 34: 571-5.

Booth, C. C., Read, A. E., and Jones, E. 1961. 'Studies on the site of fat absorption: 1. The sites of absorption of increasing doses of I-labelled triolein in the rat', *Gut*, 2: 23-31.

Brugiroux, S., Beutler, M., Pfann, C., Garzetti, D., Ruscheweyh, H. J., Ring, D., Diehl, M., Herp, S., Lotscher, Y., Hussain, S., Bunk, B., Pukall, R., Huson, D. H., Munch, P. C., McHardy, A. C., McCoy, K. D., Macpherson, A. J., Loy, A., Clavel, T., Berry, D., and Stecher, B. 2016. 'Genome-guided design of a defined mouse microbiota that confers colonization resistance against *Salmonella enterica* serovar Typhimurium', *Nat Microbiol*, 2: 16215.

Burz, S. D., Abraham, A. L., Fonseca, F., David, O., Chapron, A., Beguet-Crespel, F., Cenard, S., Le Roux, K., Patrascu, O., Levenez, F., Schwintner, C., Blottiere, H. M., Bera-Maillet, C., Lepage, P., Dore, J., and Juste, C. 2019. 'A Guide for Ex Vivo Handling and Storage of Stool Samples Intended for Fecal Microbiota Transplantation', *Sci Rep*, 9: 8897.

Campbell, C. L., Yu, R., Li, F., Zhou, Q., Chen, D., Qi, C., Yin, Y., and Sun, J. 2019. 'Modulation of fat metabolism and gut microbiota by resveratrol on high-fat diet-induced obese mice', *Diabetes Metab Syndr Obes*, 12: 97-107.

Cancello, R., Turroni, S., Rampelli, S., Cattaldo, S., Candela, M., Cattani, L., Mai, S., Vietti, R., Scacchi, M., Brigidi, P., and Invitti, C. 2019. 'Effect of Short-Term Dietary Intervention and Probiotic Mix Supplementation on the Gut Microbiota of Elderly Obese Women', *Nutrients*, 11.

Cani, P. D. 2018. 'Human gut microbiome: hopes, threats and promises', *Gut*, 67: 1716-25.

Castro-Mejia, J. L., Khakimov, B., Aru, V., Lind, M. V., Garne, E., Paulova, P., Tavakkoli, E., Hansen, L. H., Smilde, A. K., Holm, L., Engelsen, S. B., and Nielsen, D. S. 2022. 'Gut Microbiome and Its Cofactors Are Linked to Lipoprotein Distribution Profiles', *Microorganisms*, 10.

Chen-Liaw, A., Aggarwala, V., Mogno, I., Haifer, C., Li, Z., Eggers, J., Helmus, D., Hart, A., Wehkamp, J., Lamouse-Smith, E. S. N., Kerby, R. L., Rey, F. E., Colombel, J. F., Kamm, M. A., Olle, B., Norman, J. M., Menon, R., Watson, A. R., Crossette, E., Terveer, E. M., Keller, J. J., Borody, T. J., Grinspan, A., Paramsothy, S., Kaakoush, N. O., Dubinsky, M. C., and Faith, J. J. 2025. 'Gut microbiota strain richness is species specific and affects engraftment', *Nature*, 637: 422-29.

Chen, C., Fang, S., Wei, H., He, M., Fu, H., Xiong, X., Zhou, Y., Wu, J., Gao, J., Yang, H., and Huang, L. 2021. '*Prevotella copri* increases fat accumulation in pigs fed with formula diets', *Microbiome*, 9: 175.

Chen, G., Xie, M., Dai, Z., Wan, P., Ye, H., Zeng, X., and Sun, Y. 2018. 'Kudingcha and Fuzhuan Brick Tea Prevent Obesity and Modulate Gut Microbiota in High-Fat Diet Fed Mice', *Mol Nutr Food Res*, 62: e1700485.

Chen, X., and Alonzo, F., 3rd. 2019. 'Bacterial lipolysis of immune-activating ligands promotes evasion of innate defenses', *Proc Natl Acad Sci U S A*, 116: 3764-73.

Chow, S. L., and Hollander, D. 1979. 'A dual, concentration-dependent absorption mechanism of linoleic acid by rat jejunum in vitro', *J Lipid Res*, 20: 349-56.

Claus, S. P., Ellero, S. L., Berger, B., Krause, L., Bruttin, A., Molina, J., Paris, A., Want, E. J., de Waziers, I., Cloarec, O., Richards, S. E., Wang, Y., Dumas, M. E., Ross, A., Rezzi, S., Kochhar, S., Van Bladeren, P., Lindon, J. C., Holmes, E., and Nicholson, J. K. 2011. 'Colonization-induced host-gut microbial metabolic interaction', *mBio*, 2: e00271-10.

Clavel, T., Charrier, C., Braune, A., Wenning, M., Blaut, M., and Haller, D. 2009. 'Isolation of bacteria from the ileal mucosa of TNFdeltaARE mice and description of Enterorhabdus mucosicola gen. nov., sp. nov', *Int J Syst Evol Microbiol*, 59: 1805-12.

Clavel, T., Henderson, G., Engst, W., Dore, J., and Blaut, M. 2006. 'Phylogeny of human intestinal bacteria that activate the dietary lignan secoisolariciresinol diglucoside', *FEMS Microbiol Ecol*, 55: 471-8.

Clavel, T., Lepage, P., and Charrier, C. 2014. 'The Family Coriobacteriaceae.' in Rosenberg, Eugene, DeLong, Edward F., Lory, Stephen, Stackebrandt, Erko and Thompson, Fabiano (eds.), *The Prokaryotes: Actinobacteria* (Springer Berlin Heidelberg: Berlin, Heidelberg).

Cleusix, V., Lacroix, C., Vollenweider, S., Duboux, M., and Le Blay, G. 2007. 'Inhibitory activity spectrum of reuterin produced by Lactobacillus reuteri against intestinal bacteria', *BMC Microbiol*, 7: 101.

Collins, S. L., Stine, J. G., Bisanz, J. E., Okafor, C. D., and Patterson, A. D. 2023. 'Bile acids and the gut microbiota: metabolic interactions and impacts on disease', *Nat Rev Microbiol*, 21: 236-47.

Companys, J., Gosalbes, M. J., Pla-Paga, L., Calderon-Perez, L., Llaurado, E., Pedret, A., Valls, R. M., Jimenez-Hernandez, N., Sandoval-Ramirez, B. A., Del Bas, J. M., Caimari, A., Rubio, L., and Sola, R. 2021. 'Gut Microbiota Profile and Its Association with Clinical Variables and Dietary Intake in Overweight/Obese and Lean Subjects: A Cross-Sectional Study', *Nutrients*, 13.

Consortium, U. 2019. 'UniProt: a worldwide hub of protein knowledge', *Nucleic Acids Res*, 47: D506-D15.

Crusell, M. K. W., Hansen, T. H., Nielsen, T., Allin, K. H., Ruhlemann, M. C., Damm, P., Vestergaard, H., Rorbye, C., Jorgensen, N. R., Christiansen, O. B., Heinsen, F. A., Franke, A., Hansen, T., Lauenborg, J., and Pedersen, O. 2018. 'Gestational diabetes is associated with change in the

gut microbiota composition in third trimester of pregnancy and postpartum', *Microbiome*, 6: 89.

Cummings, J. H., Wiggins, H. S., Jenkins, D. J., Houston, H., Jivraj, T., Drasar, B. S., and Hill, M. J. 1978. 'Influence of diets high and low in animal fat on bowel habit, gastrointestinal transit time, fecal microflora, bile acid, and fat excretion', *J Clin Invest*, 61: 953-63.

da Silva, G. P., Mack, M., and Contiero, J. 2009. 'Glycerol: a promising and abundant carbon source for industrial microbiology', *Biotechnol Adv*, 27: 30-9.

Dave, M., Higgins, P. D., Middha, S., and Rioux, K. P. 2012. 'The human gut microbiome: current knowledge, challenges, and future directions', *Transl Res*, 160: 246-57.

De Filippis, F., Pasolli, E., Tett, A., Tarallo, S., Naccarati, A., De Angelis, M., Neviani, E., Cocolin, L., Gobbetti, M., Segata, N., and Ercolini, D. 2019. 'Distinct Genetic and Functional Traits of Human Intestinal *Prevotella copri* Strains Are Associated with Different Habitual Diets', *Cell Host Microbe*, 25: 444-53 e3.

de la Cuesta-Zuluaga, J., Mueller, N. T., Corrales-Agudelo, V., Velasquez-Mejia, E. P., Carmona, J. A., Abad, J. M., and Escobar, J. S. 2017. 'Metformin Is Associated With Higher Relative Abundance of Mucin-Degrading *Akkermansia muciniphila* and Several Short-Chain Fatty Acid-Producing Microbiota in the Gut', *Diabetes Care*, 40: 54-62.

de Vos, W. M., Tilg, H., Van Hul, M., and Cani, P. D. 2022. 'Gut microbiome and health: mechanistic insights', *Gut*, 71: 1020-32.

Demignot, S., Beilstein, F., and Morel, E. 2014. 'Triglyceride-rich lipoproteins and cytosolic lipid droplets in enterocytes: key players in intestinal physiology and metabolic disorders', *Biochimie*, 96: 48-55.

Desai, M. S., Seekatz, A. M., Koropatkin, N. M., Kamada, N., Hickey, C. A., Wolter, M., Pudlo, N. A., Kitamoto, S., Terrapon, N., Muller, A., Young, V. B., Henrissat, B., Wilmes, P., Stappenbeck, T. S., Nunez, G., and Martens, E. C. 2016. 'A Dietary Fiber-Deprived Gut Microbiota Degrades the Colonic Mucus Barrier and Enhances Pathogen Susceptibility', *Cell*, 167: 1339-53 e21.

Donaldson, G. P., Lee, S. M., and Mazmanian, S. K. 2016. 'Gut biogeography of the bacterial microbiota', *Nat Rev Microbiol*, 14: 20-32.

Dong, X., Guthrie, B. G. H., Alexander, M., Noecker, C., Ramirez, L., Glasser, N. R., Turnbaugh, P. J., and Balskus, E. P. 2022. 'Genetic manipulation of the human gut bacterium *Eggerthella lenta* reveals a widespread family of transcriptional regulators', *Nat Commun*, 13: 7624.

Doumatey, A. P., Adeyemo, A., Zhou, J., Lei, L., Adebamowo, S. N., Adebamowo, C., and Rotimi, C. N. 2020. 'Gut Microbiome Profiles Are Associated With Type 2 Diabetes in Urban Africans', *Front Cell Infect Microbiol*, 10: 63.

Dragulescu, A., and Arendt, C. 2018. "xlsx: Read, Write, Format Excel 2007 and Excel 97/2000/XP/2003 Files." In.

Drouault, S., Juste, C., Marteau, P., Renault, P., and Corthier, G. 2002. 'Oral treatment with *Lactococcus lactis* expressing *Staphylococcus hyicus* lipase enhances lipid digestion in pigs with induced pancreatic insufficiency', *Appl Environ Microbiol*, 68: 3166-8.

Eberl, C., Ring, D., Munch, P. C., Beutler, M., Basic, M., Slack, E. C., Schwarzer, M., Srutkova, D., Lange, A., Frick, J. S., Bleich, A., and Stecher, B. 2019. 'Reproducible Colonization of Germ-Free Mice With the Oligo-Mouse-Microbiota in Different Animal Facilities', *Front Microbiol*, 10: 2999.

Eckburg, P. B., Bik, E. M., Bernstein, C. N., Purdom, E., Dethlefsen, L., Sargent, M., Gill, S. R., Nelson, K. E., and Relman, D. A. 2005. 'Diversity of the human intestinal microbial flora', *Science*, 308: 1635-8.

Ecker, J., Scherer, M., Schmitz, G., and Liebisch, G. 2012. 'A rapid GC-MS method for quantification of positional and geometric isomers of fatty acid methyl esters', *J Chromatogr B Analyt Technol Biomed Life Sci*, 897: 98-104.

Edgar, R. C. 2013. 'UPARSE: highly accurate OTU sequences from microbial amplicon reads', *Nat Methods*, 10: 996-8.

Eggerth, A. H. 1935. 'The Gram-positive Non-spore-bearing Anaerobic Bacilli of Human Feces', *J Bacteriol*, 30: 277-99.

Faith, J. J., McNulty, N. P., Rey, F. E., and Gordon, J. I. 2011. 'Predicting a human gut microbiota's response to diet in gnotobiotic mice', *Science*, 333: 101-4.

Fei, N., and Zhao, L. 2013. 'An opportunistic pathogen isolated from the gut of an obese human causes obesity in germfree mice', *ISME J*, 7: 880-4.

Feng, L., Deng, Y., Song, S., Sun, Y., Cui, J., Ma, X., Jin, L., Wang, Y., James, T. D., and Wang, C. 2022. 'Visual Identification of *Trichosporon asahii*, a Gut Yeast Associated with Obesity, Using an Enzymatic NIR Fluorescent Probe', *Anal Chem*, 94: 11216-23.

Feng, Q., Lin, J., Niu, Z., Wu, T., Shen, Q., Hou, D., and Zhou, S. 2024. 'A Comparative Analysis between Whole Chinese Yam and Peeled Chinese Yam: Their Hypolipidemic Effects via Modulation of Gut Microbiome in High-Fat Diet-Fed Mice', *Nutrients*, 16.

Fischer, M., and Pleiss, J. 2003. 'The Lipase Engineering Database: a navigation and analysis tool for protein families', *Nucleic Acids Res*, 31: 319-21.

Fleissner, C. K., Huebel, N., Abd El-Bary, M. M., Loh, G., Klaus, S., and Blaut, M. 2010. 'Absence of intestinal microbiota does not protect mice from diet-induced obesity', *Br J Nutr*, 104: 919-29.

Forslund, K., Hildebrand, F., Nielsen, T., Falony, G., Le Chatelier, E., Sunagawa, S., Prifti, E., Vieira-Silva, S., Gudmundsdottir, V., Pedersen, H. K., Arumugam, M., Kristiansen, K., Voigt, A. Y., Vestergaard, H., Hercog, R., Costea, P. I., Kultima, J. R., Li, J., Jorgensen, T., Levenez, F., Dore, J., Meta, H. I. T. c., Nielsen, H. B., Brunak, S., Raes, J., Hansen, T., Wang, J., Ehrlich, S. D., Bork, P., and Pedersen, O. 2015. 'Disentangling type 2 diabetes and metformin treatment signatures in the human gut microbiota', *Nature*, 528: 262-66.

Frese, S. A., Mackenzie, D. A., Peterson, D. A., Schmaltz, R., Fangman, T., Zhou, Y., Zhang, C., Benson, A. K., Cody, L. A., Mulholland, F., Juge, N., and Walter, J. 2013. 'Molecular characterization of host-specific biofilm formation in a vertebrate gut symbiont', *PLoS Genet*, 9: e1004057.

Fu, J., Bonder, M. J., Cenit, M. C., Tigchelaar, E. F., Maatman, A., Dekens, J. A., Brandsma, E., Marczynska, J., Imhann, F., Weersma, R. K., Franke, L., Poon, T. W., Xavier, R. J., Gevers, D., Hofker, M. H., Wijmenga, C., and Zhernakova, A. 2015. 'The Gut Microbiome Contributes to a Substantial Proportion of the Variation in Blood Lipids', *Circ Res*, 117: 817-24.

Galili, T. 2015. 'dendextend: an R package for visualizing, adjusting and comparing trees of hierarchical clustering', *Bioinformatics*, 31: 3718-20.

Gallardo-Becerra, L., Cornejo-Granados, F., Garcia-Lopez, R., Valdez-Lara, A., Bikel, S., Canizales-Quinteros, S., Lopez-Contreras, B. E., Mendoza-Vargas, A., Nielsen, H., and Ochoa-Leyva, A. 2020. 'Metatranscriptomic analysis to define the Secrebiome, and 16S rRNA profiling of the gut microbiome in obesity and metabolic syndrome of Mexican children', *Microb Cell Fact*, 19: 61.

Ghadimi, D., Folster-Holst, R., Ebsen, M., Rocken, C., Dorfer, C., Uchiyama, J., Matsuzaki, S., and Bockelmann, W. 2024. 'Exploring the Interplay between Nutrients, Bacteriophages, and Bacterial Lipases in Host- and Bacteria-mediated Pathogenesis', *Endocr Metab Immune Disord Drug Targets*, 24: 930-45.

Godon, J. J., Zumstein, E., Dabert, P., Habouzit, F., and Moletta, R. 1997. 'Molecular microbial diversity of an anaerobic digestor as determined by small-subunit rDNA sequence analysis', *Appl Environ Microbiol*, 63: 2802-13.

Graffelman, J., and van Eeuwijk, F. 2005. 'Calibration of multivariate scatter plots for exploratory analysis of relations within and between sets of variables in genomic research', *Biometrical Journal*, 47: 863-79.

Gremse, F., Stark, M., Ehling, J., Menzel, J. R., Lammers, T., and Kiessling, F. 2016. 'Imalytics Preclinical: Interactive Analysis of Biomedical Volume Data', *Theranostics*, 6: 328-41.

Gu, Z., Eils, R., and Schlesner, M. 2016. 'Complex heatmaps reveal patterns and correlations in multidimensional genomic data', *Bioinformatics*, 32: 2847-9.

Gu, Z., Gu, L., Eils, R., Schlesner, M., and Brors, B. 2014. 'circlize Implements and enhances circular visualization in R', *Bioinformatics*, 30: 2811-2.

Gupta, R. S., Chen, W. J., Adeolu, M., and Chai, Y. 2013. 'Molecular signatures for the class Coriobacteriia and its different clades; proposal for division of the class Coriobacteriia into the emended order Coriobacteriales, containing the emended family Coriobacteriaceae and

Atopobiaceae fam. nov., and Eggerthellales ord. nov., containing the family Eggerthellaceae fam. nov', *Int J Syst Evol Microbiol*, 63: 3379-97.

Guzior, D. V., and Quinn, R. A. 2021. 'Review: microbial transformations of human bile acids', *Microbiome*, 9: 140.

Haiser, H. J., Gootenberg, D. B., Chatman, K., Sirasani, G., Balskus, E. P., and Turnbaugh, P. J. 2013. 'Predicting and manipulating cardiac drug inactivation by the human gut bacterium *Eggerthella lenta*', *Science*, 341: 295-8.

Harris, S. C., Devendran, S., Mendez-Garcia, C., Mythen, S. M., Wright, C. L., Fields, C. J., Hernandez, A. G., Cann, I., Hylemon, P. B., and Ridlon, J. M. 2018. 'Bile acid oxidation by *Eggerthella lenta* strains C592 and DSM 2243(T)', *Gut Microbes*, 9: 523-39.

Herp, S., Brugiroux, S., Garzetti, D., Ring, D., Jochum, L. M., Beutler, M., Eberl, C., Hussain, S., Walter, S., Gerlach, R. G., Ruscheweyh, H. J., Huson, D., Sellin, M. E., Slack, E., Hanson, B., Loy, A., Baines, J. F., Rausch, P., Basic, M., Bleich, A., Berry, D., and Stecher, B. 2019. 'Mucispirillum schaedleri Antagonizes Salmonella Virulence to Protect Mice against Colitis', *Cell Host Microbe*, 25: 681-94 e8.

Hillman, E. T., Lu, H., Yao, T., and Nakatsu, C. H. 2017. 'Microbial Ecology along the Gastrointestinal Tract', *Microbes Environ*, 32: 300-13.

Hills, R. D., Jr., Pontefract, B. A., Mishcon, H. R., Black, C. A., Sutton, S. C., and Theberge, C. R. 2019. 'Gut Microbiome: Profound Implications for Diet and Disease', *Nutrients*, 11.

Hitch, T. C. A., Masson, J. M., Streidl, T., Fischöder, T., Elling, L., and Clavel, T. 2020. 'Diversity and function of microbial lipases within the mammalian gut', *bioRxiv*: 2020.09.08.287425.

Holle, R., Happich, M., Lowel, H., Wichmann, H. E., and Group, M. K. S. 2005. 'KORA--a research platform for population based health research', *Gesundheitswesen*, 67 Suppl 1: S19-25.

Honda, A., Miyazaki, T., Iwamoto, J., Hirayama, T., Morishita, Y., Monma, T., Ueda, H., Mizuno, S., Sugiyama, F., Takahashi, S., and Ikegami, T. 2020. 'Regulation of bile acid metabolism in mouse models with hydrophobic bile acid composition', *J Lipid Res*, 61: 54-69.

Hoyles, L. 2009. 'In vitro examination of the effect of orlistat on the ability of the faecal microbiota to utilize dietary lipids', PhD thesis, University of Westminster.

Hu, P., Chen, X., Chu, X., Fan, M., Ye, Y., Wang, Y., Han, M., Yang, X., Yuan, J., Zha, L., Zhao, B., Yang, C. X., Qi, X. R., Ning, K., Debelius, J., Ye, W., Xiong, B., Pan, X. F., and Pan, A. 2021. 'Association of Gut Microbiota during Early Pregnancy with Risk of Incident Gestational Diabetes Mellitus', *J Clin Endocrinol Metab*, 106: e4128-e41.

Huerta-Cepas, J., Szklarczyk, D., Heller, D., Hernandez-Plaza, A., Forslund, S. K., Cook, H., Mende, D. R., Letunic, I., Rattei, T., Jensen, L. J., von Mering, C., and Bork, P. 2019. 'eggNOG 5.0: a hierarchical, functionally and phylogenetically annotated orthology resource based on 5090 organisms and 2502 viruses', *Nucleic Acids Res*, 47: D309-D14.

Human Microbiome Project, C. 2012. 'Structure, function and diversity of the healthy human microbiome', *Nature*, 486: 207-14.

Hungate, R. E., Smith, W., and Clarke, R. T. 1966. 'Suitability of butyl rubber stoppers for closing anaerobic roll culture tubes', *J Bacteriol*, 91: 908-9.

Hussain, M. M. 2014. 'Intestinal lipid absorption and lipoprotein formation', *Curr Opin Lipidol*, 25: 200-6.

Hyatt, D., Chen, G. L., Locascio, P. F., Land, M. L., Larimer, F. W., and Hauser, L. J. 2010. 'Prodigal: prokaryotic gene recognition and translation initiation site identification', *BMC Bioinformatics*, 11: 119.

Ioannou, A., Berkhout, M. D., Geerlings, S. Y., and Belzer, C. 2024. '*Akkermansia muciniphila*: biology, microbial ecology, host interactions and therapeutic potential', *Nat Rev Microbiol*.

Iqbal, J., and Hussain, M. M. 2009. 'Intestinal lipid absorption', *Am J Physiol Endocrinol Metab*, 296: E1183-94.

Jacobi, J., and Tsao, P. S. 2008. 'Asymmetrical dimethylarginine in renal disease: limits of variation or variation limits? A systematic review', *Am J Nephrol*, 28: 224-37.

Jang, H. R., Park, H. J., Kang, D., Chung, H., Nam, M. H., Lee, Y., Park, J. H., and Lee, H. Y. 2019. 'A protective mechanism of probiotic *Lactobacillus* against hepatic steatosis via reducing host intestinal fatty acid absorption', *Exp Mol Med*, 51: 1-14.

Javed, S., Azeem, F., Hussain, S., Rasul, I., Siddique, M. H., Riaz, M., Afzal, M., Kouser, A., and Nadeem, H. 2018. 'Bacterial lipases: A review on purification and characterization', *Prog Biophys Mol Biol*, 132: 23-34.

Jennings, S. A. V., and Clavel, T. 2024. 'Synthetic Communities of Gut Microbes for Basic Research and Translational Approaches in Animal Health and Nutrition', *Annu Rev Anim Biosci*, 12: 283-300.

Joyce, S. A., MacSharry, J., Casey, P. G., Kinsella, M., Murphy, E. F., Shanahan, F., Hill, C., and Gahan, C. G. 2014. 'Regulation of host weight gain and lipid metabolism by bacterial bile acid modification in the gut', *Proc Natl Acad Sci U S A*, 111: 7421-6.

Just, S. 2017. 'Impact of the interplay between bile acids, lipids, intestinal *Coriobacteriaceae* and diet on host metabolism', Technische Universität München.

Just, S., Mondot, S., Ecker, J., Wegner, K., Rath, E., Gau, L., Streidl, T., Hery-Arnaud, G., Schmidt, S., Lesker, T. R., Bieth, V., Dunkel, A., Strowig, T., Hofmann, T., Haller, D., Liebisch, G., Gérard, P., Rohn, S., Lepage, P., and Clavel, T. 2018. 'The gut microbiota drives the impact of bile acids and fat source in diet on mouse metabolism', *Microbiome*, 6: 134.

Kageyama, A., Benno, Y., and Nakase, T. 1999. 'Phylogenetic and phenotypic evidence for the transfer of *Eubacterium aerofaciens* to the genus *Collinsella* as *Collinsella aerofaciens* gen. nov., comb. nov', *Int J Syst Bacteriol*, 49 Pt 2: 557-65.

Kanmani, P., Aravind, J., and Kumaresan, K. 2015. 'An insight into microbial lipases and their environmental facet', *International Journal of Environmental Science and Technology*, 12: 1147-62.

Karlsson, F. H., Tremaroli, V., Nookaew, I., Bergstrom, G., Behre, C. J., Fagerberg, B., Nielsen, J., and Backhed, F. 2013. 'Gut metagenome in European women with normal, impaired and diabetic glucose control', *Nature*, 498: 99-103.

Kasahara, K., Krautkramer, K. A., Org, E., Romano, K. A., Kerby, R. L., Vivas, E. I., Mehrabian, M., Denu, J. M., Backhed, F., Lusis, A. J., and Rey, F. E. 2018. 'Interactions between *Roseburia intestinalis* and diet modulate atherogenesis in a murine model', *Nat Microbiol*, 3: 1461-71.

Kasper, H. 1970. 'Faecal fat excretion, diarrhea, and subjective complaints with highly dosed oral fat intake', *Digestion*, 3: 321-30.

Kassambara, A. 2023. "ggpubr: 'ggplot2' Based Publication Ready Plots." In.

Kennedy, K. M., de Goffau, M. C., Perez-Munoz, M. E., Arrieta, M. C., Backhed, F., Bork, P., Braun, T., Bushman, F. D., Dore, J., de Vos, W. M., Earl, A. M., Eisen, J. A., Elovitz, M. A., Ganal-Vonarburg, S. C., Ganzle, M. G., Garrett, W. S., Hall, L. J., Hornef, M. W., Huttenhower, C., Konnikova, L., Lebeer, S., Macpherson, A. J., Massey, R. C., McHardy, A. C., Koren, O., Lawley, T. D., Ley, R. E., O'Mahony, L., O'Toole, P. W., Pamer, E. G., Parkhill, J., Raes, J., Rattei, T., Salonen, A., Segal, E., Segata, N., Shanahan, F., Sloboda, D. M., Smith, G. C. S., Sokol, H., Spector, T. D., Surette, M. G., Tannock, G. W., Walker, A. W., Yassour, M., and Walter, J. 2023. 'Questioning the fetal microbiome illustrates pitfalls of low-biomass microbial studies', *Nature*, 613: 639-49.

Killgore, G. E., Starr, S. E., Del Bene, V. E., Whaley, D. N., and Dowell, V. R., Jr. 1973. 'Comparison of three anaerobic systems for the isolation of anaerobic bacteria from clinical specimens', *Am J Clin Pathol*, 59: 552-9.

Kim, M. H., Yun, K. E., Kim, J., Park, E., Chang, Y., Ryu, S., Kim, H. L., and Kim, H. N. 2020. 'Gut microbiota and metabolic health among overweight and obese individuals', *Sci Rep*, 10: 19417.

Kirpich, I. A., Gobejishvili, L. N., Bon Homme, M., Waigel, S., Cave, M., Arteel, G., Barve, S. S., McClain, C. J., and Deaciuc, I. V. 2011. 'Integrated hepatic transcriptome and proteome analysis of mice with high-fat diet-induced nonalcoholic fatty liver disease', *J Nutr Biochem*, 22: 38-45.

Klindworth, A., Pruesse, E., Schweer, T., Peplies, J., Quast, C., Horn, M., and Glockner, F. O. 2013. 'Evaluation of general 16S ribosomal RNA gene PCR primers for classical and next-generation sequencing-based diversity studies', *Nucleic Acids Res*, 41: e1.

Ko, C. W., Qu, J., Black, D. D., and Tso, P. 2020. 'Regulation of intestinal lipid metabolism: current concepts and relevance to disease', *Nat Rev Gastroenterol Hepatol*, 17: 169-83.

Koh, A., Molinaro, A., Stahlman, M., Khan, M. T., Schmidt, C., Manneras-Holm, L., Wu, H., Carreras, A., Jeong, H., Olofsson, L. E., Bergh, P. O., Gerdes, V., Hartstra, A., de Brauw, M., Perkins, R., Nieuwdorp, M., Bergstrom, G., and Backhed, F. 2018. 'Microbially Produced Imidazole Propionate Impairs Insulin Signaling through mTORC1', *Cell*, 175: 947-61 e17.

Kolde, R. 2012. 'Pheatmap: pretty heatmaps'.

Kouker, G., and Jaeger, K. E. 1987. 'Specific and sensitive plate assay for bacterial lipases', *Appl Environ Microbiol*, 53: 211-3.

Kovatcheva-Datchary, P., Shoaie, S., Lee, S., Wahlstrom, A., Nookaew, I., Hallen, A., Perkins, R., Nielsen, J., and Backhed, F. 2019. 'Simplified Intestinal Microbiota to Study Microbe-Diet-Host Interactions in a Mouse Model', *Cell Rep*, 26: 3772-83 e6.

Kraatz, M., Wallace, R. J., and Svensson, L. 2011. '*Olsenella umbonata* sp. nov., a microaerotolerant anaerobic lactic acid bacterium from the sheep rumen and pig jejunum, and emended descriptions of *Olsenella, Olsenella uli* and *Olsenella profusa*', *Int J Syst Evol Microbiol*, 61: 795-803.

Kübeck, R., Bonet-Ripoll, C., Hoffmann, C., Walker, A., Müller, V. M., Schüppel, V. L., Lagkouvardos, I., Scholz, B., Engel, K. H., Daniel, H., Schmitt-Kopplin, P., Haller, D., Clavel, T., and Klingenspor, M. 2016. 'Dietary fat and gut microbiota interactions determine diet-induced obesity in mice', *Mol Metab*, 5: 1162-74.

Lagkouvardos, I., Fischer, S., Kumar, N., and Clavel, T. 2017. 'Rhea: a transparent and modular R pipeline for microbial profiling based on 16S rRNA gene amplicons', *PeerJ*, 5: e2836.

Lagkouvardos, I., Joseph, D., Kapfhammer, M., Giritli, S., Horn, M., Haller, D., and Clavel, T. 2016. 'IMNGS: A comprehensive open resource of processed 16S rRNA microbial profiles for ecology and diversity studies', *Sci Rep*, 6: 33721.

Le Chatelier, E., Nielsen, T., Qin, J., Prifti, E., Hildebrand, F., Falony, G., Almeida, M., Arumugam, M., Batto, J. M., Kennedy, S., Leonard, P., Li, J., Burgdorf, K., Grarup, N., Jorgensen, T., Brandslund, I., Nielsen, H. B., Juncker, A. S., Bertalan, M., Levenez, F., Pons, N., Rasmussen, S., Sunagawa, S., Tap, J., Tims, S., Zoetendal, E. G., Brunak, S., Clement, K., Dore, J., Kleerebezem, M., Kristiansen, K., Renault, P., Sicheritz-Ponten, T., de Vos, W. M., Zucker, J. D., Raes, J., Hansen, T., Meta, H. I. T. c., Bork, P., Wang, J., Ehrlich, S. D., and Pedersen, O. 2013. 'Richness of human gut microbiome correlates with metabolic markers', *Nature*, 500: 541-6.

Leiby, J. S., McCormick, K., Sherrill-Mix, S., Clarke, E. L., Kessler, L. R., Taylor, L. J., Hofstaedter, C. E., Roche, A. M., Mattei, L. M., Bittinger, K., Elovitz, M. A., Leite, R., Parry, S., and Bushman, F. D. 2018. 'Lack of detection of a human placenta microbiome in samples from preterm and term deliveries', *Microbiome*, 6: 196.

Letunic, I., and Bork, P. 2021. 'Interactive Tree Of Life (iTOL) v5: an online tool for phylogenetic tree display and annotation', *Nucleic Acids Res*, 49: W293-W96.

Ley, R. E., Turnbaugh, P. J., Klein, S., and Gordon, J. I. 2006. 'Microbial ecology: human gut microbes associated with obesity', *Nature*, 444: 1022-3.

Lin, J., Zhang, R., Liu, H., Zhu, Y., Dong, N., Qu, Q., Bi, H., Zhang, L., Luo, O., Sun, L., Ma, M., and You, J. 2024. 'Multi-omics analysis of the biological mechanism of the pathogenesis of non-alcoholic fatty liver disease', *Front Microbiol*, 15: 1379064.

Lin, X., Hu, T., Chen, J., Liang, H., Zhou, J., Wu, Z., Ye, C., Jin, X., Xu, X., Zhang, W., Jing, X., Yang, T., Wang, J., Yang, H., Kristiansen, K., Xiao, L., and Zou, Y. 2023. 'The genomic landscape of reference genomes of cultivated human gut bacteria', *Nat Commun*, 14: 1663.

Liu, L., Aigner, A., and Schmid, R. D. 2011. 'Identification, cloning, heterologous expression, and characterization of a NADPH-dependent 7beta-hydroxysteroid dehydrogenase from Collinsella aerofaciens', *Appl Microbiol Biotechnol*, 90: 127-35.

Liu, X., Cheng, Y. W., Shao, L., Sun, S. H., Wu, J., Song, Q. H., Zou, H. S., and Ling, Z. X. 2021. 'Gut microbiota dysbiosis in Chinese children with type 1 diabetes mellitus: An observational study', *World J Gastroenterol*, 27: 2394-414.

Lobo, M. V., Huerta, L., Ruiz-Velasco, N., Teixeiro, E., de la Cueva, P., Celdran, A., Martin-Hidalgo, A., Vega, M. A., and Bragado, R. 2001. 'Localization of the lipid receptors CD36 and CLA-1/SR-BI in

the human gastrointestinal tract: towards the identification of receptors mediating the intestinal absorption of dietary lipids', *J Histochem Cytochem*, 49: 1253-60.

Lucas, L. N., Barrett, K., Kerby, R. L., Zhang, Q., Cattaneo, L. E., Stevenson, D., Rey, F. E., and Amador-Noguez, D. 2021. 'Dominant Bacterial Phyla from the Human Gut Show Widespread Ability To Transform and Conjugate Bile Acids', *mSystems*: e0080521.

Lv, Y., Liu, R., Jia, H., Sun, X., Gong, Y., Ma, L., Qiu, W., and Wang, X. 2023. 'Alterations of the gut microbiota in type 2 diabetics with or without subclinical hypothyroidism', *PeerJ*, 11: e15193.

Lynch, J. B., Gonzalez, E. L., Choy, K., Faull, K. F., Jewell, T., Arellano, A., Liang, J., Yu, K. B., Paramo, J., and Hsiao, E. Y. 2023. 'Gut microbiota *Turicibacter* strains differentially modify bile acids and host lipids', *Nat Commun*, 14: 3669.

Lynch, S. V., and Pedersen, O. 2016. 'The Human Intestinal Microbiome in Health and Disease', *N Engl J Med*, 375: 2369-79.

Maini Rekdal, V., Bess, E. N., Bisanz, J. E., Turnbaugh, P. J., and Balskus, E. P. 2019. 'Discovery and inhibition of an interspecies gut bacterial pathway for Levodopa metabolism', *Science*, 364.

Maini Rekdal, V., Nol Bernadino, P., Luescher, M. U., Kiamehr, S., Le, C., Bisanz, J. E., Turnbaugh, P. J., Bess, E. N., and Balskus, E. P. 2020. 'A widely distributed metalloenzyme class enables gut microbial metabolism of host- and diet-derived catechols', *Elife*, 9.

Makki, K., Deehan, E. C., Walter, J., and Backhed, F. 2018. 'The Impact of Dietary Fiber on Gut Microbiota in Host Health and Disease', *Cell Host Microbe*, 23: 705-15.

Mandic, A. D., Woting, A., Jaenicke, T., Sander, A., Sabrowski, W., Rolle-Kampcyk, U., von Bergen, M., and Blaut, M. 2019. '*Clostridium ramosum* regulates enterochromaffin cell development and serotonin release', *Sci Rep*, 9: 1177.

Mansbach, C. M., 2nd, and Gorelick, F. 2007. 'Development and physiological regulation of intestinal lipid absorption. II. Dietary lipid absorption, complex lipid synthesis, and the intracellular packaging and secretion of chylomicrons', *Am J Physiol Gastrointest Liver Physiol*, 293: G645-50.

Marchesi, J. R. 2011. 'Human distal gut microbiome', *Environ Microbiol*, 13: 3088-102.

Marchesi, J. R., and Ravel, J. 2015. 'The vocabulary of microbiome research: a proposal', *Microbiome*, 3: 31.

Marion, S., Desharnais, L., Studer, N., Dong, Y., Notter, M. D., Poudel, S., Menin, L., Janowczyk, A., Hettich, R. L., Hapfelmeier, S., and Bernier-Latmani, R. 2020. 'Biogeography of microbial bile acid transformations along the murine gut', *J Lipid Res*, 61: 1450-63.

Martin, S., and Parton, R. G. 2006. 'Lipid droplets: a unified view of a dynamic organelle', *Nat Rev Mol Cell Biol*, 7: 373-8.

Martinez-Guryn, K., Hubert, N., Frazier, K., Urlass, S., Musch, M. W., Ojeda, P., Pierre, J. F., Miyoshi, J., Sontag, T. J., Cham, C. M., Reardon, C. A., Leone, V., and Chang, E. B. 2018. 'Small Intestine Microbiota Regulate Host Digestive and Absorptive Adaptive Responses to Dietary Lipids', *Cell Host Microbe*, 23: 458-69 e5.

Martinez, I., Perdicaro, D. J., Brown, A. W., Hammons, S., Carden, T. J., Carr, T. P., Eskridge, K. M., and Walter, J. 2013. 'Diet-induced alterations of host cholesterol metabolism are likely to affect the gut microbiota composition in hamsters', *Appl Environ Microbiol*, 79: 516-24.

Maukonen, J., Simoes, C., and Saarela, M. 2012. 'The currently used commercial DNA-extraction methods give different results of clostridial and actinobacterial populations derived from human fecal samples', *FEMS Microbiol Ecol*, 79: 697-708.

McCurry, M. D., D'Agostino, G. D., Walsh, J. T., Bisanz, J. E., Zalosnik, I., Dong, X., Morris, D. J., Korzenik, J. R., Edlow, A. G., Balskus, E. P., Turnbaugh, P. J., Huh, J. R., and Devlin, A. S. 2024. 'Gut bacteria convert glucocorticoids into progestins in the presence of hydrogen gas', *Cell*, 187: 2952-68 e13.

Mitchell, A. L., Attwood, T. K., Babbitt, P. C., Blum, M., Bork, P., Bridge, A., Brown, S. D., Chang, H. Y., El-Gebali, S., Fraser, M. I., Gough, J., Haft, D. R., Huang, H., Letunic, I., Lopez, R., Luciani, A., Madeira, F., Marchler-Bauer, A., Mi, H., Natale, D. A., Necci, M., Nuka, G., Orengo, C., Pandurangan, A. P., Paysan-Lafosse, T., Pesseat, S., Potter, S. C., Qureshi, M. A., Rawlings, N. D., Redaschi, N., Richardson, L. J., Rivoire, C., Salazar, G. A., Sangrador-Vegas, A., Sigrist, C. J.

A., Sillitoe, I., Sutton, G. G., Thanki, N., Thomas, P. D., Tosatto, S. C. E., Yong, S. Y., and Finn, R. D. 2019. 'InterPro in 2019: improving coverage, classification and access to protein sequence annotations', *Nucleic Acids Res*, 47: D351-D60.

Miyazaki, H., Matsuoka, H., Cooke, J. P., Usui, M., Ueda, S., Okuda, S., and Imaizumi, T. 1999. 'Endogenous nitric oxide synthase inhibitor: a novel marker of atherosclerosis', *Circulation*, 99: 1141-6.

Moore, W. E., and Holdeman, L. V. 1974. 'Human fecal flora: the normal flora of 20 Japanese-Hawaiians', *Appl Microbiol*, 27: 961-79.

Morales, C., Rojas, G., Rebolledo, C., Rojas-Herrera, M., Arias-Carrasco, R., Cuadros-Orellana, S., Maracaja-Coutinho, V., Saavedra, K., Leal, P., Lanas, F., Salazar, L. A., and Saavedra, N. 2022. 'Characterization of microbial communities from gut microbiota of hypercholesterolemic and control subjects', *Front Cell Infect Microbiol*, 12: 943609.

Nassir, F., Wilson, B., Han, X., Gross, R. W., and Abumrad, N. A. 2007. 'CD36 is important for fatty acid and cholesterol uptake by the proximal but not distal intestine', *J Biol Chem*, 282: 19493-501.

Nesci, A., Carnuccio, C., Ruggieri, V., D'Alessandro, A., Di Giorgio, A., Santoro, L., Gasbarrini, A., Santoliquido, A., and Ponziani, F. R. 2023. 'Gut Microbiota and Cardiovascular Disease: Evidence on the Metabolic and Inflammatory Background of a Complex Relationship', *Int J Mol Sci*, 24.

Nirmalkar, K., Murugesan, S., Pizano-Zarate, M. L., Villalobos-Flores, L. E., Garcia-Gonzalez, C., Morales-Hernandez, R. M., Nunez-Hernandez, J. A., Hernandez-Quiroz, F., Romero-Figueroa, M. D. S., Hernandez-Guerrero, C., Hoyo-Vadillo, C., and Garcia-Mena, J. 2018. 'Gut Microbiota and Endothelial Dysfunction Markers in Obese Mexican Children and Adolescents', *Nutrients*, 10.

Noecker, C., Sanchez, J., Bisanz, J. E., Escalante, V., Alexander, M., Trepka, K., Heinken, A., Liu, Y., Dodd, D., Thiele, I., DeFelice, B. C., and Turnbaugh, P. J. 2023. 'Systems biology elucidates the distinctive metabolic niche filled by the human gut microbe *Eggerthella lenta*', *PLoS Biol*, 21: e3002125.

Nouioui, I., Carro, L., Garcia-Lopez, M., Meier-Kolthoff, J. P., Woyke, T., Kyrpides, N. C., Pukall, R., Klenk, H. P., Goodfellow, M., and Goker, M. 2018. 'Genome-Based Taxonomic Classification of the Phylum Actinobacteria', *Front Microbiol*, 9: 2007.

Nuttall, G. H. F., and Thierfelder., H. 1896. 'Thierisches Leben ohne Bakterien im Verdauungskanal', *Biological Chemistry*, 21: 109-21.

O'Hara, A. M., and Shanahan, F. 2006. 'The gut flora as a forgotten organ', *EMBO Rep*, 7: 688-93.

Ogiwara, A., Uchiyama, I., Takagi, T., and Kanehisa, M. 1996. 'Construction and analysis of a profile library characterizing groups of structurally known proteins', *Protein Sci*, 5: 1991-9.

Oksanen, J., Simpson, G., Blanchet, F. G., Kindt, R., Legendre, P., Minchin, P., hara, R., Solymos, P., Stevens, H., Szöcs, E., Wagner, H., Barbour, M., Bedward, M., Bolker, B., Borcard, D., Carvalho, G., Chirico, M., De Cáceres, M., Durand, S., and Weedon, J. 2022. "vegan: Community Ecology Package. R package version 2.6-2." In.

Paik, D., Yao, L., Zhang, Y., Bae, S., D'Agostino, G. D., Zhang, M., Kim, E., Franzosa, E. A., Avila-Pacheco, J., Bisanz, J. E., Rakowski, C. K., Vlamakis, H., Xavier, R. J., Turnbaugh, P. J., Longman, R. S., Krout, M. R., Clish, C. B., Rastinejad, F., Huttenhower, C., Huh, J. R., and Devlin, A. S. 2022. 'Human gut bacteria produce Tau(Eta)17-modulating bile acid metabolites', *Nature*, 603: 907-12.

Panzer, J. J., Romero, R., Greenberg, J. M., Winters, A. D., Galaz, J., Gomez-Lopez, N., and Theis, K. R. 2023. 'Is there a placental microbiota? A critical review and re-analysis of published placental microbiota datasets', *BMC Microbiol*, 23: 76.

Park, S. E., Kwon, S. J., Cho, K. M., Seo, S. H., Kim, E. J., Unno, T., Bok, S. H., Park, D. H., and Son, H. S. 2020. 'Intervention with kimchi microbial community ameliorates obesity by regulating gut microbiota', *J Microbiol*, 58: 859-67.

Pedersen, H. K., Gudmundsdottir, V., Nielsen, H. B., Hyotylainen, T., Nielsen, T., Jensen, B. A., Forslund, K., Hildebrand, F., Prifti, E., Falony, G., Le Chatelier, E., Levenez, F., Dore, J., Mattila, I., Plichta, D. R., Poho, P., Hellgren, L. I., Arumugam, M., Sunagawa, S., Vieira-Silva, S., Jorgensen, T., Holm, J. B., Trost, K., Meta, H. I. T. C., Kristiansen, K., Brix, S., Raes, J., Wang, J., Hansen, T., Bork, P.,

Brunak, S., Oresic, M., Ehrlich, S. D., and Pedersen, O. 2016. 'Human gut microbes impact host serum metabolome and insulin sensitivity', *Nature*, 535: 376-81.

Pedersen, K. J., Haange, S. B., Zizalova, K., Viehof, A., Clavel, T., Lenicek, M., Engelmann, B., Wick, L. Y., Schaap, F. G., Jehmlich, N., Rolle-Kampczyk, U., and von Bergen, M. 2022. '*Eggerthella lenta* DSM 2243 Alleviates Bile Acid Stress Response in Clostridium ramosum and Anaerostipes caccae by Transformation of Bile Acids', *Microorganisms*, 10.

Perez-Munoz, M. E., Arrieta, M. C., Ramer-Tait, A. E., and Walter, J. 2017. 'A critical assessment of the "sterile womb" and "in utero colonization" hypotheses: implications for research on the pioneer infant microbiome', *Microbiome*, 5: 48.

Perino, A., Demagny, H., Velazquez-Villegas, L., and Schoonjans, K. 2021. 'Molecular Physiology of Bile Acid Signaling in Health, Disease, and Aging', *Physiol Rev*, 101: 683-731.

Peterson, B. G., Carl, P., Boudt, K., Bennett, R., Ulrich, J., Zivot, E., Lestel, M., Balkissoon, K., and Wuertz, D. 2014. "PerformanceAnalytics: Econometric tools for performance and risk analysis." In.

Plagge, J. 2023. 'The role of gut microbiota in intestinal lipid absorption and systemic lipid metabolism', Technische Universität München.

Pleasants, J. R. 1959. 'Rearing germfree cesarean-born rats, mice, and rabbits through weaning', *Ann N Y Acad Sci*, 78: 116-26.

Plovier, H., Everard, A., Druart, C., Depommier, C., Van Hul, M., Geurts, L., Chilloux, J., Ottman, N., Duparc, T., Lichtenstein, L., Myridakis, A., Delzenne, N. M., Klievink, J., Bhattacharjee, A., van der Ark, K. C., Aalvink, S., Martinez, L. O., Dumas, M. E., Maiter, D., Loumaye, A., Hermans, M. P., Thissen, J. P., Belzer, C., de Vos, W. M., and Cani, P. D. 2017. 'A purified membrane protein from *Akkermansia muciniphila* or the pasteurized bacterium improves metabolism in obese and diabetic mice', *Nat Med*, 23: 107-13.

Pruesse, E., Peplies, J., and Glockner, F. O. 2012. 'SINA: accurate high-throughput multiple sequence alignment of ribosomal RNA genes', *Bioinformatics*, 28: 1823-9.

Purohit, A., Kandiyal, B., Kumar, S., Pragasam, A. K., Kamboj, P., Talukdar, D., Verma, J., Sharma, V., Sarkar, S., Mahajan, D., Yadav, R., Ahmed, R., Nanda, R., Dikshit, M., Banerjee, S. K., Shalimar, and Das, B. 2024. '*Collinsella aerofaciens* linked with increased ethanol production and liver inflammation contribute to the pathophysiology of NAFLD', *iScience*, 27: 108764.

Qin, J., Li, R., Raes, J., Arumugam, M., Burgdorf, K. S., Manichanh, C., Nielsen, T., Pons, N., Levenez, F., Yamada, T., Mende, D. R., Li, J., Xu, J., Li, S., Li, D., Cao, J., Wang, B., Liang, H., Zheng, H., Xie, Y., Tap, J., Lepage, P., Bertalan, M., Batto, J. M., Hansen, T., Le Paslier, D., Linneberg, A., Nielsen, H. B., Pelletier, E., Renault, P., Sicheritz-Ponten, T., Turner, K., Zhu, H., Yu, C., Li, S., Jian, M., Zhou, Y., Li, Y., Zhang, X., Li, S., Qin, N., Yang, H., Wang, J., Brunak, S., Dore, J., Guarner, F., Kristiansen, K., Pedersen, O., Parkhill, J., Weissenbach, J., Meta, H. I. T. C., Bork, P., Ehrlich, S. D., and Wang, J. 2010. 'A human gut microbial gene catalogue established by metagenomic sequencing', *Nature*, 464: 59-65.

Qin, J., Li, Y., Cai, Z., Li, S., Zhu, J., Zhang, F., Liang, S., Zhang, W., Guan, Y., Shen, D., Peng, Y., Zhang, D., Jie, Z., Wu, W., Qin, Y., Xue, W., Li, J., Han, L., Lu, D., Wu, P., Dai, Y., Sun, X., Li, Z., Tang, A., Zhong, S., Li, X., Chen, W., Xu, R., Wang, M., Feng, Q., Gong, M., Yu, J., Zhang, Y., Zhang, M., Hansen, T., Sanchez, G., Raes, J., Falony, G., Okuda, S., Almeida, M., LeChatelier, E., Renault, P., Pons, N., Batto, J. M., Zhang, Z., Chen, H., Yang, R., Zheng, W., Li, S., Yang, H., Wang, J., Ehrlich, S. D., Nielsen, R., Pedersen, O., Kristiansen, K., and Wang, J. 2012. 'A metagenome-wide association study of gut microbiota in type 2 diabetes', *Nature*, 490: 55-60.

Quince, C., Walker, A. W., Simpson, J. T., Loman, N. J., and Segata, N. 2017. 'Shotgun metagenomics, from sampling to analysis', *Nat Biotechnol*, 35: 833-44.

Quinn, R. A., Melnik, A. V., Vrbanac, A., Fu, T., Patras, K. A., Christy, M. P., Bodai, Z., Belda-Ferre, P., Tripathi, A., Chung, L. K., Downes, M., Welch, R. D., Quinn, M., Humphrey, G., Panitchpakdi, M., Weldon, K. C., Aksenov, A., da Silva, R., Avila-Pacheco, J., Clish, C., Bae, S., Mallick, H., Franzosa, E. A., Lloyd-Price, J., Bussell, R., Thron, T., Nelson, A. T., Wang, M., Leszczynski, E., Vargas, F., Gauglitz, J. M., Meehan, M. J., Gentry, E., Arthur, T. D., Komor, A. C., Poulsen, O., Boland, B. S., Chang, J. T., Sandborn, W. J., Lim, M., Garg, N., Lumeng, J. C., Xavier, R. J., Kazmierczak, B. I., Jain, R., Egan, M., Rhee, K. E., Ferguson, D., Raffatellu, M., Vlamakis, H.,

Haddad, G. G., Siegel, D., Huttenhower, C., Mazmanian, S. K., Evans, R. M., Nizet, V., Knight, R., and Dorrestein, P. C. 2020. 'Global chemical effects of the microbiome include new bile-acid conjugations', *Nature*, 579: 123-29.

Rabot, S., Membrez, M., Bruneau, A., Gérard, P., Harach, T., Moser, M., Raymond, F., Mansourian, R., and Chou, C. J. 2010. 'Germ-free C57BL/6J mice are resistant to high-fat-diet-induced insulin resistance and have altered cholesterol metabolism', *Faseb j*, 24: 4948-59.

Ramirez Garcia, A., Zhang, J., Greppi, A., Constancias, F., Wortmann, E., Wandres, M., Hurley, K., Pascual-Garcia, A., Ruscheweyh, H. J., Sturla, S. J., Lacroix, C., and Schwab, C. 2021. 'Impact of manipulation of glycerol/diol dehydratase activity on intestinal microbiota ecology and metabolism', *Environ Microbiol*, 23: 1765-79.

Ran, C., He, S., Yang, Y., Huang, L., and Zhou, Z. 2015. 'A Novel Lipase as Aquafeed Additive for Warm-Water Aquaculture', *PLoS One*, 10: e0132049.

Reitmeier, S., Hitch, T. C. A., Treichel, N., Fikas, N., Hausmann, B., Ramer-Tait, A. E., Neuhaus, K., Berry, D., Haller, D., Lagkouvardos, I., and Clavel, T. 2021. 'Handling of spurious sequences affects the outcome of high-throughput 16S rRNA gene amplicon profiling', *ISME Commun*, 1: 31.

Ridaura, V. K., Faith, J. J., Rey, F. E., Cheng, J., Duncan, A. E., Kau, A. L., Griffin, N. W., Lombard, V., Henrissat, B., Bain, J. R., Muehlbauer, M. J., Ilkayeva, O., Semenkovich, C. F., Funai, K., Hayashi, D. K., Lyle, B. J., Martini, M. C., Ursell, L. K., Clemente, J. C., Van Treuren, W., Walters, W. A., Knight, R., Newgard, C. B., Heath, A. C., and Gordon, J. I. 2013. 'Gut microbiota from twins discordant for obesity modulate metabolism in mice', *Science*, 341: 1241214.

Ridlon, J. M., Kang, D. J., and Hylemon, P. B. 2006. 'Bile salt biotransformations by human intestinal bacteria', *J Lipid Res*, 47: 241-59.

Ritchie, M. E., Phipson, B., Wu, D., Hu, Y., Law, C. W., Shi, W., and Smyth, G. K. 2015. 'limma powers differential expression analyses for RNA-sequencing and microarray studies', *Nucleic Acids Res*, 43: e47.

Rodriguez Jovita, M., Collins, M. D., Sjoden, B., and Falsen, E. 1999. 'Characterization of a novel Atopobium isolate from the human vagina: description of Atopobium vaginae sp. nov', *Int J Syst Bacteriol*, 49 Pt 4: 1573-6.

Rohart, F., Gautier, B., Singh, A., and Le Cao, K. A. 2017. 'mixOmics: An R package for 'omics feature selection and multiple data integration', *PLoS Comput Biol*, 13: e1005752.

Romo-Vaquero, M., Cortes-Martin, A., Loria-Kohen, V., Ramirez-de-Molina, A., Garcia-Mantrana, I., Collado, M. C., Espin, J. C., and Selma, M. V. 2019. 'Deciphering the Human Gut Microbiome of Urolithin Metabotypes: Association with Enterotypes and Potential Cardiometabolic Health Implications', *Mol Nutr Food Res*, 63: e1800958.

Roume, H., Mondot, S., Saliou, A., Le Fresne-Languille, S., and Dore, J. 2023. 'Multicenter evaluation of gut microbiome profiling by next-generation sequencing reveals major biases in partial-length metabarcoding approach', *Sci Rep*, 13: 22593.

Round, J. L., and Mazmanian, S. K. 2009. 'The gut microbiota shapes intestinal immune responses during health and disease', *Nat Rev Immunol*, 9: 313-23.

Routy, B., Le Chatelier, E., Derosa, L., Duong, C. P. M., Alou, M. T., Daillere, R., Fluckiger, A., Messaoudene, M., Rauber, C., Roberti, M. P., Fidelle, M., Flament, C., Poirier-Colame, V., Opolon, P., Klein, C., Iribarren, K., Mondragon, L., Jacquelot, N., Qu, B., Ferrere, G., Clemenson, C., Mezquita, L., Masip, J. R., Naltet, C., Brosseau, S., Kaderbhai, C., Richard, C., Rizvi, H., Levenez, F., Galleron, N., Quinquis, B., Pons, N., Ryffel, B., Minard-Colin, V., Gonin, P., Soria, J. C., Deutsch, E., Loriot, Y., Ghiringhelli, F., Zalcman, G., Goldwasser, F., Escudier, B., Hellmann, M. D., Eggermont, A., Raoult, D., Albiges, L., Kroemer, G., and Zitvogel, L. 2018. 'Gut microbiome influences efficacy of PD-1-based immunotherapy against epithelial tumors', *Science*, 359: 91-97.

Russell, D. W. 2003. 'The enzymes, regulation, and genetics of bile acid synthesis', *Annu Rev Biochem*, 72: 137-74.

Saha, J. R., Butler, V. P., Jr., Neu, H. C., and Lindenbaum, J. 1983. 'Digoxin-inactivating bacteria: identification in human gut flora', *Science*, 220: 325-7.

Sakai, R., Winand, R., Verbeiren, T., Moere, A. V., and Aerts, J. 2014. 'dendsort: modular leaf ordering methods for dendrogram representations in R', *F1000Res*, 3: 177.

Sannasiddappa, T. H., Lund, P. A., and Clarke, S. R. 2017. 'In Vitro Antibacterial Activity of Unconjugated and Conjugated Bile Salts on *Staphylococcus aureus*', *Front Microbiol*, 8: 1581.

Santa Maria, J., Vallance, P., Charles, I. G., and Leiper, J. M. 1999. 'Identification of microbial dimethylarginine dimethylaminohydrolase enzymes', *Mol Microbiol*, 33: 1278-9.

Sayin, S. I., Wahlstrom, A., Felin, J., Jantti, S., Marschall, H. U., Bamberg, K., Angelin, B., Hyotylainen, T., Oresic, M., and Backhed, F. 2013. 'Gut microbiota regulates bile acid metabolism by reducing the levels of tauro-beta-muricholic acid, a naturally occurring FXR antagonist', *Cell Metab*, 17: 225-35.

Schaedler, R. W., Dubs, R., and Costello, R. 1965. 'Association of Germfree Mice with Bacteria Isolated from Normal Mice', *J Exp Med*, 122: 77-82.

Schaubeck, M., Clavel, T., Calasan, J., Lagkouvardos, I., Haange, S. B., Jehmlich, N., Basic, M., Dupont, A., Hornef, M., von Bergen, M., Bleich, A., and Haller, D. 2016. 'Dysbiotic gut microbiota causes transmissible Crohn's disease-like ileitis independent of failure in antimicrobial defence', *Gut*, 65: 225-37.

Seedorf, H., Griffin, N. W., Ridaura, V. K., Reyes, A., Cheng, J., Rey, F. E., Smith, M. I., Simon, G. M., Scheffrahn, R. H., Woebken, D., Spormann, A. M., Van Treuren, W., Ursell, L. K., Pirrung, M., Robbins-Pianka, A., Cantarel, B. L., Lombard, V., Henrissat, B., Knight, R., and Gordon, J. I. 2014. 'Bacteria from diverse habitats colonize and compete in the mouse gut', *Cell*, 159: 253-66.

Semova, I., Carten, J. D., Stombaugh, J., Mackey, L. C., Knight, R., Farber, S. A., and Rawls, J. F. 2012. 'Microbiota regulate intestinal absorption and metabolism of fatty acids in the zebrafish', *Cell Host Microbe*, 12: 277-88.

Sender, R., Fuchs, S., and Milo, R. 2016. 'Revised Estimates for the Number of Human and Bacteria Cells in the Body', *PLoS Biol*, 14: e1002533.

Senior, J. R. 1964. 'INTESTINAL ABSORPTION OF FATS', *J Lipid Res*, 5: 495-521.

Shalon, D., Culver, R. N., Grembi, J. A., Folz, J., Treit, P. V., Shi, H., Rosenberger, F. A., Dethlefsen, L., Meng, X., Yaffe, E., Aranda-Diaz, A., Geyer, P. E., Mueller-Reif, J. B., Spencer, S., Patterson, A. D., Triadafilopoulos, G., Holmes, S. P., Mann, M., Fiehn, O., Relman, D. A., and Huang, K. C. 2023. 'Profiling the human intestinal environment under physiological conditions', *Nature*, 617: 581-91.

Sheng, Y., Ren, H., Limbu, S. M., Sun, Y., Qiao, F., Zhai, W., Du, Z. Y., and Zhang, M. 2018. 'The Presence or Absence of Intestinal Microbiota Affects Lipid Deposition and Related Genes Expression in Zebrafish (Danio rerio)', *Front Microbiol*, 9: 1124.

Shiau, Y. F., Popper, D. A., Reed, M., Umstetter, C., Capuzzi, D., and Levine, G. M. 1985. 'Intestinal triglycerides are derived from both endogenous and exogenous sources', *Am J Physiol*, 248: G164-9.

Sim, K., Cox, M. J., Wopereis, H., Martin, R., Knol, J., Li, M. S., Cookson, W. O., Moffatt, M. F., and Kroll, J. S. 2012. 'Improved detection of bifidobacteria with optimised 16S rRNA-gene based pyrosequencing', *PLoS One*, 7: e32543.

Slezak, K., Krupova, Z., Rabot, S., Loh, G., Levenez, F., Descamps, A., Lepage, P., Dore, J., Bellier, S., and Blaut, M. 2014. 'Association of germ-free mice with a simplified human intestinal microbiota results in a shortened intestine', *Gut Microbes*, 5: 176-82.

Snipes, R. L. 1977. 'Limited fat absorption in the large intestine of mice. A morphological study', *Acta Anat (Basel)*, 99: 435-9.

Sonnhammer, E. L., von Heijne, G., and Krogh, A. 1998. 'A hidden Markov model for predicting transmembrane helices in protein sequences', *Proc Int Conf Intell Syst Mol Biol*, 6: 175-82.

Sorbara, M. T., Littmann, E. R., Fontana, E., Moody, T. U., Kohout, C. E., Gjonbalaj, M., Eaton, V., Seok, R., Leiner, I. M., and Pamer, E. G. 2020. 'Functional and Genomic Variation between Human-Derived Isolates of Lachnospiraceae Reveals Inter- and Intra-Species Diversity', *Cell Host Microbe*, 28: 134-46 e4.

Sperry, J. F., and Wilkins, T. D. 1976. 'Arginine, a growth-limiting factor for *Eubacterium lentum*', *J Bacteriol*, 127: 780-4.

Spiess, A.-N. 2018. "qpcR: Modelling and Analysis of Real-Time PCR Data." In.

Sprotte, S., Rasmussen, T. S., Cho, G. S., Brinks, E., Lametsch, R., Neve, H., Vogensen, F. K., Nielsen, D. S., and Franz, C. 2022. 'Morphological and Genetic Characterization of *Eggerthella lenta* Bacteriophage PMBT5', *Viruses*, 14.

Streidl, T. 2021. 'Effects of the bacterial conversion of lipids in the gut on mouse metabolism', PhD thesis, RWTH Aachen University.

Streidl, T., Karkossa, I., Segura Munoz, R. R., Eberl, C., Zaufel, A., Plagge, J., Schmaltz, R., Schubert, K., Basic, M., Schneider, K. M., Afify, M., Trautwein, C., Tolba, R., Stecher, B., Doden, H. L., Ridlon, J. M., Ecker, J., Moustafa, T., von Bergen, M., Ramer-Tait, A. E., and Clavel, T. 2021. 'The gut bacterium *Extibacter muris* produces secondary bile acids and influences liver physiology in gnotobiotic mice', *Gut Microbes*, 13: 1-21.

Studer, N., Desharnais, L., Beutler, M., Brugiroux, S., Terrazos, M. A., Menin, L., Schurch, C. M., McCoy, K. D., Kuehne, S. A., Minton, N. P., Stecher, B., Bernier-Latmani, R., and Hapfelmeier, S. 2016. 'Functional Intestinal Bile Acid 7alpha-Dehydroxylation by Clostridium scindens Associated with Protection from Clostridium difficile Infection in a Gnotobiotic Mouse Model', *Front Cell Infect Microbiol*, 6: 191.

Sung, J. Y., Shaffer, E. A., and Costerton, J. W. 1993. 'Antibacterial activity of bile salts against common biliary pathogens. Effects of hydrophobicity of the molecule and in the presence of phospholipids', *Dig Dis Sci*, 38: 2104-12.

Surdacki, A., Nowicki, M., Sandmann, J., Tsikas, D., Boeger, R. H., Bode-Boeger, S. M., Kruszelnicka-Kwiatkowska, O., Kokot, F., Dubiel, J. S., and Froelich, J. C. 1999. 'Reduced urinary excretion of nitric oxide metabolites and increased plasma levels of asymmetric dimethylarginine in men with essential hypertension', *J Cardiovasc Pharmacol*, 33: 652-8.

Suzuki, A., Mizumoto, A., Rerknimitr, R., Sarr, M. G., and DiMango, E. P. 1999. 'Effect of bacterial or porcine lipase with low- or high-fat diets on nutrient absorption in pancreatic-insufficient dogs', *Gastroenterology*, 116: 431-7.

Suzuki, A., Mizumoto, A., Sarr, M. G., and DiMagno, E. P. 1997. 'Bacterial lipase and high-fat diets in canine exocrine pancreatic insufficiency: a new therapy of steatorrhea?', *Gastroenterology*, 112: 2048-55.

Sze, M. A., and Schloss, P. D. 2016. 'Looking for a Signal in the Noise: Revisiting Obesity and the Microbiome', *mBio*, 7.

Takagaki, A., and Nanjo, F. 2015. 'Bioconversion of (-)-epicatechin, (+)-epicatechin, (-)-catechin, and (+)-catechin by (-)-epigallocatechin-metabolizing bacteria', *Biol Pharm Bull*, 38: 789-94.

Tang, Q., Huang, H., Xu, H., Xia, H., Zhang, C., Ye, D., and Bi, F. 2024. 'Endogenous Coriobacteriaceae enriched by a high-fat diet promotes colorectal tumorigenesis through the CPT1A-ERK axis', *NPJ Biofilms Microbiomes*, 10: 5.

Thomas, A. M., and Segata, N. 2019. 'Multiple levels of the unknown in microbiome research', *BMC Biol*, 17: 48.

Thorasin, T., Hoyles, L., and McCartney, A. L. 2015. 'Dynamics and diversity of the 'Atopobium cluster' in the human faecal microbiota, and phenotypic characterization of 'Atopobium cluster' isolates', *Microbiology (Reading)*, 161: 565-79.

Tian, Y., Gui, W., Koo, I., Smith, P. B., Allman, E. L., Nichols, R. G., Rimal, B., Cai, J., Liu, Q., and Patterson, A. D. 2020. 'The microbiome modulating activity of bile acids', *Gut Microbes*, 11: 979-96.

Tims, S., Derom, C., Jonkers, D. M., Vlietinck, R., Saris, W. H., Kleerebezem, M., de Vos, W. M., and Zoetendal, E. G. 2013. 'Microbiota conservation and BMI signatures in adult monozygotic twins', *ISME J*, 7: 707-17.

Trexler, P. C., and Reynolds, L. I. 1957. 'Flexible film apparatus for the rearing and use of germfree animals', *Appl Microbiol*, 5: 406-12.

Truong, D. T., Tett, A., Pasolli, E., Huttenhower, C., and Segata, N. 2017. 'Microbial strain-level population structure and genetic diversity from metagenomes', *Genome Res*, 27: 626-38.

Turnbaugh, P. J., Hamady, M., Yatsunenko, T., Cantarel, B. L., Duncan, A., Ley, R. E., Sogin, M. L., Jones, W. J., Roe, B. A., Affourtit, J. P., Egholm, M., Henrissat, B., Heath, A. C., Knight, R., and Gordon, J. I. 2009. 'A core gut microbiome in obese and lean twins', *Nature*, 457: 480-4.

Turnbaugh, P. J., Ley, R. E., Mahowald, M. A., Magrini, V., Mardis, E. R., and Gordon, J. I. 2006. 'An obesity-associated gut microbiome with increased capacity for energy harvest', *Nature*, 444: 1027-31.

van Greevenbroek, M. M., and de Bruin, T. W. 1998. 'Chylomicron synthesis by intestinal cells in vitro and in vivo', *Atherosclerosis*, 141 Suppl 1: S9-16.

van Tilburg Bernardes, E., Pettersen, V. K., Gutierrez, M. W., Laforest-Lapointe, I., Jendzjowsky, N. G., Cavin, J. B., Vicentini, F. A., Keenan, C. M., Ramay, H. R., Samara, J., MacNaughton, W. K., Wilson, R. J. A., Kelly, M. M., McCoy, K. D., Sharkey, K. A., and Arrieta, M. C. 2020. 'Intestinal fungi are causally implicated in microbiome assembly and immune development in mice', *Nat Commun*, 11: 2577.

Velagapudi, V. R., Hezaveh, R., Reigstad, C. S., Gopalacharyulu, P., Yetukuri, L., Islam, S., Felin, J., Perkins, R., Boren, J., Oresic, M., and Backhed, F. 2010. 'The gut microbiota modulates host energy and lipid metabolism in mice', *J Lipid Res*, 51: 1101-12.

Viehof, A., Haange, S. B., Streidl, T., Schubert, K., Engelmann, B., Haller, D., Rolle-Kampczyk, U., von Bergen, M., and Clavel, T. 2024. 'The human intestinal bacterium *Eggerthella lenta* influences gut metabolomes in gnotobiotic mice', *Microbiome Res Rep*, 3: 14.

Vital, M., Rud, T., Rath, S., Pieper, D. H., and Schluter, D. 2019. 'Diversity of Bacteria Exhibiting Bile Acid-inducible 7alpha-dehydroxylation Genes in the Human Gut', *Comput Struct Biotechnol J*, 17: 1016-19.

Wade, W. G., Downes, J., Dymock, D., Hiom, S. J., Weightman, A. J., Dewhirst, F. E., Paster, B. J., Tzellas, N., and Coleman, B. 1999. 'The family Coriobacteriaceae: reclassification of Eubacterium exiguum (Poco et al. 1996) and Peptostreptococcus heliotrinreducens (Lanigan 1976) as Slackia exigua gen. nov., comb. nov. and Slackia heliotrinireducens gen. nov., comb. nov., and Eubacterium lentum (Prevot 1938) as Eggerthella lenta gen. nov., comb. nov', *Int J Syst Bacteriol*, 49 Pt 2: 595-600.

Wahlstrom, A., Sayin, S. I., Marschall, H. U., and Backhed, F. 2016. 'Intestinal Crosstalk between Bile Acids and Microbiota and Its Impact on Host Metabolism', *Cell Metab*, 24: 41-50.

Walker, A. W., and Hoyles, L. 2023. 'Human microbiome myths and misconceptions', *Nat Microbiol*, 8: 1392-96.

Walker, A. W., Ince, J., Duncan, S. H., Webster, L. M., Holtrop, G., Ze, X., Brown, D., Stares, M. D., Scott, P., Bergerat, A., Louis, P., McIntosh, F., Johnstone, A. M., Lobley, G. E., Parkhill, J., and Flint, H. J. 2011. 'Dominant and diet-responsive groups of bacteria within the human colonic microbiota', *ISME J*, 5: 220-30.

Walker, B. E., Kelleher, J., Davies, T., Smith, C. L., and Losowsky, M. S. 1973. 'Influence of dietary fat on fecal fat', *Gastroenterology*, 64: 233-9.

Walter, J., Armet, A. M., Finlay, B. B., and Shanahan, F. 2020. 'Establishing or Exaggerating Causality for the Gut Microbiome: Lessons from Human Microbiota-Associated Rodents', *Cell*, 180: 221-32.

Walters, W. A., Xu, Z., and Knight, R. 2014. 'Meta-analyses of human gut microbes associated with obesity and IBD', *FEBS Lett*, 588: 4223-33.

Wang, Z., Karkossa, I., Grosskopf, H., Rolle-Kampczyk, U., Hackermuller, J., von Bergen, M., and Schubert, K. 2021. 'Comparison of quantitation methods in proteomics to define relevant toxicological information on AhR activation of HepG2 cells by BaP', *Toxicology*, 448: 152652.

Wegner, K., Just, S., Gau, L., Mueller, H., Gerard, P., Lepage, P., Clavel, T., and Rohn, S. 2017. 'Rapid analysis of bile acids in different biological matrices using LC-ESI-MS/MS for the investigation of bile acid transformation by mammalian gut bacteria', *Anal Bioanal Chem*, 409: 1231-45.

Wei, T., and Simko, V. 2017. "R package "corrplot": Visualization of a Correlation Matrix." In.

Weitkunat, K., Schumann, S., Petzke, K. J., Blaut, M., Loh, G., and Klaus, S. 2015. 'Effects of dietary inulin on bacterial growth, short-chain fatty acid production and hepatic lipid metabolism in gnotobiotic mice', *J Nutr Biochem*, 26: 929-37.

Wickham, H. 2007. 'Reshaping Data with the reshape Package', *Journal of Statistical Software*, 21: 1 - 20.

———. 2016a. 'Data Analysis.' in Wickham, Hadley (ed.), *ggplot2: Elegant Graphics for Data Analysis* (Springer International Publishing: Cham).

Wickham, H. 2016b. "ggplot2: Elegant Graphics for Data Analysis." In.: Springer-Verlag New York.

Winkler, F. K., D'Arcy, A., and Hunziker, W. 1990. 'Structure of human pancreatic lipase', *Nature*, 343: 771-4.

Woese, C. R., and Fox, G. E. 1977. 'Phylogenetic structure of the prokaryotic domain: the primary kingdoms', *Proc Natl Acad Sci U S A*, 74: 5088-90.

Wostmann, B. S. 1981. 'The germfree animal in nutritional studies', *Annu Rev Nutr*, 1: 257-79.

Woting, A., Clavel, T., Loh, G., and Blaut, M. 2010. 'Bacterial transformation of dietary lignans in gnotobiotic rats', *FEMS Microbiol Ecol*, 72: 507-14.

Woting, A., Pfeiffer, N., Loh, G., Klaus, S., and Blaut, M. 2014. '*Clostridium ramosum* promotes high-fat diet-induced obesity in gnotobiotic mouse models', *mBio*, 5: e01530-14.

Wu, C., Yang, F., Zhong, H., Hong, J., Lin, H., Zong, M., Ren, H., Zhao, S., Chen, Y., Shi, Z., Wang, X., Shen, J., Wang, Q., Ni, M., Chen, B., Cai, Z., Zhang, M., Cao, Z., Wu, K., Gao, A., Li, J., Liu, C., Xiao, M., Li, Y., Shi, J., Zhang, Y., Xu, X., Gu, W., Bi, Y., Ning, G., Wang, W., Wang, J., and Liu, R. 2024. 'Obesity-enriched gut microbe degrades myo-inositol and promotes lipid absorption', *Cell Host Microbe*, 32: 1301-14 e9.

Wu, H., Tremaroli, V., Schmidt, C., Lundqvist, A., Olsson, L. M., Kramer, M., Gummesson, A., Perkins, R., Bergstrom, G., and Backhed, F. 2020. 'The Gut Microbiota in Prediabetes and Diabetes: A Population-Based Cross-Sectional Study', *Cell Metab*, 32: 379-90 e3.

Wyss, M., and Kaddurah-Daouk, R. 2000. 'Creatine and creatinine metabolism', *Physiol Rev*, 80: 1107-213.

Xiao, N. 2018. "Scientific Journal and Sci-Fi Themed Color Palettes for 'ggplot2'." In.

Yan, H., Fei, N., Wu, G., Zhang, C., Zhao, L., and Zhang, M. 2016. 'Regulated Inflammation and Lipid Metabolism in Colon mRNA Expressions of Obese Germfree Mice Responding to Enterobacter cloacae B29 Combined with the High Fat Diet', *Front Microbiol*, 7: 1786.

Yoon, H. S., Cho, C. H., Yun, M. S., Jang, S. J., You, H. J., Kim, J. H., Han, D., Cha, K. H., Moon, S. H., Lee, K., Kim, Y. J., Lee, S. J., Nam, T. W., and Ko, G. 2021. '*Akkermansia muciniphila* secretes a glucagon-like peptide-1-inducing protein that improves glucose homeostasis and ameliorates metabolic disease in mice', *Nat Microbiol*, 6: 563-73.

Yun, K. E., Kim, J., Kim, M. H., Park, E., Kim, H. L., Chang, Y., Ryu, S., and Kim, H. N. 2020. 'Major Lipids, Apolipoproteins, and Alterations of Gut Microbiota', *J Clin Med*, 9.

Yun, Y., Kim, H. N., Kim, S. E., Heo, S. G., Chang, Y., Ryu, S., Shin, H., and Kim, H. L. 2017. 'Comparative analysis of gut microbiota associated with body mass index in a large Korean cohort', *BMC Microbiol*, 17: 151.

Zairis, M. N., Patsourakos, N. G., Tsiaousis, G. Z., Theodossis Georgilas, A., Melidonis, A., Makrygiannis, S. S., Velissaris, D., Batika, P. C., Argyrakis, K. S., Tzerefos, S. P., Prekates, A. A., and Foussas, S. G. 2012. 'Plasma asymmetric dimethylarginine and mortality in patients with acute decompensation of chronic heart failure', *Heart*, 98: 860-4.

Zhang, H., DiBaise, J. K., Zuccolo, A., Kudrna, D., Braidotti, M., Yu, Y., Parameswaran, P., Crowell, M. D., Wing, R., Rittmann, B. E., and Krajmalnik-Brown, R. 2009. 'Human gut microbiota in obesity and after gastric bypass', *Proc Natl Acad Sci U S A*, 106: 2365-70.

Zhang, J., Sturla, S., Lacroix, C., and Schwab, C. 2018. 'Gut Microbial Glycerol Metabolism as an Endogenous Acrolein Source', *mBio*, 9.

Zhang, X., Smits, A. H., van Tilburg, G. B., Ovaa, H., Huber, W., and Vermeulen, M. 2018. 'Proteome-wide identification of ubiquitin interactions using UbIA-MS', *Nat Protoc*, 13: 530-50.

Zhao, L., Zhang, Q., Ma, W., Tian, F., Shen, H., and Zhou, M. 2017. 'A combination of quercetin and resveratrol reduces obesity in high-fat diet-fed rats by modulation of gut microbiota', *Food Funct*, 8: 4644-56.

Zilversmit, D. B. 1968. 'The surface coat of chylomicrons: lipid chemistry', *J Lipid Res*, 9: 180-6.

Curriculum vitae

Persönliche Daten

Name	Alina Viehof-Beckmann (geb. Viehof)
Geburtsdatum	29.11.1993
Geburtsort	Neuss

Wissenschaftliche Tätigkeit

Seit 11/2019	**Wissenschaftliche Mitarbeiterin**
	Institut für Medizinische Mikrobiologie, Uniklinik RWTH Aachen
07/2017 - 12/2017	**Studentische Hilfskraft**
	Institut für Angewandte Mikrobiologie, RWTH Aachen

Ausbildung

10/2016 – 11/2019	**Master of Science, Biologie**
	RWTH Aachen
	Schwerpunkt: Mikrobiologie und Genetik
10/2013 - 09/2016	**Bachelor of Science, Biologie**
	RWTH Aachen
	Schwerpunkt: Mikrobiologie und Genetik
08/2004 - 07/2013	**Abitur**
	Gymnasium Korschenbroich

Publikationen

Afrizal, A., Hitch, T. C. A., **Viehof, A**., Treichel, N., Riedel, T., Abt, B., Buhl, E. M., Kohlheyer, D., Overmann, J., and Clavel, T. 2022. **'Anaerobic single-cell dispensing facilitates the cultivation of human gut bacteria'**, Environ Microbiol, 24: 3861-81.

Afrizal, A., Jennings, S. A. V., Hitch, T. C. A., Riedel, T., Basic, M., Panyot, A., Treichel, N., Hager, F. T., Wong, E. O., Wolter, B., **Viehof, A.**, von Strempel, A., Eberl, C., Buhl, E. M., Abt, B., Bleich, A., Tolba, R., Blank, L. M., Navarre, W. W., Kiessling, F., Horz, H. P., Torow, N., Cerovic, V., Stecher, B., Strowig, T., Overmann, J., and Clavel, T. 2022. **'Enhanced cultured diversity of the mouse gut microbiota enables custom-made synthetic communities'**, Cell Host Microbe, 30: 1630-45 e25.

Hitch, T. C. A., Masson, J. M., Pauvert, C., Bosch, J., Nuchtern, S., Treichel, N. S., Baloh, M., Razavi, S., Afrizal, A., Kousetzi, N., Aguirre, A. M., Wylensek, D., Coates, A. C., Jennings, S. A. V., Panyot, A., **Viehof, A.**, Schmitz, M. A., Stuhrmann, M., Deis, E. C., Bisdorf, K., Chiotelli, M. D., Lissin, A., Schober, I., Witte, J., Cramer, T., Riedel, T., Wende, M., Winter, K. A., Amend, L., Riva, A., Trinh, S., Mitchell, L., Hartman, J., Berry, D., Seitz, J., Bossert, L. C., Grognot, M., Allers, T., Strowig, T., Pester, M., Abt, B., Reimer, L. C., Overmann, J., and Clavel, T. 2025. **'HiBC: a publicly available collection of bacterial strains isolated from the human gut'**, Nat Commun, 16: 4203.

Kister, B., **Viehof, A.**, Rolle-Kampczyk, U., Schwentker, A., Treichel, N. S., Jennings, S. A. V., Wirtz, T. H., Blank, L. M., Hornef, M. W., von Bergen, M., Clavel, T., and Kuepfer, L. 2023. **'A physiologically based model of bile acid metabolism in mice'**, iScience, 26: 107922.

Pedersen, K. J., Haange, S. B., Zizalova, K., **Viehof, A.**, Clavel, T., Lenicek, M., Engelmann, B., Wick, L. Y., Schaap, F. G., Jehmlich, N., Rolle-Kampczyk, U., and von Bergen, M. 2022. **'*Eggerthella lenta* DSM 2243 Alleviates Bile Acid Stress Response in *Clostridium ramosum* and *Anaerostipes caccae* by Transformation of Bile Acids'**, Microorganisms, 10.

Viehof, A., Haange, S. B., Streidl, T., Schubert, K., Engelmann, B., Haller, D., Rolle-Kampczyk, U., von Bergen, M., and Clavel, T. 2024. **'The human intestinal bacterium *Eggerthella lenta* influences gut metabolomes in gnotobiotic mice'**, Microbiome Res Rep, 3: 14.

Eidesstattliche Erklärung

Ich, Alina Viehof-Beckmann, erkläre hiermit, dass diese Dissertation und die darin dargelegten Inhalte die eigenen sind und selbstständig, als Ergebnis der eigenen originären Forschung, generiert wurden.

Hiermit erkläre ich an Eides statt

1. Diese Arbeit wurde vollständig oder größtenteils in der Phase als Doktorand dieser Fakultät und Universität angefertigt;
2. Sofern irgendein Bestandteil dieser Dissertation zuvor für einen akademischen Abschluss oder eine andere Qualifikation an dieser oder einer anderen Institution verwendet wurde, wurde dies klar angezeigt;
3. Wenn immer andere eigene- oder Veröffentlichungen Dritter herangezogen wurden, wurden diese klar benannt;
4. Wenn aus anderen eigenen- oder Veröffentlichungen Dritter zitiert wurde, wurde stets die Quelle hierfür angegeben. Diese Dissertation ist vollständig meine eigene Arbeit, mit der Ausnahme solcher Zitate;
5. Alle wesentlichen Quellen von Unterstützung wurden benannt;
6. Wenn immer ein Teil dieser Dissertation auf der Zusammenarbeit mit anderen basiert, wurde von mir klar gekennzeichnet, was von anderen und was von mir selbst erarbeitet wurde;
7. Ein Teil dieser Arbeit wurden zuvor veröffentlicht und zwar in:

   Viehof, A., Haange, S. B., Streidl, T., Schubert, K., Engelmann, B., Haller, D., Rolle-Kampczyk, U., von Bergen, M., and Clavel, T. 2024. 'The human intestinal bacterium *Eggerthella lenta* influences gut metabolomes in gnotobiotic mice', Microbiome Res Rep, 3: 14.

_____ _____

Ort, Datum (Alina Viehof-Beckmann)